UNIVERZITET U NOVOM SADU
FAKULTET TEHNIČKIH NAUKA U NOVOM SADU

Aleksandar Minja

ODREĐIVANJE PERFORMANSI DEKODERA ZAŠTITNIH KODOVA

DOKTORSKA DISERTACIJA

Novi Sad, 2018.

УНИВЕРЗИТЕТ У НОВОМ САДУ ● **ФАКУЛТЕТ ТЕХНИЧКИХ НАУКА**
21000 НОВИ САД, Трг Доситеја Обрадовића 6

КЉУЧНА ДОКУМЕНТАЦИЈСКА ИНФОРМАЦИЈА

Редни број, **РБР**:		
Идентификациони број, **ИБР**:		
Тип документације, **ТД**:		Монографска документација
Тип записа, **ТЗ**:		Текстуални штампани материјал
Врста рада, **ВР**:		Докторска дисертација
Аутор, **АУ**:		Александар Миња
Ментор, **МН**:		др Војин Шенк, редовни професор
Наслов рада, **НР**:		Одређивање перформанси декодера заштитних кодова
Језик публикације, **ЈП**:		Енглески
Језик извода, **ЈИ**:		Српски / Енглески
Земља публиковања, **ЗП**:		Република Србија
Уже географско подручје, **УГП**:		Војводина
Година, **ГО**:		2018
Издавач, **ИЗ**:		Ауторски репринт
Место и адреса, **МА**:		Факултет техничких наука, Трг Доситеја Обрадовића 6, 21000 Нови Сад
Физички опис рада, **ФО**: (поглавља/страна/ цитата/табела/слика/графика/прилога)		7 / 130 /143 / 5 / 28 / 0 / 0
Научна област, **НО**:		Електротехничко и рачунарско инжењерство
Научна дисциплина, **НД**:		Телекомуникације и обрада сигнала
Предметна одредница/Кључне речи, **ПО**:		Дигиталне телекомуникације, моделовање и симулација, квази-аналитички поступак, кодовање, теорија информација,
УДК		
Чува се, **ЧУ**:		Библиотека ФТН, Нови Сад
Важна напомена, **ВН**:		
Извод, **ИЗ**:		Ова дисертација садржи неке од резултата аутора добијених током његовог постдипломског истраживања у областима моделовања комуникационих система и теорије информација и заштитног кодовања. Резултати су представљени у математичком формату и верификовани су нумеричким симулацијама. Већина њих је мотивисана проблемима који се појављују приликом развоја и стандрадизације 5G комуникационих система и имају велики научни и практични значај. Дисертација је подељена у два дела. Први део уводи нови квазианалитички поступак за естимацију вероватноће грешке декодера заштитних кодова. Математички је показано и експериментално потврђено да је нови симулациони поступак значајно бржи од постојећих симулационих постпупака (монте карло и поступак узорковања по значајности) који се користе у пракси. У другом делу тезе представљен је проблем конструкције вишедимензионалне трелис кодоване модулације (енг. Trellis Coded Modulation - TCM) помоћу сферичних кодова. Развијен је нови алгоритам за конструкцију сферичних кодова који су прилагођени структури TCM кода и показано је да такви TCM кодови имају знатно боље перформансе од постојећих. Вероватноћа грешке ових нових TCM кодова је естимирана применом симулационог поступка који је дат у првом делу дисертације.
Датум прихватања теме, **ДП**:		14. 09. 2017. године
Датум одбране, **ДО**:		
Чланови комисије, **КО**:	Председник:	др Драгана Бајовић
	Члан:	др Душан Јаковетић
	Члан:	др Владо Делић
	Члан:	др Зорица Николић
	Члан, ментор:	др Војин Шенк

UNIVERSITY OF NOVI SAD ● **FACULTY OF TECHNICAL SCIENCES**
21000 NOVI SAD, Trg Dositeja Obradovića 6

KEY WORDS DOCUMENTATION

Accession number, **ANO**:			
Identification number, **INO**:			
Document type, **DT**:		Monograph publication	
Type of record, **TR**:		Textual printed material	
Contents code, **CC**:		PhD thesis	
Author, **AU**:		Aleksadnar Minja	
Mentor, **MN**:		dr Vojin Šenk	
Title, **TI**:		Determining Performance of Channel Decoders	
Language of text, **LT**:		English	
Language of abstract, **LA**:		Serbian / English	
Country of publication, **CP**:		Republic of Serbia	
Locality of publication, **LP**:		Vojvodina	
Publication year, **PY**:		2018	
Publisher, **PB**:		Author's reprint	
Publication place, **PP**:		Faculty of Technical Sciences, Trg Dositeja Obradovića 6, 21000 Novi Sad	
Physical description, **PD**: (chapters/pages/ref./tables/pictures/graphs/appendixes)		7 / 130 /143 / 5 / 28 / 0 / 0	
Scientific field, **SF**:		Electrical and computer engineering	
Scientific discipline, **SD**:		Telecommunications and signal processing	
Subject/Key words, **S/KW**:		Digital communications, modeling and simulation, quasi-analytical method, coding, information theory,	
UC			
Holding data, **HD**:		Library of Faculty of technical sciences, Novi Sad	
Note, **N**:			
Abstract, **AB**:		This thesis contains some of the results obtained by the author in the course of his postgraduate research in the fields of Communication system modeling and Information and coding theory. The results are presented in mathematical form and are verified by numerical simulations. Most of them are motivated by challenges arising in the design and standardization of 5G communication systems and are of practical and scientific relevance. Main contributions of the thesis are divided into two parts. In the first part of this thesis we introduce a novel SNR-invariant quasi-analytical technique for estimating the error rate of a communication link over the geodesic channel. We compared this technique to the Monte Carlo and Importance Sampling methods and it has been found out that it outperforms other methods in both accuracy and speed. In the second part of the thesis we introduce an optimization procedure, based on the variable force repulsion method, for the design of spherical codes that are tailored to the TCM and achieve lower error rates at high SNR, then their counterparts that are optimized for minimum distance. The performance of these codes is verified using the method developed in part I of this thesis which is suitable for simulating error rates at high SNR.	
Accepted by the Scientific Board on, **ASB**:		September 14th, 2017	
Defended on, **DE**:			
Defended Board, **DB**:	President:	Dragana Bajović, PhD	
	Member:	Dušan Jakovetić, PhD	
	Member:	Vlado Delić, PhD	
	Member:	Zorica Nikolić, PhD	
	Member, Mentor:	Vojin Šenk, PhD	

Determining Performance of Channel Decoders

by
Aleksandar Minja

for the degree of

Doctor of Technical Sciences

A dissertation submitted to the

Department of Power, Electronics
and Telecommunication Engineering,
Faculty of Technical Sciences,
University of Novi Sad,
Serbia.

2018.

Advisors: Prof. Dr Vojin Šenk,
Department of Power, Electronics
and Telecommunication Engineering,
Faculty of Technical Sciences,
University of Novi Sad, Serbia.

Thesis Committee Members:

Assistant Prof. Dr Dragana Bajović, chair
Department of Power, Electronics
and Telecommunication Engineering,
Faculty of Technical Sciences,
University of Novi Sad, Serbia.

Assistant Prof. Dr Dušan Jakovetić,
Department of Mathematics and Informatics,
Faculty of Sciences,
University of Novi Sad, Serbia.

Prof. Dr Vlado Delić
Department of Power, Electronics
and Telecommunication Engineering,
Faculty of Technical Sciences,
University of Novi Sad, Serbia.

Prof Dr Zorica Nikolić,
Department of Telecommunications,
Faculty of Electronic Engineering,
University of Niš, Serbia.

To my parents

Contents

Acknowledgments **v**

Rezime **vii**

Abstract **xix**

List of Figures **xxi**

List of Tables **xxiii**

1 Introduction and Motivation **1**

I Novel Quasi-Analytical Simulation Method **11**

2 System Model **13**

2.1 Geodesic Channel Model 13

2.2 Metric Star Domain Decoders 15

2.2.1 Ordered Statistics Decoder 18

2.2.2 Polar Successive Cancellation Decoder 21

2.3 Error Probability of Star Domain Decoders 24

3 Simulation of a Communication Link **27**
3.1 General Simulation Framework 27
3.2 Monte Carlo Simulation Method 28
3.3 Importance Sampling Simulation Method 29
3.3.1 IS techniques for AWGN Channel 31
3.3.2 Minimum Variance IS for BSC 32

4 Quasi-Analytical Simulation Method **33**
4.1 General QA Simulation Method 33
4.1.1 QA Simulation for the BSC 44
4.1.2 QA Simulation for the AWGN Channel 46
4.2 Analysis of the QA Simulation Method 48

5 Numerical Results **53**
5.1 Comparison of Different Simulation Methods 53
5.2 Conclusion 59

II Trellis Coded Modulation Design by Optimized Set Partitioning **61**

6 Multidimensional Coded Modulation **63**
6.1 Multidimensional Modulation 63
6.1.1 Lattice Constellations 65
6.1.2 Spherical Codes 65
6.2 Visualization of 3D Spherical Codes 66
6.3 Design of Spherical Codes 67
6.4 Trellis Coded Modulation 69
6.4.1 Set Partitioning 69
6.4.2 TCM Encoding 73
6.4.3 Viterbi Decoding 74

7 Optimized Set Partitioning **75**
7.1 Problem Formulation and Algorithm 75
7.2 Simulation Results 78
7.3 Conclusion 81

Bibliography **85**

Acknowledgments

First of all, I would like to thank Smiljana and my parents for their love and support. I have been very fortunate to be raised and surrounded throughout my life by wonderful people; they have always been, and always will be, my driving force and source of inspiration. I would like to dedicate this thesis to my parents, Speranca and Đorđe, whose wisdom, kindness and caring have always guided me unmistakably in the right direction and to the memory of my grandparents.

On the professional side, I would like to express my sincere gratitude to my advisor, Prof. Vojin Šenk, for inspiring me to pursue research in Information and coding theory. I would also like to thank Professors Dejan Vukobratović, Dragana Bajović and Dušan Jakovetić and to Dr Mladen Kovačević for teaching me a lot about the fields of wireless communications and information theory and about research itself, and for their invaluable help and advice.

There are also many other people who have influenced my work and helped me in my career in various ways, and to whom I am deeply grateful, in the first place prof. Vlado Delić, prof. Vladimir Milošević and prof. Milan Narandžić. Special thanks are also due to Branka Stojković and to my friends and colleagues Đorđe Starčević, Vladimir Ostojić and Gorana Mijatović. Finally, I would like to thank all members of the Communications and Signal Processing Group at the Department of Power, Electronic and Telecommunication Engineering, for building

and maintaining such a stimulating and friendly environment. It has been a pleasure working with them.

I would also like to express my gratitude to the team at The Centre for IoT and Telecommunications with the University of Sydney, Australia, for their assistance. I would especially like to thank prof. Branka Vučetić, prof. Yonghui Li, Dr Mahyar Shirvanimoghaddam and Ms Rana Abbas.

Aleksandar Minja
Novi Sad
October 9, 2018

Rezime

Ova teza sadrži neke od rezultata autora dobijenih tokom njegovog postdiplomskog istraživanja u oblastima modelovanja komunikacionih sistema i teorije informacija i zaštitnog kodovanja. Rezultati su predstavljeni u matematičkom formatu i verifikovani su numeričkim simulacijama. Većina njih je motivisana problemima koji se pojavljuju prilikom razvoja i standradizacije 5G komunikacionih sistema i imaju veliki naučni i praktični značaj.

Ova disertacija je podeljena u dva dela. Prvi deo uvodi novi kvazianalitički postupak za estimaciju verovatnoće greške dekodera zaštitnih kodova. Matematički je pokazano i eksperimentalno potvrđeno da je novi simulacioni postupak značajno brzi od postojećih simulacionih postpupaka koji se koriste u praksi. U drugom delu teze predstavljen je problem konstrukcije višedimenzionalne trelis kodovane modulacije (eng. Trellis Coded Modulation - TCM) pomoću sferičnih kodova. Razvijen je novi algoritam za konstrukciju sferičnih kodova koji su prilagođeni strukturi TCM koda i pokazano je da takvi TCM kodovi imaju znatno bolje performanse od postojećih. Verovatnoća greške ovih novih TCM kodova je estimirana primenom simulacionog postupka koji je dat u prvom delu disertacije.

U nastavku navodimo najbitnije teorijske rezultate ove disertacije. Dokazi teorema i analize predstavljenih rezultata su detaljno opisani u samoj tezi.

Novi kvazianalitički simulacioni postupak

Prilikom dizajna, performansa komunikacionih sistema obično se izražava kao verovatnoća greške koja može biti definisana na nivou bita (eng. Bit Error Rate - BER) ili na nivou bloka (eng. Block Error Rate - BLER). U ovoj disertaciji razmatramo samo BLER. Verovatnoća greške se obično izražava kao funkcija odnosa-signal-šum (eng. signal-to-noise ratio - SNR) ili normalizovanog SNR (E_b/N_0). U praksi, verovatnoća greške ne može da se odredi analitički već mora da se estimira pomoću nekog simulacionog postupka. Osnovni postupak za estimaciju verovatnoće greške komunikacionog sistema jeste Monte Karlo metod (eng. Monte Carlo - MC). Velika mana MC metoda jeste veliki broj potrebnih uzoraka za estimaciju verovatnoće greške, posebno pri velikim SNR vrednostima. Klasičan postupak za ubrzavanje MC metoda jeste uzorkovanje po značajnosti (eng. Importance Sampling - IS). MC i IS metod koriste indikatorsku funkciju da sakriju rad dekodra, što daje veliku fleksibilnost ovih postupaka. Uvođenjem nekih pretpostavki o samom dekoderu, moguće je značajno ubrzati simulacioni postupak.

Da bismo razvili novi kvazianalitički simulacioni postupak, prvo uvodimo novi formalni model komunikacionog kanala - **geodezijski kanal**, koji objedinjuje veliki broj postojećih modela koji se često sreću u praksi i omogućava njihov zajednički tretman. Ovde spadaju binarni kanal sa brisanjem (eng. Binary Erasure Channel - BEC), binarni simetrični kanal (eng. Binary Symmetric Channel - BSC) i kanal sa belim aditivnim Gausovim šumom (eng. Additive White Gaussian Noise - AWGN).

Neka skup $\mathcal{Y}$ predstavlja prostor kanala (eng. channel space), a $\mathcal{C} \subseteq \mathcal{Y}$ predstavlja kod koji se koristi za prenos informacija kroz proizvoljni kanal. Kanal $\Omega : \mathcal{C} \to \mathcal{Y}$ jeste matematički model smetnje prilikom prenosa i obično je prikazan kao slučajno preslikavanje definisano uslovnom verovatnoćom $P[\boldsymbol{Y}|\boldsymbol{X}]$, gde $\boldsymbol{X} \in \mathcal{C}$ predstavlja sučajno odabranu kodnu reč, a $\boldsymbol{Y} = \Omega(\boldsymbol{X}) \in \mathcal{Y}$ predstavlja izlaz iz kanala. Dekoder je bilo koja funkcija $D : \mathcal{Y} \to \mathcal{C}$, koja zadovoljava $D(\boldsymbol{x}) = \boldsymbol{x}, \forall \boldsymbol{x} \in \mathcal{C}$.

Neka je data funkcija $d : \mathcal{Y} \times \mathcal{Y} \to \mathbb{R}$, koja za bilo koje vrednosti $\boldsymbol{x}, \boldsymbol{y}, \boldsymbol{z} \in \mathcal{Y}$ zadovoljava sledeće osobine:

1. $d(\boldsymbol{x}, \boldsymbol{y}) = d(\boldsymbol{y}, \boldsymbol{x})$
2. $d(\boldsymbol{x}, \boldsymbol{y}) \geq 0$, sa jednakošću akko $\boldsymbol{x} = \boldsymbol{y}$.
3. $d(\boldsymbol{x}, \boldsymbol{y}) + d(\boldsymbol{y}, \boldsymbol{z}) \geq d(\boldsymbol{x}, \boldsymbol{z})$ (nejednakost trougla).

Tada kažemo da je $d(\cdot)$ metrika, a $(\mathcal{Y}, d)$ metrički prostor. Ukoliko je za dati kanal Ω odlučivanje po maksimalnoj verodostojnosti ekvivalentno odlučivanju po minimalnom rastojanju, u odnosu na metriku $d(\cdot)$, tj.

$$\arg\max_{\boldsymbol{x} \in \mathcal{C}} P[\boldsymbol{Y} = \boldsymbol{y} | \boldsymbol{x}] = \arg\min_{\boldsymbol{x} \in \mathcal{C}} d(\boldsymbol{x}, \boldsymbol{Y} = \boldsymbol{y}), \ \forall \boldsymbol{x} \in \mathcal{C}, \forall \boldsymbol{y} \in \mathcal{Y}, \quad (1)$$

kažemo da su Ω i $d(\cdot)$ "upareni".

Geodezijski segment $\gamma_{[\boldsymbol{x}, \boldsymbol{y}]}$ jeste lokalno minimizujuća kriva, definisana kao preslikavanje $\gamma : [0, 1] \to \mathcal{Y}$, koja spaja tačke $\boldsymbol{x} \in \mathcal{Y}$ i $\boldsymbol{y} \in \mathcal{Y}$. Ako između bilo koje dve tačke u metričkom prostoru postoji geodezijski segment, kazemo da je $(\mathcal{Y}, d)$ geodezijski prostor.

Prirodna parametrizacija geodezijskog segmenta, definisana kao

$$d(\gamma(t_1), \gamma(t_2)) = \alpha |t_1 - t_2|, \ t_1, t_2 \in [0, 1], \ \alpha \in \mathbb{R}, \quad (2)$$

omogućava razvoj brzih algoritama pretrage zasnovanih na metodu polovljenja.

Sa ciljem razvoja brzih algoritama za simulaciju i zbog potrebe za zajedničkim tretmanom diskretnih i kontinualnih kanala, uvodimo novi formalni model komunikacionog kanala koji nazivamo **geodezijski kanal**.

Definicija 1. *Geodezijski kanal jeste bilo koji kanal* $\Omega : \mathcal{C} \subseteq \mathcal{Y} \to \mathcal{Y}$, *koji sadrži uparenu metriku* d, *takvu da* $(\mathcal{Y}, d)$ *čini geodezijski prostor.*

Oblast odlučivanja dekodera $\mathcal{D}_m \subseteq \mathcal{Y}$ koja pripada kodnoj reči $\boldsymbol{x}_m$ dat je izrazom

$$\mathcal{D}_m = \{\boldsymbol{y} \in \mathcal{Y} : D(\boldsymbol{y}) = \boldsymbol{x}_m\}. \quad (3)$$

Bitno je primetiti da $\mathcal{D}_m$ zavisi od koda $\mathcal{C}$, kanala Ω i algoritma za dekodovanje i može se promeniti ako se bilo koji od njih promeni.

Za dati kod $\mathcal{C} \subseteq \mathcal{Y}$ i odgovoarajući geodezijski kanal Ω, neka *zvezda domen dekoder* $D : \mathcal{Y} \to \mathcal{C}$ bude algoritam za dekodovanje, takav da svaki njegov region odlučivanja bude $\mathcal{D}_m$ predstavlja *metrički zvezda domen.*

Definicija 2. *Region odlučivanja $\mathcal{D}_m$ koji pripada kodnoj reči $\boldsymbol{x}_m \in \mathcal{C} \subseteq \mathcal{Y}$ jeste metrički zvezda domen ako i samo ako za svaki geodezijski segment $\gamma_{[\boldsymbol{x}_m, \boldsymbol{y}]}$, $\gamma(0) = \boldsymbol{x}_m$ i $\gamma(1) = \boldsymbol{y} \in \mathcal{D}_m$ važi*

$$\forall k \in [0,1] \Rightarrow \gamma(k) \in \mathcal{D}_m. \tag{4}$$

Odlučivanje po minimalnom rastojanju (eng. minimum distance decoder) i odlučivanje na osnovu poređenja sa pragom (eng bounded distance decoder) po definiciji su zvezda domen dekoderi. Mnogi dekoderi koji se danas koriste u praksi spadaju u ovu kategoriju. U drugom poglavlju je pokazano da su OSD (eng. Ordered Statistics Decoder) i PSCD (eng Polar Successive Cancellation Decoder) takođe zvezda domen dekoderi.

Za $\boldsymbol{x}_m \in \mathcal{C}$ i odgovarajući region odlučivanja $\mathcal{D}_m$, verovatnoća greške je data izrazom

$$P_{\mathrm{e}}^{(m)} = P[\boldsymbol{Y} \notin \mathcal{D}_m \mid \boldsymbol{x}_m]. \tag{5}$$

Verovatnoća greške koda $\mathcal{C}$ tada je definisana kao

$$P_{\mathrm{e}} = E[P_{\mathrm{e}}^{(m)}]. \tag{6}$$

Ukoliko su sve kodne reči jednako verovatne i ako je kod geometrijski uniforman (svi regioni odlučivanja su jednaki), važi

$$P_{\mathrm{e}} = \frac{1}{M} \sum_{m=1}^{M} P_{\mathrm{e}}^{(M)} = P_{\mathrm{e}}^{(M)}. \tag{7}$$

Sledi da se verovatnoća greške može definisati sa aspekta bilo koje kodne reči $\boldsymbol{x}_m = \boldsymbol{x}$, sa odgovarajućim regionom odlučivanja $\boldsymbol{x}_m = \boldsymbol{x}$ i $\mathcal{D}_m = \mathcal{D}$, kao

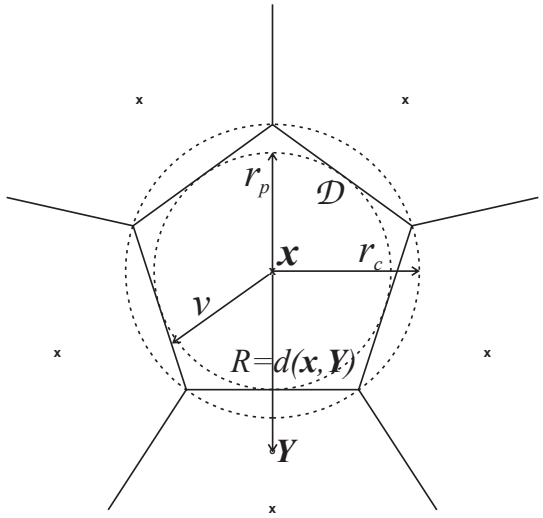

Slika 1: *Region odlučivanja $\mathcal{D}$ koji pripada kodnoj reči $\boldsymbol{x}$. Izlaz iz kanala $\boldsymbol{Y}$ nalazi se izvan regiona $\mathcal{D}$ što dovodi do greške dekodovanja. r_p je poluprečnik upisane sfere, a r_c poluprečnik opisane sfere. v - rastojanje između $\boldsymbol{x}$ i granice regiona $\mathcal{D}$.*

$$P_{\mathrm{e}} = P[\boldsymbol{Y} \notin \mathcal{D} \mid \boldsymbol{x}]. \tag{8}$$

Greška nastaje kada izlaz iz kanala $\boldsymbol{Y} = \Omega(\boldsymbol{x})$ ispadne izvan regiona odlučivanja koji pripada kodnoj reči $\boldsymbol{x}$. Uprošćeni izgled regiona odlučivanja prikazan je na slici 1. Slučajna promenljiva $R = d(\boldsymbol{x}, \boldsymbol{Y})$ predstavlja rastojanje između kodne reči i izlaza iz kanala, dok r_p i r_c predstavljaju poluprečnike upisane, odnosno opisane sfere. Za bilo koje $\boldsymbol{y} \in \mathcal{Y}$, uvek važi

$$\begin{aligned} d(\boldsymbol{x}, \boldsymbol{y}) \leq r_p &\Rightarrow \boldsymbol{y} \in \mathcal{D} \\ d(\boldsymbol{x}, \boldsymbol{y}) > r_c &\Rightarrow \boldsymbol{y} \notin \mathcal{D}. \end{aligned} \tag{9}$$

Za svaki geodezijski segment $\gamma_{[\boldsymbol{x},\boldsymbol{y}]}$, $\gamma(0) = \boldsymbol{x}$ i $\gamma(1) = \boldsymbol{y} \notin \mathcal{D}$, postoji

najdalja tačka (eng. distance point) $\boldsymbol{z} = \gamma(k^*) \in \mathcal{D}$ koja je najdalja od $\boldsymbol{x}$ (u odnosu na rastojanje d), sa osobinom

$$\boldsymbol{z} = \underset{d(\boldsymbol{x},\gamma(k))}{\arg\max}\{k \in [0,1] : \gamma(k) \in \mathcal{D}\}. \tag{10}$$

Neka je $\boldsymbol{Z}$ slučajna *najdalja tačka*. Tada se verovatnoća greške u odnosu na realizaciju $\boldsymbol{Z} = \boldsymbol{z}$ može definisati kao

$$P_{\mathrm{e}}(\boldsymbol{z}) = P[R > d(\boldsymbol{x}, \boldsymbol{Z}) | \boldsymbol{Z} = \boldsymbol{z}]. \tag{11}$$

Sledi da je verovatnoća greške koda data izrazom

$$P_{\mathrm{e}} = E_{\boldsymbol{Z}}[P_{\mathrm{e}}(\boldsymbol{Z})] = P[R > V], \tag{12}$$

gde je $V = d(\boldsymbol{x}, \boldsymbol{Z})$ pomoćna slučajna promenljiva koja predstavlja rastojanje između kodne reči i slučajne najdalje tačke.

Teorema 3. *Verovatnoća greške zvezda domen dekodera definisana je izrazom*

$$P_e = E_V[\overline{F}_R(V)] = E_R[F_V(R)]. \tag{13}$$

Sledi da se verovatnoća greške može estimirati pomoću izraza

$$\widehat{P}_{\mathrm{e}}^{\,\mathrm{QA}} = \frac{1}{J}\sum_{j=1}^{J} \overline{F}_R(v_j), \tag{14}$$

gde J predstavlja unapred definisani broj potrebnih merenja. Ovo je kvazianalitički (eng. Quasi-Analytical - QA) postupak za estimaciju verovatnoće greške zato što se šum ne simulira već se računa analitički preko funkcije $\overline{F}_R(\cdot)$. Procena verovatnoće greške ne zavisi od varijanse šuma, već samo od izmerenog rastojanja v, i može da se preračuna za različite vrednosti SNRa.

Teorema 4. *Varijansa QA estimatora ograničena je sa gornje strane izrazom*

$$Var[\widehat{P}_e^{\,QA}] \leq \frac{1}{J} P_e \overline{F}_R(r_p) \tag{15}$$

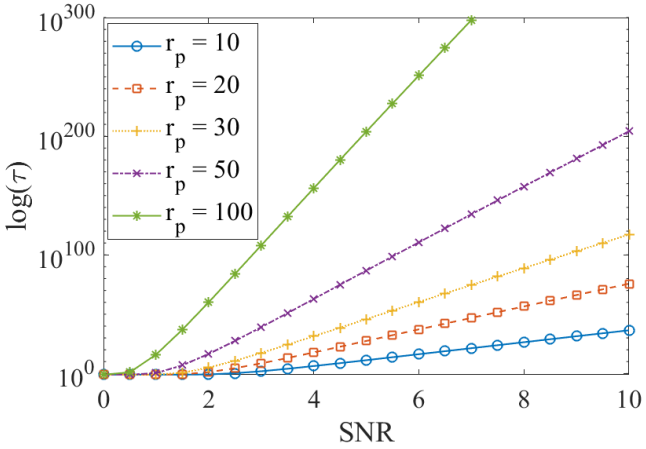

Slika 2: *Ubrzanje kao funkcija SNRa za slučaj BSC kanala i dužinu koda* $N = 512$.

Ubrzanje našeg QA postupka u odnosu na MC metod (pri estimaciji verovatnoće greške P_{e} uz odstupanje δ) data je izrazom

$$\tau = \frac{\mathscr{T}_{\mathrm{MC}}(\delta, P_{\mathrm{e}})}{\mathscr{T}_{\mathrm{QA}}(\delta, P_{\mathrm{e}})} = \mathcal{O}\left(\frac{1}{\overline{F}_R(r_p)\log_2 N}\right). \tag{16}$$

Slike 2. i 3. prikazuju ubrzanje QA postupka u odnosu na MC metod za slučaj BSC kanala i dužinu koda $N = 512$. Slika 2. prikazuje ubrzanje kao funkciju SNRa, dok je r_p fiksan, dok Slika 3. prikazuje ubrzanje kao funkciju r_p za razne vrednosti SNRa.

Ukoliko se koristi dekoder sa grubim odlučivanjem za prenos podataka kroz diskretni kanal, verovatnoća greške 13 može da se napiše u obliku sume

$$P_{\mathrm{e}} = \sum_{v=r_p}^{r_c} p_V(v)\overline{F}_R(v), \tag{17}$$

gde $p_V(\cdot)$ predstavlja funkciju raspodele slučajne promenljive V. U

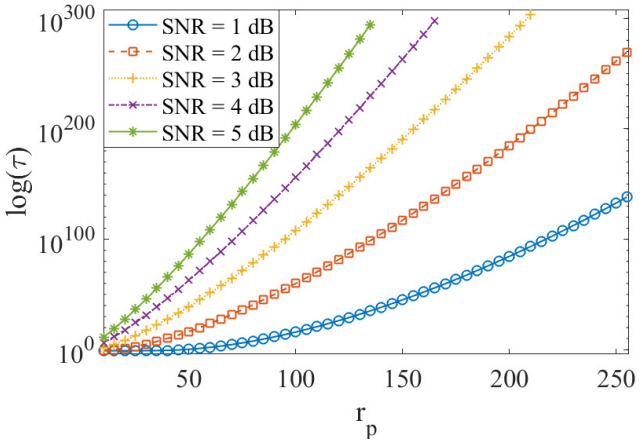

Slika 3: *Ubrzanje kao funkcija r_p za slučaj BSC kanala i dužinu koda $N = 512$.*

ovom slučaju QA estimator (14) može da se napiše kao

$$\widehat{P}_{\mathrm{e}}^{\mathrm{QA}} = \sum_{v} \overline{F}_R(v)\widehat{p}_V(v), \tag{18}$$

gde $\widehat{p}_V(\cdot)$ predstavlja funkciju raspodele nepoznatu slučajne promenljive V koju je potrebno estimirati.

Teorema 5. *Za diskretni kanal i dekoder sa grubim odlučivanjem, varijansa estimatora je deinisana izrazom*

$$Var[\widehat{P}_e^{QA}] = \sum_{v} \overline{F}_R^2(v)\,\frac{p_V(v)(1-p_V(v))}{J}. \tag{19}$$

Teorema 6. *Za diskretni kanal i dekoder sa grubim odlučivanjem, broj simulacija J potrebnih za dostizanje tačnosti δ ograničen je sa gornje strane izrazom*

$$J \le \frac{1}{\delta^2}\sum_{v}\frac{1-p_V(v)}{p_V(v)}. \tag{20}$$

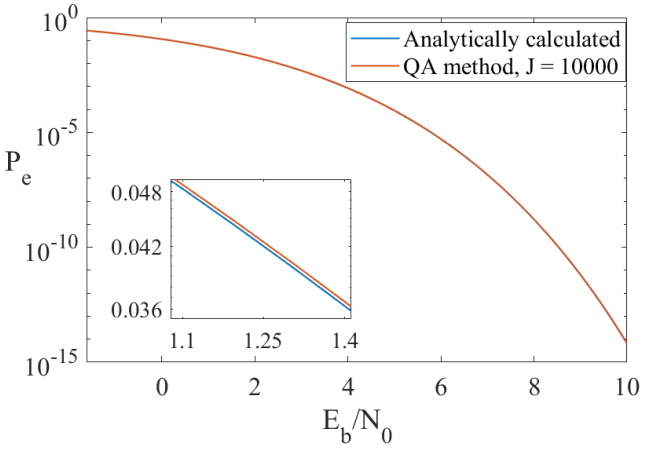

Slika 4: *QA estimirana i analitički izračunata verovatnoća greške RM(1, 5) koda za prenos kroz BSC kanal.*

Slika 4. prikazuje QA estimiranu i analitički izračunatu verovatnoću greške za primer BSC kanala i RM(1, 5) koda.

U poglavlju pet dati su numerički rezultati. Naš QA postupak poređen je sa MC i IS metodima po pitanju tačnosti i brzine za slučaj AWGN i BSC kanala. Rezultati jasno pokazuju da je novi QA postupak za istu tačnost bar 10^3 puta brži od MC metoda, a bar 10 puta brži od IS metoda.

TCM dizajn pomoću sferičnih kodova prirpemljenih za podelu skupa

Trelis kodovana modulacija (eng. Trellis Coded Modulation - TCM), kao što i samo ime kaže, kombinuje zaštitno kodovanje i modulaciju i time značajno povećava spektralnu efikasnost digitalnog prenosa. Glavna ideja TCMa jeste da se maksimizuje kvadratno Euklidsko rastojanje između sekvenci modulacionih simbola, umesto Hemingovog rastojanja,

sto je bio slučaj kod klasičnog zaštitnog kodovanja.

Obično se za TCM koriste 1D i 2D modulacije, ali napredak u MIMO i optičkim komunikacijama omogućava korišćenje 3D i 4D modulacija (i njihovih umnožaka). TCM zasnovan na ovim modulacijama naziva se višedimenzionalni TCM.

Konstelacija je algebarska reprezentacija skupa modulacionih signala (eng. modulation signal space). Konstelacija N-dimenzionalne modulacije predstavlja konačan skup ($\mathcal{C} \subset \mathbb{R}^N$) N-dimenzionalnih vekora (modulacioni simboli ili tačke konstelacije), a veličina konstelacije, $M = |\mathcal{C}|$, predstavlja broj tačaka u skupu. Rastojanje između dve tačke $\boldsymbol{x}_i$, $\boldsymbol{x}_j \in \mathcal{C}$ $(i \neq j)$ definisano je kao

$$d_{i,j} = \|\boldsymbol{x}_i - \boldsymbol{x}_j\|, \tag{21}$$

dok je minimalno rastojanje u konstelaciji

$$d_{\min} = \min_{i \neq j} d_{i,j}. \tag{22}$$

Konstelacija $\mathcal{C}(M, N)$, gde svi N-dimenzionalni vektori imaju jediničnu normu (tačke leže na površini sfere) naziva se sferični kod. Problem konstrukcije sferičnih kodova ekvivalentan je problemu raspoređivanja tačaka na površini sfere i najčešće se koristi Metod promenljive odbojne sile (eng. Variable Repulsion Force Method), gde se tačke na sferi modeluju generalizovanim elektronima koji se odbijaju. Sledi klasičan optimizacioni problem za konstrukciju sferičnih kodova

Optimizacioni problem 1 *Minimizacija ukupnog potencijala*

$$\begin{aligned} &\text{minimizuj} \quad V = \sum_{i<j} V_{ij}^{\beta-2} \\ &\text{tako da} \qquad \|\boldsymbol{x}_i\| = 1;\ i = 1, \ldots, M. \end{aligned} \tag{23}$$

V_{ij} predstavlja potencijal između tačaka $\boldsymbol{x}_i$ i $\boldsymbol{x}_j$ i definisan je kao

$$V_{ij} = \frac{\gamma}{\|\boldsymbol{x}_j - \boldsymbol{x}_i\|}. \tag{24}$$

V predstavlja ukupan potencijal generalizovanih elektrona koji se odbijaju pod dejstvom centralne sile. Konstanta γ služi da bi se izbegli problemi prilikom numeričkog izračunavanja, i obično se bira da bude

$$\gamma = \min_{i\in\{1,\dots,M\}\setminus\{j\}} \|\boldsymbol{x}_j - \boldsymbol{x}_i\|. \tag{25}$$

Centralna ideja TCMa jeste tzv. podela skupa (eng. set partitioning), gde se tačke u konstelaciji dele u podskupove sa ciljem povećavanja minimalnog rastojanja unutar podskupa. Obično se polazi od postojećeg koda koji ima dobro minimalno rastojanje i zatim se pravi podela skupa. Ovi skupovi se zatim dodeljuju granama u TCM trelisu.

U poglavlju 7 predložen je optimizacioni problem za generisanje sferičnih kodova, sa ciljem raspoređivanja tačaka na površini sfere tako da se

1. maksimizuje minimalno euklidsko rastojanje između tačaka unutar jednog podskupa,
2. maksimizuje minimalno euklidsko rastojanje između podskupova.

Optimizacioni problem 2 *Optimizovana podela skupa*

$$\begin{aligned} \text{minimizuj} \quad & V = (1-\lambda)\sum_{i<j}\left(V_{ij}(\alpha_1)\mathbb{1}_{\mathcal{X}_i}(\boldsymbol{x}_j)\right)^{\beta} \\ & \qquad +\lambda\sum_{i<j}\left(V_{ij}(\alpha_2)\overline{\mathbb{1}}_{\mathcal{X}_i}(\boldsymbol{x}_j)\right)^{\beta} \\ \text{tako da} \quad & \|\boldsymbol{x}_i\| = 1;\ i = 1,\dots,M. \end{aligned} \tag{26}$$

$$V_{ij}(\alpha) = \frac{\gamma}{\alpha\|\boldsymbol{x}_j - \boldsymbol{x}_i\|},\ \alpha = \begin{cases} \alpha_1, & \mathbb{1}_{\mathcal{X}_i}(\boldsymbol{x}_j) = 1 \\ \alpha_2, & \text{otherwise} \end{cases}. \tag{27}$$

Indikatorska funkcija $\mathbb{1}$ (i njen komplement $\overline{\mathbb{1}}$) proverava da li tačke pripadaju istom podskupu, a α_1, α_2 ($\alpha_2 > \alpha_1$) i λ predstavljaju optimizacione konstante.

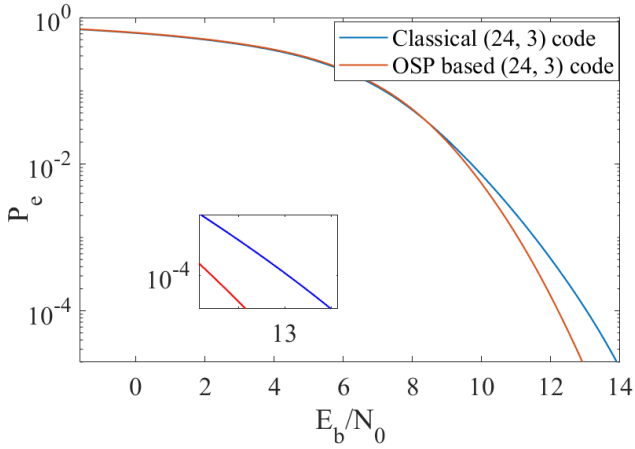

Slika 5: *QA estimacija BLERa za dva (24, 3) sferična koda*

Ovaj problem je rešen primenom metoda promenljive odbojne sile, a sam postupak nazivamo optimizovana podela skupa (eng. Optimized Set Partitioning - OSP).

Pomoću OSP algoritma, konstruisani su novi 3D sferični kodovi sa $M = 12, 16$ i 24. Primećeno je da novi sferični kodovi, iako slabiji od najboljih klasičnih sferičnih kodova (kodovi sa dobrim minimalnim rastojanjem), u kombinaciji sa TCMom postižu bolje performanse, čak i do $1dB$ (Slika 5).

Abstract

This thesis contains some of the results obtained by the author in the course of his postgraduate research in the fields of Communication system modeling and Information and coding theory. The results are presented in mathematical form and are verified by numerical simulations. Most of them are motivated by challenges arising in the design and standardization of 5G communication systems and are of practical and scientific relevance.

Evaluating the error rate of a digital communication system is usually done using the Monte Carlo simulation method. The Monte Carlo method is an unbiased estimator that is independent of the channel model or the decoding algorithm. The main drawback of the Monte Carlo method is the need of a huge sample size for estimating low error rates. Other methods commonly used are the importance sampling technique and the quasi-analytical method. Both Monte Carlo and importance sampling methods use the indicator function to hide the details of the decoding algorithm used. It is possible to achieve significant improvements by taking into account the structure of the decoder and the decoding region.

In the first part of this thesis we first introduce the *geodesic channel model* (a generalization of a vast number of commonly used channels, including BSC, BEC and AWGN channel) and the *metric star domain decoder*. We show that many practical decoders like the ordered statis-

tics decoder and the polar successive cancellation decoder have a *star domain* decision region. Finally, we introduce a novel SNR-invariant quasi-analytical technique for estimating the error rate of a communication link over the geodesic channel. We compared this technique to the Monte Carlo and Importance Sampling methods and it has been found out that it outperforms other methods in both accuracy and speed. It is shown that our quasi-analytical method is at least 10^3 times faster than MC and 10 times faster than IS for the same accuracy.

Trellis coded modulation (TCM) is a modulation technique that uses ideas from channel coding theory (specifically from convolutional/trellis codes) in order to improve the reliability of a digital transmission system without compromising bandwidth efficiency. The key idea of TCM is *set partitioning* in which an existing modulation (e.g. a spherical code with a good minimum distance) is partitioned into sets that are then mapped onto a trellis. This approach is not necessarily optimal.

In the second part of the thesis we introduce an optimization procedure, based on the variable force repulsion method, for the design of spherical codes that are tailored to the TCM and achieve lower error rates at high SNR, then their counterparts that are optimized for minimum distance. We call this approach *TCM design by optimized set partitioning*. The performance of these codes is verified using the method developed in part I of this thesis which is suitable for simulating error rates at high SNR.

List of Figures

1.1 URLLC service requirements 2

2.1 Examples of star domain sets 16
2.2 Octahedron code 17
2.3 Algorithmic Complexity of OSD 19
2.4 Tree structure of an (8, 4) polar code 23
2.5 Decoding region of the octahedron code 25

4.1 Decoding region and the channel output 34
4.2 Calculating the error probability of the RM(1,5) code . . 37
4.3 QA speedup over the MC method 40
4.4 Decoding region of the bounded distance decoder 43
4.5 QA Estimator accuracy as a function of measured distances 50
4.6 QA Estimator accuracy as a function of E_b/N_0 51
4.7 QA estimated and Analytical BLER 52

5.1 QA estimated BLER of Polar Codes 56
5.2 QA estimated BLER of RM(1,5) Code 56
5.3 BLER comparison for (256,128) polar code 57
5.4 BLER comparison for (127,8,31) BCH code 58

6.1 Icosahedron code 66
6.2 Set Partitioning of an 8-PSK modulation 70
6.3 Set Partitioning of the icosahedron code 71
6.4 TCM encoder 73
6.5 Trellis representation of TCM 73

7.1 Set partitions of icosahedron and cuboctahedron cdoes . 79
7.2 Set partitions of two (16,3) spherical codes 80
7.3 Set partitions of two (24,3) spherical codes 81
7.4 QA estimated BLER of (12,3) spherical codes 81
7.5 QA estimated BLER of (16,3) spherical codes 82
7.6 QA estimated BLER of (24,3) spherical codes 82

List of Tables

2.1 List of octahedron codewords 17

5.1 Simulation Run time comparison of (N,K) Polar Codes . 55
5.2 Simulation Run time comparison of RM(1,5) Code . . . 55
5.3 Simulation Run time comparison of (N,K,T) BCH Codes 55

7.1 Distance gain 79

Chapter 1
Introduction and Motivation

This chapter provides an overview of the thesis structure and the summary of its contributions. The current state of the art of 5G communication systems is given and main design problems are presented. The thesis is divided into two parts. In the first part we introduce a novel quasi-analytical technique for estimating the error rate performance of a communication link over the *geodesic channel* (a generalization of a vast number of commonly used channels, including BSC, BEC and the AWGN channel). The second part describes a new algorithm for designing spherical codes *optimized for set partitioning*. The error rate performance of these codes is estimated using the algorithm described in the first part of the thesis. The mathematical notation is provided at the end of this chapter.

Novel Quasi-Analytical Simulation Method

The third generation partnership project (3GPP) has defined three main service categories in 5G – enhanced mobile broadband (eMBB), massive machine-type communication (mMTC) and ultra reliable low latency communication (URLLC) [1–3]. The eMBB category is designed for services with high bandwidth requirements (e.g. virtual reality, augmented reality, high-resolution video streaming, etc). The mMTC category supports a massive number of Internet of Things (IoT) devices, which are only sporadically active and send small data payloads [4, 5]. The most innovative feature brought in 5G is the URLLC cate-

gory [3, 6, 7], which focuses on delay sensitive services and applications (see Fig. 1.1) like factory automation, tele-surgery, smart grid, tactile internet and many others, some of which are yet unknown [1, 2, 6, 8].

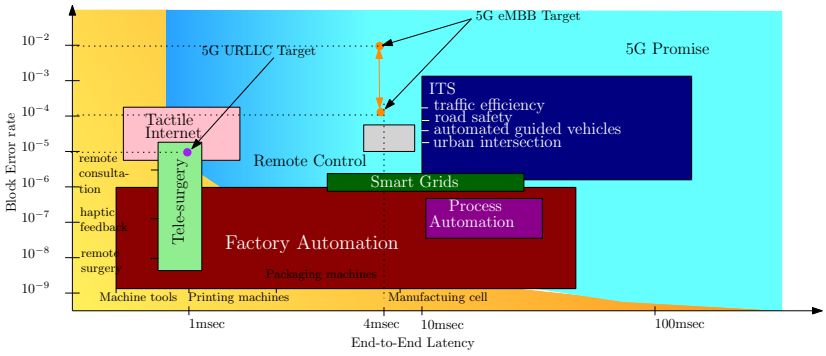

Figure 1.1: *Latency reliability requirement for different URLLC services [1].*

It is clear that URLLC should satisfy two conflicting requirements: ultra-low latency and ultra-high reliability. The most promissing approach is to use short packets to reduce latency which in turn causes a severe loss in coding gain. It is possible to enhance reliability by using different retransmission techniques [9–11] and feedback [12–14], but this will significantly increassy lattency. Alternatively, the system bandwidth should be widened, which is not always possible. The second part of this thesis will present a technique for better spectrum utilization. It has been clearly specified that channel coding for URLLC should be further studied, especially for information blocks of less than 1000 bits [1, 15]. This has reopened the interest in short and medium blocklength code design [1, 16–18] and the corresponding decoding algorithms. Due to short-block length regime, maximum likelihood (ML) and near maximum likelihood decoders like ordered statistics decoder (OSD) [19,20] are also being considered for future applications [1,16,17]. It is well known that feedback does not improve the capacity of a discrete memoryless channel [21], but it can improve its error expo-

nent [22, 23]. Variable-length codes with a short average blocklength, that rely on incremental redundancy (controlled using feedback) have been shown to achieve a rate near capacity [14, 24]. Variable-length codes with incremental redundancy *without feedback*, introduced in [25], show good error performance with low latency.

Machine-type communication systems require the use of low cost and power efficient hardware to connect many devices and sensors and provide URLLC between them [26] in order to support future applications like reliable remote links, production automation, autonomous driving and many others. With these applications in mind, different coding schemes are being investigated and compared in terms of error performance and encoding/decoding complexity [1, 16–18]. Error performance is usually mesaured as bit error rate (BER) or block error rate (BLER) and is usually presented as a function of signal-to-noise ratio (SNR), or more commonly of bit SNR: energy per bit to noise power spectral density ratio (E_b/N_0) [27].

In general, error rate is hard to calculate analytically but it can be estimated. It is of paramount importance to find a fast and accurate simulation method which will allow the comparison of coding and decoding algorithms (in terms of error performance) for these future applications. It can be seen in Fig. 1.1 that tele-surgery and factory automation have the strictest requirements of 1ms end-to-end latency and BLER as low as 10^{-9}. Other services such as smart grids and process automation have more relaxed requirements (latency of 10ms and more, and BLER between 10^{-3} and 10^{-6}). As 3GPP defines a minimal success probability of $1 - 10^{-5}$ of transmitting a layer 2 protocol data unit [28, 29] for mission critical URLLC demands, in this thesis we concentrate only on the BLER, where generalization to BER is straightforward.

The basic method for simulating the error performance of communication systems is the Monte Carlo (MC) method. Monte Carlo refers to a broad class of computational algorithms that rely on repeated random sampling to obtain numerical results. The MC method is an

unbiased estimator, but it requires a huge sample size to achieve certain efficiency [30–34].

One of the most efficient ways to speed up the MC method is to use the Importance Sampling (IS) technique. The IS technique is a general variance reduction technique for estimating properties of the original distribution while samples are being generated from some other biased distribution. IS techniques have attracted a lot of attention over the years. A number of sub-optimal solutions have been proposed [32, 35, 36]. A minimum variance IS technique for linear codes over the Binary Symmetric Channel (BSC) is presented in [37]. An SNR invariant IS technique was first presented in [38, 39] and later in [40]. It is possible to achieve significant improvements over [38, 40] by introducing the so-called dummy simulations so that the total variance of the estimator becomes much lower in the high SNR region [39]. A detailed theoretical background of various IS techniques is given in [30–34].

Simulations in which only some input processes are simulated explicitly, while the effects of other processes are handled using analytical techniques, are called quasi-analytical (QA) or semi-analytical (SA). QA methods usually assume existence of some a priori knowledge that can be evaluated analytically and this allows for simulation speedup. There is no unique QA method [31], and the best combination of simulation and analysis is generally problem dependent, [30, 41–44].

Other methods used for simulating communication systems include tail extrapolation [30, 31] and extreme-value theory [30, 45]. These methods provide a good indicator of the error rate trend but are less accurate at high SNR and therefore are not applicable for our use case.

Our main result in this part of the thesis is the establishment of a novel QA method which is shown to outperform the MC and IS method in both run time and accuracy. The main contributions are as follows:

- introduction and definition of the geodesic channel model and the metric star domain decoder,
- proof that the OSD and the polar successive decoder (PSCD) are

metric star domain decoders,

- establishment of a novel QA method for estimating the error rate of a communication system with a star domain decoder and a general algorithm for performing the simulation.

Furthermore we also give a detailed theoretical analysis of the proposed QA method and provide illustrative numerical examples of the given algorithm.

We show that two most frequently used channels, additive white Gaussian noise (AWGN) and binary symmetric channel (BSC) are geodesic, and compare the results of our QA method with the MC and IS simulation methods over them.

In Chapter 2 we introduce the *geodesic channel model* and show that the binary erasure channel (BEC) [46] falls into this category. Given a geodesic channel model we define a *metric star domain* decoder and show that many popular decoders fall into this category. Ordered statistics decoder (OSD) is considered for future URLLC applications as it allows for complexity/reliability trade off [1]. Polar codes [47, 48] are the first codes with explicit construction to provably achieve the channel capacity for the symmetric binary-input, discrete, memoryless channels. PSCD is a low complexity decoder with good error performances at long blocklengths and with no error-floor [48–51]. Several modifications of the PSCD were proposed to improve the short and medium length performance of polar codes [52,53], which makes them suitable for many mMTC applications [54–59]. We give explicit proof that both the OSD and the PSCD are star domain. Finally we give the formula for the error probability of a metric star domain decoder that will be used throughout the thesis.

In Chapter 3 we will give a general simulation framework for estimating the error rate of a communication link. We will also introduce the accuracy of the estimator and give two metrics for calculating the accuracy, namely the estimated relative precision and the average relative error. We finish this chapter with a detailed description of the MC

and IS techniques and give some notes on their implementation.

Our main results are presented in Chapter 4. We first introduce a QA procedure for the general geodesic channel model. Unlike the MC and IS method, where we estimate the error probability for one SNR value, our QA method is SNR invariant. We will give a more specific mathematical interpretation of the error probability with respect to a metric star domain decoder and comment on it. We will also derive the upper bound on the variance of our QA method using the Edmundson-Madansky inequality, which will allow us to express the time complexity of the proposed method. We show that both AWGN and BSC are a special case of the geodesic channel model, and give details on implementing the QA method for the discrete and continuous case. We conclude this chapter with an analysis of the proposed QA method.

Chapter 5 concludes Part I of the thesis. We will demonstrate our QA method for the case of the AWGN and the BSC and compare it to the MC and IS methods in terms of accuracy and speed. Some comments about future work is given at the end of this chapter.

The results presented in Part I of the thesis are based on the following works:

- M. Shirvanimoghaddam, M. Sadegh Mohamadi, R. Abbas, A. Minja, C. Yue, B. Matuz, G. Han, Z. Lin,Y. Li, S. Johnson, B. Vucetic, "Short Block-length Codes for Ultra-Reliable Low-Latency Communications," *IEEE Commun. Magazine* accepted for publication.

- A. Minja and V. Šenk, "Quasi-Analytical Simulation Method for estimating the Error Probability of Star Domain Decoders,", submitted for publication.

- A. Minja, I. Stanojevic and V. Šenk, "Novel quasi-analytical simulation method for estimating the error probability in AWGN channel," *37th Conference on TSP.*, pp. 1–5 , Jul. 2014.

- A. Minja, I. Stanojevic and V. Šenk, "Novel quasi-analytical simulation method for estimating the error probability over the BSC" *38th Conference on TSP.*, pp. 309–313, Jul. 2015.

TCM Design by Optimized Set Partitioning

As was descirbed in the previous section, emerging technologies, such as 5G cellular networks and millimeter wave communications, internet of things [8, 60], and visible light communications [61], and the ever increasing data transfer require better spectrum utilization and higher user throughput for short length communications.

In fiber-optic communication systems a coherent receiver maps the optical signal to the electrical domain and in so enables the detection of all four quadratures of the optical signal (in-phase and quadrature-phase components of the two orthogonal polarizations) [62, 63]. In order to achieve better spectral efficiency (to fully utilize the available spectrum) a four dimensional (4D) modulation is used [63–65]. Recent advances in orbital angular momentum (OAM) for free-space optical and radio-wave communications demonstrated that OAM can benefit the transmission with very high spectrum efficiency [66–68]. It was shown in [69, 70] that in a wireless communication system with circular phased arrays OAM mode can be considered as an additional dimension of the modulation constellation, which results in a 3D multilevel modulation. It is possible to further expand the number of dimensions by using multiple transmitters coupled with a single-point detector, multiple time slots or even multiple wavelengths in the case of optical communications.

Trellis coded modulation (TCM) [64,65,69–75] combines coding and modulation techniques for digital transmission, so as to achieve significant coding gains over conventional uncoded modulations without compromising bandwidth efficiency. The main idea of TCM is to partition the modulation signal set into subsets in such a way as to increase

the Euclidean distance inside a subset (set partitioning), rather then to increase the Hamming distance between the codewords, as was accomplished with conventional coding alone. At high signal-to-noise ratio (SNR) the error probability is completely characterized by the minimum Euclidean distance between members of a subset. We will call this distance *intra-partition* distance. Classical TCM design uses an existing constellation which is partitioned into subsets. This approach is not necessarily optimal. TCM design based on combining 2D constellations into higher-dimensional constellations was presented in [64, 65, 70] and a heuristic approach based on small 3D spherical codes was investigated in [75]

The main contribution of this part of the thesis is the development of an optimization method for designing a spherical code [76] optimized for set partitioning by optimizing the intra-partition distance (rather then the minimum distance) of the modulation constellation. This method is tailored to the TCM and achieves lower error rate at high SNR, compared to the classical modulation schemes. An iterative algorithm, based on the variable repulsive force method [77, 78] is presented and evaluated. Recent advances in spherical code design allow for fast implementation of the proposed algorithm on dedicated hardware [78].

In Chapter 6 we introduce multidimensional modulations and spherical codes - a multidimensional generalization of the phase shift keying (PSK) modulation. We present the problem of finding good spherical codes and give an overview of existing procedures for designing them. We conclude this chapter with a short overview of the TCM technique with emphasis on encoding and decoding algorithms.

In Chapter 7 we develop the Optimized Set Partitioning algorithm for designing spherical codes that are tailored to the TCM. We compare codes that are generated using our algorithm to classical spherical codes that correspond to densest packings, and show that it is possible to achieve a modest but crucial coding gain over best known codes. We conclude this chapter with numerical results, followed by a short

discussion and an overview of future work.

The results presented in Part II of the thesis are based on the following works:

- A. Minja and V. Šenk, "Coded Modulation Design by Optimized Set Partitioning,",
  in preparation
- A. Minja, I. Stanojevic and V. Šenk, "TCM Design Optimizing set partitioning of 3-dimensional spherical codes," *21st TELFOR*, pp. 373–376 , Nov. 2013.

Notation

Throughout the thesis, uppercase letters represent random variables, lowercase letters represent realizations of the corresponding random variables, uppercase bold letters represent random points in a metric space and lowercase bold letters represent their realization. In the case of a normed vector space, the i-th component of a vector $\boldsymbol{x}$ is denoted x_i and $\|\boldsymbol{x}\|$ represents the 2 - norm of $\boldsymbol{x}$. $p_X(\cdot)$ represents both the probability density function and the probability mass function of a random variable X and $F_X(\cdot)$ and $\overline{F}_X(\cdot) = 1 - F_X(\cdot)$ are used to denote the corresponding cumulative distribution function and the tail distribution function respectively. $P[\cdot]$ represents the probability of an event, $E[\cdot]$ represents the mean of a random variable and $\mathrm{Var}[\cdot]$ represents the variance of a random variable. Cursive uppercase letters represent sets (or their subsets), and $\mathcal{A}^N$ represents the set of all N-tuples of a set $\mathcal{A}$. Sometimes a set will be defined only by its elements, i.e $\{a_1, a_2, \ldots a_N\}$. Given a set $\mathcal{C}$ and $\boldsymbol{x}_i \in \mathcal{C}$, let $\mathcal{X}_i$ be a subset of $\mathcal{C}$, such that $\boldsymbol{x}_i \in \mathcal{X}_i$ ($\boldsymbol{x}_i \in \mathcal{X}_i \subset \mathcal{C}$). For convenience, $\overline{\mathbb{1}}_{\mathcal{A}}(\mathbf{a}) = 1 - \mathbb{1}_{\mathcal{A}}(\mathbf{a})$ represents the inverse indicator function and $\overline{\mathbb{1}}_{\mathcal{A}}(\mathbf{a}) = 0$ if $\mathbf{a} \in \mathcal{A}$ and $\overline{\mathbb{1}}_{\mathcal{A}}(\mathbf{a}) = 1$ if $\mathbf{a} \notin \mathcal{A}$.

Part I

Novel Quasi-Analytical Simulation Method

Chapter 2

System Model

In this chapter we introduce the geodesic channel model and argue that many important models like the BEC are a special case of the geodesic channel. We define the metric star domain decoder and show that many common decoders like the Berlekamp-Massey algorithm, the OSD and the PSCD fall into this category. Finally we give a formula for calculating the error probability of a star domain decoder that will be used throughout this thesis.

2.1 Geodesic Channel Model

Given the channel space $\mathcal{Y}$, and some code $\mathcal{C} \subseteq \mathcal{Y}$, an arbitrary channel $\Omega : \mathcal{C} \to \mathcal{Y}$ is a random mapping defined by a conditional probability $P[\boldsymbol{Y}|\boldsymbol{X}]$, where $\boldsymbol{X} \in \mathcal{C}$ is a random codeword and $\boldsymbol{Y} = \Omega(\boldsymbol{X}) \in \mathcal{Y}$ is the channel output. We define the decoder as any mapping $D : \mathcal{Y} \to \mathcal{C}$, that satisfies $D(\boldsymbol{x}) = \boldsymbol{x}, \forall \boldsymbol{x} \in \mathcal{C}$.

Let $(\mathcal{Y}, d)$ be a metric space with a metric (distance function) $d : \mathcal{Y} \times \mathcal{Y} \to \mathbb{R}$, such that for any $\boldsymbol{x}, \boldsymbol{y}, \boldsymbol{z} \in \mathcal{Y}$:

1. $d(\boldsymbol{x}, \boldsymbol{y}) = d(\boldsymbol{y}, \boldsymbol{x})$

2. $d(\boldsymbol{x}, \boldsymbol{y}) \geq 0$, with equality if and only if $\boldsymbol{x} = \boldsymbol{y}$.

3. $d(\boldsymbol{x}, \boldsymbol{y}) + d(\boldsymbol{y}, \boldsymbol{z}) \geq d(\boldsymbol{x}, \boldsymbol{z})$ (triangle inequality).

If the maximum likelihood (ML) [1] decoding on Ω coincides with the minimum distance (MD) decoding with respect to d, Ω and d are said to be *matched* [79], or more precisely

$$\arg\max_{\boldsymbol{x}\in\mathcal{C}} P[\boldsymbol{Y}=\boldsymbol{y}|\boldsymbol{x}] = \arg\min_{\boldsymbol{x}\in\mathcal{C}} d(\boldsymbol{x},\boldsymbol{Y}=\boldsymbol{y}),\ \forall \boldsymbol{x}\in\mathcal{C}, \forall \boldsymbol{y}\in\mathcal{Y}. \tag{2.1}$$

A curve ξ in a metric space $(\mathcal{Y},d)$ is a continuous mapping $\xi : [0,1]\to\mathcal{Y}$, from the interval $[0,1]$ into $\mathcal{Y}$. The length $L(\xi)\in[0,\infty]$ of ξ is defined by [80]

$$L(\xi) = \sup\sum_{i=1}^{n} d\left(\xi(t_i),\xi(t_{i-1})\right),\ n\in\mathbb{N}, t_0=0, t_n=1, \tag{2.2}$$

where the supremum is taken over all $n\in\mathbb{N}$ and all partitions $\{t_0,t_1,...,t_n\}$ of $[0,1]$.

Metric space $(\mathcal{Y},d)$ is called a length space if for any curve $\xi : [0,1]\to\mathcal{Y}$, with $\xi(0)=\boldsymbol{x},\xi(1)=\boldsymbol{y}\in\mathcal{Y}$, the following holds true

$$d(\boldsymbol{x},\boldsymbol{y}) = \inf L(\xi). \tag{2.3}$$

Given a length space $(\mathcal{Y},d)$, a geodesic segment $\gamma_{[\boldsymbol{x},\boldsymbol{y}]}$, from $\boldsymbol{x}\in\mathcal{Y}$ to $\boldsymbol{y}\in\mathcal{Y}$ is locally the shortest metric curve ($\gamma:[0,1]\to\mathcal{Y}$, with $\gamma(0)=\boldsymbol{x}$ and $\gamma(1)=\boldsymbol{y}$) between $\boldsymbol{x}$ and $\boldsymbol{y}$. If any two points of $\mathcal{Y}$ are joined by a geodesic segment, $(\mathcal{Y},d)$ is called a *geodesic metric space* [80,81]. Note that a geodesic segment $\gamma_{[\boldsymbol{x},\boldsymbol{y}]}$ need not be unique, as will be shown in Example 2.2.4. If the geodesic segment is unique (as in the case of the AWGN channel - Section 4.1.2), $(\mathcal{Y},d)$ is called a uniquely geodesic metric space.

A geodesic segment γ is usually equipped with a natural parametrization given by

$$d(\gamma(t_1),\gamma(t_2)) = \alpha|t_1-t_2|,\ t_1,t_2\in[0,1],\ \alpha\in\mathbb{R}, \tag{2.4}$$

[1] Note that a similar claim can be made for the maximum a posteriori probability decoder [79]

which allows for designing of fast search algorithms based on the bisection method.

In order to have a fast algorithm and a unified model and analysis for both discrete and continuous channels (that are not necessarily additive) we hereby introduce the notion of a *geodesic channel* as a special case of the matched channel:

Definition 2.1.1. Geodesic channel is any channel $\Omega : \mathcal{C} \subseteq \mathcal{Y} \to \mathcal{Y}$, with a matched metrics d, such that $(\mathcal{Y}, d)$ is a geodesic metric space.

Example 2.1.2. Binary erasure channel with erasure probability p,

$$BEC(p) : \mathcal{C} \subseteq \{0,1\}^N \to \mathcal{Y} = \{0,1,\infty\}^N, \tag{2.5}$$

together with a matched Hamming metric, defined as

$$d_H(\boldsymbol{x}, \boldsymbol{y}) = \sum_{n=1}^{N} \overline{\mathbb{1}}_{\{x_n\}}(y_n), \tag{2.6}$$

forms a *geodesic channel*. Similarly as in [79], we consider $BEC(p)$ to be a channel operating on the set $\{0,1\}^N$, rather than N uses of a channel defined on $\{0,1\}$. Channel output can be defined as $\boldsymbol{Y} = \boldsymbol{X} + \boldsymbol{W}$, where $\boldsymbol{W} \in \{0,\infty\}^N$ is a random erasure vector such that each component of $\boldsymbol{W}$ is either "∞" with some erasure probability p or "0" with probability $1-p$.

A geodesic segment $\gamma_{[\boldsymbol{x},\boldsymbol{y}]}$ is defined by a discrete line $\boldsymbol{x} + \mathcal{W}$, where $\mathcal{W} = \{\boldsymbol{w}_0, \boldsymbol{w}_1 \dots \boldsymbol{w}_K\}$ is a set of erasure patterns such that $\boldsymbol{w}_0$ is the all zero vector, $\boldsymbol{y} = \boldsymbol{x} + \boldsymbol{w}_K$ and $d_{\mathrm{H}}(\boldsymbol{w}_k, \boldsymbol{w}_{k+1}) = 1$, $k = 1 \dots K-1$.

2.2 Metric Star Domain Decoders

The decoding region $\mathcal{D}_m \subseteq \mathcal{Y}$ associated with a codeword $\boldsymbol{x}_m$ is defined as

$$\mathcal{D}_m = \{\boldsymbol{y} \in \mathcal{Y} : D(\boldsymbol{y}) = \boldsymbol{x}_m\}. \tag{2.7}$$

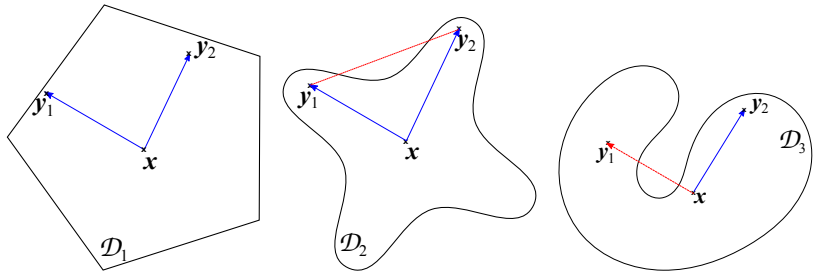

(a) Convex set (b) Star domain (c) Neither

Figure 2.1: *Examples of star domain sets in* $\mathbb{R}^2$. *Set* $\mathcal{D}_1$ *is convex and also a star domain. Set* $\mathcal{D}_2$ *is not convex, but it is a star domain. Set* $\mathcal{D}_3$ *is neither convex nor a star domain, as there is not a line segment between* $\boldsymbol{x}$ *and* $\boldsymbol{y}_1$.

Note that $\mathcal{D}_m$ is dependent on the code $\mathcal{C}$, channel Ω, and the decoding algorithm and can change if any of these are changed.

Given a code $\mathcal{C} \subseteq \mathcal{Y}$ and the coresponding geodesic channel Ω, let the *star domain decoder* $D : \mathcal{Y} \to \mathcal{C}$ be a decoding algorithm for which every decoding region $\mathcal{D}_m$ is a *metric star domain* (named as an analogy to the star domain in Euclidean space Fig. 2.1, [82]) defined as:

Definition 2.2.1. Decoding region $\mathcal{D}_m$ associated to codeword $\boldsymbol{x}_m \in \mathcal{C} \subseteq \mathcal{Y}$ is said to be a *metric star domain* if and only if for every geodesic segment $\gamma_{[\boldsymbol{x}_m, \boldsymbol{y}]}$, with $\gamma(0) = \boldsymbol{x}_m$ and $\gamma(1) = \boldsymbol{y} \in \mathcal{D}_m$ the following holds true:

$$\forall k \in [0,1] \Rightarrow \gamma(k) \in \mathcal{D}_m. \tag{2.8}$$

Example 2.2.2. A set $\mathcal{D} \subseteq \mathbb{R}^N$ is called a star domain (or star convex) if there exists a point $\boldsymbol{x} \in \mathcal{D}$, such that there is a straight line between $\boldsymbol{x}$ and any other $\boldsymbol{y} \in \mathcal{D}$ that is also in $\mathcal{D}$. It can be said that $\mathcal{D}$ is convex with respect to $\boldsymbol{x}$. The set $\mathcal{D}_1$ in Fig. 2.1a is convex, so it is also a star domain with respect to every $\boldsymbol{y} \in \mathcal{D}_1$. The set $\mathcal{D}_2$ in Fig 2.1b is a star domain with respect to $\boldsymbol{x}$ but it is not convex as there is no line segment from $\boldsymbol{y}_1$ to $\boldsymbol{y}_2$ that is also in $\mathcal{D}_2$. The set $\mathcal{D}_3$ in Fig 2.1c is neither convex nor star convex.

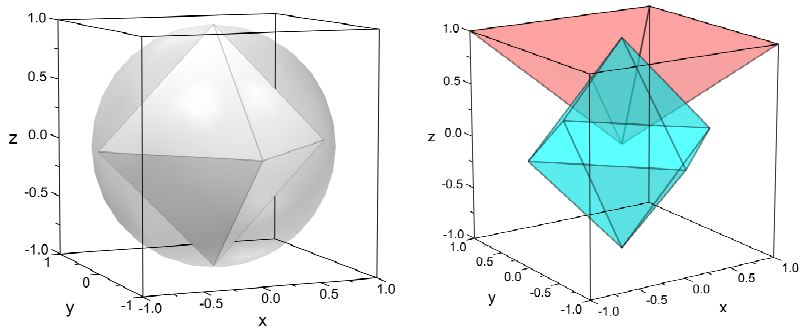

(a) Octahedron inscribed in a unit sphere (b) Decoding region

Figure 2.2: *Octahedron code and its decoding region.*

Example 2.2.3. Consider a simple spherical code $\mathcal{C}_6 \subset \mathbb{R}^3$ corresponding to an octahedron (Fig. 2.2a) coupled with an MD decoder. Each one of the six points of the octahedron represent a codeword (Table 2.2.3) and the MD decoder is defined as

$$D(\boldsymbol{y}) = \underset{\boldsymbol{x}\in\mathcal{C}_6}{\arg\min}\, d(\boldsymbol{x}, \boldsymbol{y}). \tag{2.9}$$

$\boldsymbol{x}_1$	$[1,\ 0,\ 0]$
$\boldsymbol{x}_2$	$[-1,\ 0,\ 0]$
$\boldsymbol{x}_3$	$[0,\ 1,\ 0]$
$\boldsymbol{x}_4$	$[0, -1,\ 0]$
$\boldsymbol{x}_5$	$[0,\ 0,\ 1]$
$\boldsymbol{x}_6$	$[0,\ 0, -1]$

Table 2.1: *Codewords of the octahedron code*

The decoding region corresponding to any codeword $\boldsymbol{x}_m$, $(m = 1, 2, ..., 6)$, has the shape of an open pyramid, which is shown in Fig.

2.2b. The octahedron code is a very important example that will be used throughout the thesis.

Example 2.2.4. Consider a binary erasure channel $BEC(p)$

$$BEC(p) : \mathcal{C} = \{[0,0,0],[1,1,1]\} \to \{0,1,\infty\}^3. \tag{2.10}$$

If a codeword $\boldsymbol{x} = [0,0,0]$ is sent over the $BEC(p)$ channel and a channel output $\boldsymbol{y} = [0,\infty,\infty]$ is received, there are two possible geodesic segments between $\boldsymbol{x}$ and $\boldsymbol{y}$. $\gamma^{(1)}_{[\boldsymbol{x},\boldsymbol{y}]} = \{[0,0,0],[0,0,\infty],[0,\infty,\infty]\}$ and $\gamma^{(2)}_{[\boldsymbol{x},\boldsymbol{y}]} = \{[0,0,0],[0,\infty,0],[0,\infty,\infty]\}$. If the output of the decoder is $D([0,\infty,\infty]) = [0,0,0]$ it must also be $D([0,0,\infty]) = D([0,\infty,0]) = [0,0,0]$ in order for $D(\cdot)$ to be a metric star domain decoder.

MD decoders and bounded distance (BD) decoders such as spherical decoder [83, 84] and Berlekamp-Massey algorithm [85] are by definition star domain decoders. It can be shown that many popular near-ML decoders, such as OSD and the PSCD, are also star domain. In Section 2.2.1 we show that the OSD also falls in this category. The metric star domain property of the PSCD decoder follows directly from the definition of the channel polarization [47], which is shown in Section 2.2.2. For completeness, a description of the PSCD algorithm is also given.

2.2.1 Ordered Statistics Decoder

Ordered statistics decoder [19] is a soft decision decoding algorithm for a binary linear (N, K) code with a known generator matrix G. Bose–Chaudhuri–Hocquenghem (BCH) codes are known to have good performance at short blocklength. Coupled with a flexible near-ML decoder like the OSD, they are strong contenders for use in the future URLLC applications.

Recent advances in OSD have shown significant complexity reduction [20, 86–93] while maintaining rate efficiency. By reducing complexity, we also reduce processing latency. It is possible to achieve a trade

off between error performance and complexity (latency) by using OSD with bounded complexity, which means that the same coding scheme can be used for multiple applications with different reliability-latency requirements [1]. Compleixty-performance tradeoff of different coding schemes is shown in Fig 2.3. The algorithmic complexity is given as the number of binary operations per information bit and is taken from [18]. The performance is given as a gap to the Polyanskiy-Poor-Verdu (PPV) bound [94], which is applicable for finite blocklengths. For more detail see [1].

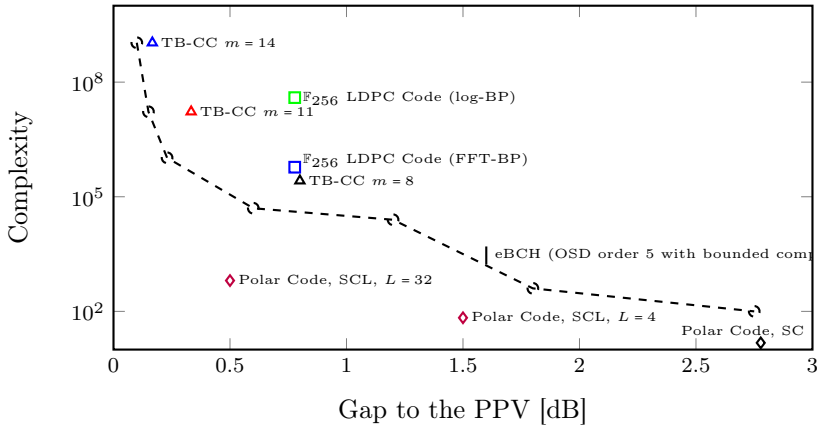

Figure 2.3: *Algorithmic complexity versus performance for different rate-1/2 channel codes with block length $N = 128$ at BLER= 10^{-4} [1]. The algorithmic complexity for different decoders are obtained from [18].*

Without loss of generality, we assume an all-zero codeword $\boldsymbol{c}$ is mapped into a BPSK symbol sequence $\boldsymbol{x} = 2\boldsymbol{c} - 1$ ($x_i = -1, 1 \leq i \leq N$) and is transmitted over the AWGN channel. Channel output is an N-dimensional vector of real values, $\boldsymbol{y} = [y_1, y_2, ..., y_N]$ where y_i represents the i-th component of channel output $\boldsymbol{y}$ associated with the i-th column of matrix G. If a hard decision decoder is used, estimate $\hat{\boldsymbol{c}}$ is generated as

$$\hat{c}_i = \begin{cases} 0, & y_i \le 0 \\ 1, & y_i > 0 \end{cases}$$

Note that hard decision decoder is star convex. This follows from

$$\begin{aligned} y_i = x_i + w_i \le 0 \Rightarrow x_i + \alpha w_i \le 0,\ 1 \le i \le N, \\ w_i \in \mathbb{R},\ \alpha \in [0,1],\ x_i = -1. \end{aligned} \tag{2.11}$$

The inverse is also true

$$\begin{aligned} y_i = x_i + w_i > 0 \Rightarrow x_i + \alpha w_i > 0,\ 1 \le i \le N, \\ w_i \in \mathbb{R},\ \alpha \in \left(\frac{1}{w_i}, \infty\right),\ x_i = -1. \end{aligned} \tag{2.12}$$

The idea of OSD is to use the reliability of the received vector $\boldsymbol{y}$ to get a better estimate. The first step is to sort the channel output $\boldsymbol{y}$ in the decreasing order of reliability value $|y_i|$ for $1 \le i \le N$, and apply the corresponding permutation $\pi_1(\cdot)$ to the columns of matrix G. The reordered generator matrix is transformed into a systematic form via Gaussian elimination. An additional permutation $\pi_2(\cdot)$ may be needed in order to get the most reliable basis. This gives the generator matrix $\widetilde{G}$, and the reorderd channel output $\widetilde{\boldsymbol{y}} = \pi_2(\pi_1(\boldsymbol{y}))$. Now we perform hard decision decoding of the first K most reliable symbols of the vector $\widetilde{\boldsymbol{y}}$ to get the binary vector $\widetilde{\boldsymbol{a}}$ of length K. Decoded sequence $\hat{\boldsymbol{c}}$ is obtained by re-encoding vector $\widetilde{\boldsymbol{a}}$ via the matrix $\widetilde{G}$ and applying the inverse permutations π_1^{-1} and π_2^{-1}

$$\hat{\boldsymbol{c}} = \pi_1^{-1}\left(\pi_2^{-1}\left(\widetilde{\boldsymbol{a}}\widetilde{G}\right)\right). \tag{2.13}$$

This solution corresponds to the hard decision decoding based on the reliability of information and can be reprocessed and improved progressively in stages. Reprocessing step consists of generating test error patterns $\boldsymbol{e}_j$ of increasing weight, finding the codeword $\overline{\boldsymbol{c}}_j = (\widetilde{\boldsymbol{a}} + \boldsymbol{e}_j)\widetilde{G}$ and determining its corresponding BPSK sequence $\overline{\boldsymbol{x}}_j$. We compare the squared Euclidean distance between $\overline{\boldsymbol{x}}_j$ and the ordered received

sequence $\widetilde{\boldsymbol{y}}$ and choose $\overline{\boldsymbol{x}}^*$ (and the corresponding $\overline{\boldsymbol{c}}^*$) which is closest to $\widetilde{\boldsymbol{y}}$. The refactoring algorithm is terminated after a predefined number of generated test error patterns or when a desired error performance is achieved.

In order to show that the hard decision decoding based on reliability of information preserves star convexity we must prove that it is impossible for an incorrect symbol to become more reliable than a correct symbol after noise reduction, i.e.

$$\begin{gathered} |x_i + w_i| > |x_j + w_j| \Rightarrow |x_i + \alpha w_i| > |x_j + \alpha w_j| \\ x_i = x_j = -1,\ \alpha \in [0,1],\ w_i \in (-\infty, 1],\ w_j \in (1, \infty). \end{gathered} \tag{2.14}$$

By using the definition of absolute value it can easily be verified that

$$\begin{gathered} -(w_i - 1) > (w_j - 1) \Leftrightarrow \\ w_i + w_j < 2 \Rightarrow \alpha(w_j + w_i) < 2, \\ \alpha \in [0,1],\ w_i \in (-\infty, 1],\ w_j \in (1, \infty). \end{gathered} \tag{2.15}$$

Refactoring step also preserves star convexity. This follows from the fact that after the noise reduction, the Euclidean distance between the received vector and the correct codeword will be reduced and a correct estimate will remain correct.

2.2.2 Polar Successive Cancellation Decoder

The polar transform $G_2^{\otimes \log_2 N}$ converts N copies of some binary memoryless symmetric channel (BMSC), $\Omega : \{0,1\} \to \mathcal{Y}$ (defined by $P[Y|X]$), into a mixture of N *polarized* channels, $\Omega_N : \{0,1\}^N \to \mathcal{Y}^N$, that ideally polarize to either a noiseless or completely noisy channel, in a way that preserves the symmetric capacity of the channel Ω, as best as possible [47].

Given a binary random data vector of length N, $\boldsymbol{U} \in \mathbb{F}_2^N$, containing K information bits and $N-K$ frozen bits (usually set to zero), encoding is realized as

$$\boldsymbol{C} = \boldsymbol{U} G_2^{\otimes \log_2 N} \tag{2.16}$$

The mixed channel (Ω_N) is then defined by a conditional probability

$$P_N[\boldsymbol{Y}|\boldsymbol{U}] = \prod_{n=1}^{N} P[Y_n|C_n]. \tag{2.17}$$

The i-th subchannel, $\Omega_N^{(i)} : \{0,1\} \to \mathbb{R}^N$, associated with the bit U_i, is defined by [47, 95]

$$P_N^{(i)}[\boldsymbol{Y}; U_1, \dots U_{i-1}|U_i] = \frac{1}{2^{N-1}} \sum_{U_{i+1},\dots,U_N} P_N[\boldsymbol{Y}|\boldsymbol{U}]. \tag{2.18}$$

In order to achieve the symmetric capacity with low complexity, a SCD algorithm is introduced in [47], where the information bits are decoded sequentially in the ascending order of their indices using the following rule [95]

$$\hat{U}_i(\boldsymbol{y}; \hat{u}_1, \dots, \hat{u}_{i-1}) = \underset{u_i \in \{0,1\}}{\arg\max}\, P_N^{(i)}[\boldsymbol{y}; \hat{u}_1, \dots, \hat{u}_{i-1}|u_i]. \tag{2.19}$$

It has been shown in [95,96] that $\Omega_N^{(i)}$ is a tree channel [97] and that SCD corresponds to a belief propagation decoding on a tree graph, which is equivalent to an ML estimation [97] of the bit U_i, given the channel output $\boldsymbol{y}$. We asume that every free bit U_i has been correctly estimated using a different bit-ML decoder (which is by definition a metric star domain decoder). After noise reduction every free bit will remain correct so it follows that SCD is also a metric star domain decoder.

Consider a binary input AWGN channel with noise variance σ^2, $\Omega(\sigma) : \{-1,1\}^N \to \mathbb{R}^N$. Let $\boldsymbol{x}$ be a BPSK modulated polar codeword, and $\boldsymbol{Y} = \boldsymbol{x} + \boldsymbol{W}$ be a corresponding channel output. Then multiplying the noise vector by $\alpha \in [0,1]$, ($\boldsymbol{Y}_\alpha = \boldsymbol{x} + \alpha\boldsymbol{W}$), is equivalent to replacing the channel $\Omega(\sigma)$ with a "better" channel $\Omega(\alpha\sigma)$ (i.e $\Omega(\sigma)$ is degraded with respect to $\Omega(\alpha\sigma)$). As the performance of a belief propagation decoding on a tree graph improves if the channel improves (monotonicity of the decoder with respect to channel) [97], it follows that the SCD is

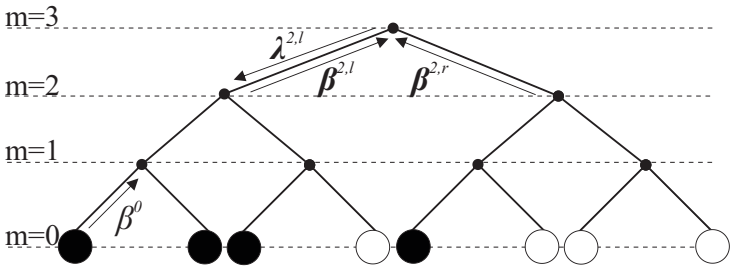

Figure 2.4: *Tree representation of an (8, 4) polar code. Black circles represent frozen bits.*

a metric star domain decoder:

$$\mathrm{SCD}(\boldsymbol{y}) = \boldsymbol{x} \Rightarrow \mathrm{SCD}(\boldsymbol{y}_\alpha) = \boldsymbol{x}, \forall \alpha \in [0,1]. \tag{2.20}$$

This holds true for any BMSC [97].

Because of its recursive construction, the structure of an (N, K) polar code is usually represented using a full binary tree (Fig. 2.4) of height $M = \log_2 N$ and with N leaf nodes [56, 98].

Successive cancellation decoding algorithm can be implemented as a depth-first traversal [99] of the polar tree. At each node of height m a vector $\boldsymbol{\lambda}^m \in \mathbb{R}^{N_m}$ of soft logarithmic likelihood ratio (LLR) values is passed from the parent to the child nodes, while a vector of hard bit estimates, $\boldsymbol{\beta}^m \in \mathbb{F}_2^{N_m}$, follows the opposite direction [56].

At each node of height m, $1 \le m \le M$, a vector $\boldsymbol{\lambda}^m$, of size $N_m = 2^m$, is recursively divided into $\boldsymbol{\lambda}^{m-1,l}$ and $\boldsymbol{\lambda}^{m-1,r}$, of size $N_{m-1} = 2^{m-1}$, which are passed to the left and right child node, respectively.

$$\lambda_i^{m-1,l} = 2 \operatorname{arctanh}\left(\tanh\left(\frac{\lambda_i^m}{2}\right)\tanh\left(\frac{\lambda_{i+N_{m-1}}^m}{2}\right)\right), \tag{2.21}$$

$$\lambda_i^{m-1,r} = \lambda_{i+N_{m-1}}^m + (1 - 2\beta_i^{m-1,l})\lambda_i^m. \tag{2.22}$$

In most practical systems the following approximation of Equation (2.21) is usually used [56, 100]

$$\lambda_i^{m-1,l} = \operatorname{sign}(\lambda_i^m)\operatorname{sign}(\lambda_{i+N_{m-1}}^m)\min(|\lambda_i^m|, |\lambda_{i+N_{m-1}}^m|). \tag{2.23}$$

This is repeated until the leaf node is reached where the appropriate bit, $\hat{u}$, is estimated as

$$\hat{u} = \begin{cases} 0, & \lambda^0 \geq 0 \\ 1, & \text{otherwise.} \end{cases} \tag{2.24}$$

At each node of height m, $1 \leq m \leq M$, a vector $\boldsymbol{\beta}^m$, of size $N_m = 2^m$, is calculated using the vectors $\boldsymbol{\beta}^{m-1,l}$ and $\boldsymbol{\beta}^{m-1,r}$, received from the child nodes.

$$\beta_i^m = \begin{cases} \beta_i^{m-1,l} + \beta_i^{m-1,r}, & i \leq N_{m-1} \\ \beta_{i-N_{m-1}}^{m-1,r}, & \text{otherwise,} \end{cases} \tag{2.25}$$

with β^0 equal to the corresponding $\hat{u}$.

The procedure is terminated once all leaf nodes are visited. Different decoding algorithms correspond to different tree search algorithms.

2.3 Error Probability of Star Domain Decoders

Given a codeword $\boldsymbol{x}_m \in \mathcal{C}$ and its associated decoding region $\mathcal{D}_m$, error probability is correspondingly defined as

$$P_{\mathrm{e}} = E[P_{\mathrm{e}}^{(m)}], \tag{2.26}$$

where

$$P_{\mathrm{e}}^{(m)} = P[\boldsymbol{Y} \notin \mathcal{D}_m \mid \boldsymbol{x}_m]. \tag{2.27}$$

For simplicity of notation (and without the loss of generality) we assume that all codewords are equally likely and that their associated decoding regions are isomorphic. This allows for the error probability to be to be considered from aspect of any single codeword $\boldsymbol{x}_m = \boldsymbol{x}$ (i.e. $P_{\mathrm{e}}^{(m)} = P_{\mathrm{e}}$). Although such a choice may seem restrictive, many codes used in practice satisfy this property (e.g. coset and linear block codes, trellis codes with binary or M-ary phase shift keying symbols

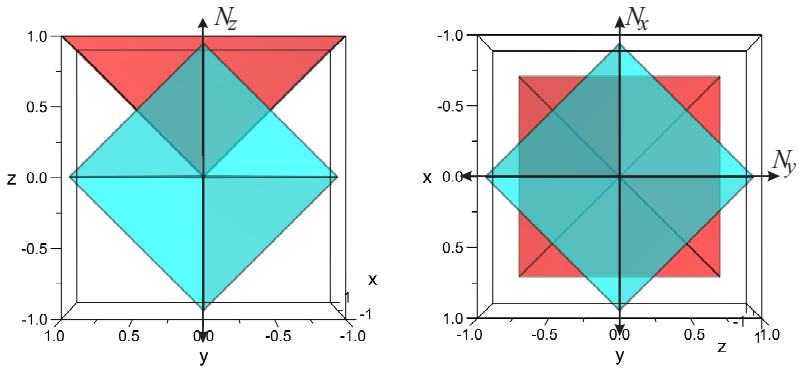

Figure 2.5: *Side (a) and top (b) view of the octahedron code.*

and a more general class of geometrically uniform codes [101]). If the decoding region associated with the codeword $\boldsymbol{x}_m = \boldsymbol{x}$ is $\mathcal{D}_m = \mathcal{D}$, the error probability can be defined as

$$P_{\mathrm{e}} = P[\boldsymbol{Y} \notin \mathcal{D} \mid \boldsymbol{x}]. \tag{2.28}$$

For convenience, let $P[\boldsymbol{Y} = \boldsymbol{y} | \boldsymbol{X} = \boldsymbol{x}] = p_{\boldsymbol{Y}}(\boldsymbol{y})$.

Example 2.3.1. We will derive the error probability of the $\mathcal{C}_6$ octahedron code in the case of the AWGN channel. Following (2.28), an error occurs if the output of the channel falls in the decoding region of another codeword. Side and top view of the octahedron code, and the decoding region corresponding to the codeword $\boldsymbol{x}$ are shown in Fig. 2.5a. and Fig. 2.5b. respectively.

To calculate the error probability of the octahedron code we decompose the AWGN noise into three components, N_x, N_y and N_z, acting in the directions x, y and z respectively (Fig. 2.5a. and Fig. 2.5b). The N_z component of the AWGN noise is point noise with probability density function

$$p_{N_z}(n_z) = \frac{1}{\sqrt{2\pi}\sigma} e^{-\frac{{n_z}^2}{2\sigma^2}}, \tag{2.29}$$

If $n_z \in (-\infty, -1]$ an error certainly occurs, otherwise that depends on N_x and N_y components.

The probability that no error occurs in case of a fixed $N_z = n_z$ is

$$P_{cxy} = \left(1 - 2Q\left(\frac{1 - n_z}{\sigma}\right)\right)^2, \tag{2.30}$$

where

$$Q(x) = \frac{1}{\sqrt{2\pi}} \int_x^\infty e^{-\frac{u^2}{2}} du \tag{2.31}$$

represents the tail probability of the standard normal distribution.

Probability that no error occurs is thus

$$P_c = \int_{-1}^{\infty} P_{cxy} p_{N_z}(n_z)\, dn_z, \tag{2.32}$$

and the error probability is then

$$P_e = 1 - P_c = 1 - \int_{-1}^{\infty} p_{N_z}(n_z) \left(1 - 2Q\left(\frac{1 - n_z}{\sigma}\right)\right)^2 dn_z. \tag{2.33}$$

This function is evaluated using numerical integration.

Chapter 3

Simulation of a Communication Link

In this chapter we introduce a general simulation framework for estimating the error probability of a communication system. We define the accuracy of the estimator and give two metrics for evaluating its performance. We show that both the MC and IS methods fit into this framework and give some details about their implementation that will be used in future chapters.

3.1 General Simulation Framework

The problem of simulating the error probability of a communication system is usually stated as an expectation of some random variable T (i.e. $P_e = E[T]$). The simplest method for estimating this expectation is to generate a set of J independent observations $\{t_1, t_2, \cdots t_J\}$ according to the distribution $p_T(\cdot)$ and calculate the sample mean as

$$\widehat{P}_e = \frac{1}{J} \sum_{j=1}^{j} t_j. \tag{3.1}$$

Relative precission (aka normalized standard error) of the estimator is usally used as a measure of accuracy and it is defined as [30]

$$\delta = \frac{\sqrt{\mathrm{Var}\left[\widehat{P}_e\right]}}{P_e}, \tag{3.2}$$

where the variance of the estimator [30, 31, 36, 37, 102] is given by

$$\mathrm{Var}\left[\widehat{P}_\mathrm{e}\right] = \frac{\mathrm{Var}[T]}{J} = \frac{1}{J}\left(E\left[T^2\right] - P_\mathrm{e}^2\right). \tag{3.3}$$

It follows that the variance can be made arbitrarily small as J grows. The smaller the variance, the better the estimator, but there is a trade-off between the accuracy of the estimator and the simulation run-time (the number of generated samples J).

The true variance of the estimator cannot generally be calculated as it depends on P_e (which is the true value of the parameter being estimated), so sample variance is used instead [30, 31]

$$S^2\left[\widehat{P}_\mathrm{e}\right] = \frac{1}{J-1}\sum_{j=1}^{J}\left(t_j - \widehat{P}_\mathrm{e}\right)^2. \tag{3.4}$$

The estimated relative precision [30] is usually used as a simulation stopping rule and it is defined as

$$\widehat{\delta} = \frac{\sqrt{S^2\left[\widehat{P}_\mathrm{e}\right]}}{\widehat{P}_\mathrm{e}}. \tag{3.5}$$

In rare cases when P_e is known, the average relative error [103] may be used as a measure of estimator accuracy

$$\rho = \frac{1}{I}\sum_{i=1}^{I}\frac{|P_\mathrm{e} - \widehat{P}_{\mathrm{e}i}|}{P_\mathrm{e}}, \tag{3.6}$$

where I is the total number of estimates.

The time complexity $\mathscr{T}(\delta, P_\mathrm{e})$ of the estimator is usually given as the number of simulation runs (decoder calls) needed to estimate P_e with some accuracy δ, and may differ from J.

3.2 Monte Carlo Simulation Method

Given the channel output $\boldsymbol{Y}$ the error probability in (2.28) can be expressed in terms of the indicator function (or more precisely its inverse)

as [30]

$$P_{\mathrm{e}} = E_{\boldsymbol{Y}}\left[\overline{\mathbb{1}}_{\mathcal{D}}(\boldsymbol{Y})\right] = \int \overline{\mathbb{1}}_{\mathcal{D}}(\boldsymbol{y}) p_{\boldsymbol{Y}}(\boldsymbol{y}) d\boldsymbol{y}, \tag{3.7}$$

which corresponds to $T = \overline{\mathbb{1}}_{\mathcal{D}}(\boldsymbol{Y})$.

The variance of the MC estimator [30, 31, 36, 37, 102] is given by

$$\mathrm{Var}\left[\widehat{P}_{\mathrm{e}}^{\,\mathrm{MC}}\right] = \frac{P_{\mathrm{e}}\left(1 - P_{\mathrm{e}}\right)}{J}. \tag{3.8}$$

Relative precision of the MC estimator is then equal to

$$\delta = \sqrt{\frac{1 - P_{\mathrm{e}}}{P_{\mathrm{e}} J}}. \tag{3.9}$$

For small P_{e} ($P_{\mathrm{e}} \ll 1$) the relative error is approximated as

$$\delta \approx \frac{1}{\sqrt{P_{\mathrm{e}} J}}. \tag{3.10}$$

The time complexity of the MC estimator is given by [30]

$$\mathscr{T}_{\mathrm{MC}}(\delta, P_{\mathrm{e}}) = \mathcal{O}(J) = \mathcal{O}\left(\frac{1}{\delta^2 P_{\mathrm{e}}}\right). \tag{3.11}$$

Algorithm 1 represents a generic implementation of the MC simulation method for estimation of the error probability. $CONDITION$ represents some terminating condition which is chosen so as to provide a predefined confidence interval [30].

3.3 Importance Sampling Simulation Method

If $p_{\boldsymbol{Y}^*}(\boldsymbol{y})$ is a distribution function, called the biased distribution, the error probability in (3.7) is equivalent to

$$P_{\mathrm{e}} = \int \overline{\mathbb{1}}_{\mathcal{D}}(\boldsymbol{y}) p_{\boldsymbol{Y}^*}(\boldsymbol{y}) \frac{p_{\boldsymbol{Y}}(\boldsymbol{y})}{p_{\boldsymbol{Y}^*}(\boldsymbol{y})} d\boldsymbol{y} = E_{\boldsymbol{Y}^*}\left[\overline{\mathbb{1}}_{\mathcal{D}}(\boldsymbol{Y}^*) W(\boldsymbol{Y}^*)\right], \tag{3.12}$$

Algorithm 1 *Generic MC Simulation method*

$\boldsymbol{x} \leftarrow \boldsymbol{X}$ {Initialize codeword}
$j \leftarrow 0$ {Total number of simulations}
$e \leftarrow 0$ {Total number of detected errors}
$\widehat{P}_{\mathrm{e}} \leftarrow 0$ {Estimated error probability}
while $CONDITION$ **do**
  $j \leftarrow j + 1$
  $\boldsymbol{y} \leftarrow \boldsymbol{Y} = \Omega(\boldsymbol{x})$ {Generate the channel output}
  $\hat{\boldsymbol{x}} \leftarrow D(\boldsymbol{y})$
  if $\boldsymbol{x} \neq \hat{\boldsymbol{x}}$ **then**
    $e \leftarrow e + 1$
  end if
  $\widehat{P}_{\mathrm{e}} \leftarrow \frac{e}{j}$ {Update $\widehat{P}_{\mathrm{e}}$}
end while

where $\boldsymbol{y}$ is now a realization of $\boldsymbol{Y}^*$ and the ratio

$$W(\boldsymbol{y}) = \frac{p_{\boldsymbol{Y}}(\boldsymbol{y})}{p_{\boldsymbol{Y}^*}(\boldsymbol{y})} \tag{3.13}$$

is called the likelihood ratio or weighing function [30, 31]. IS method can be stated as the estimation of the expectation of a random variable $T = \overline{\mathbb{1}}_{\mathcal{D}}(\boldsymbol{Y}^*)W(\boldsymbol{Y}^*)$. As the variance of the IS estimator depends on the choice of the biased distribution, it cannot be expressed in closed form.

The optimal biased distribution is theoretically known, but since it depends on the parameter that is to be estimated, it cannot be effectively used. There are many methods of choosing a good biased distribution but in this thesis we limit ourselves to the adaptive IS with variance scaling [30, 34] for the AWGN channel and the state of the art minimum variance IS estimator [36] for BSC.

Likelihood ratio (3.13) is usually defined as a function of some parameter θ (usually mean or variance of the biased distribution)

$$W(\boldsymbol{y};\theta) = \frac{p_{\boldsymbol{Y}}(\boldsymbol{y})}{p_{\boldsymbol{Y}^*}(\boldsymbol{y};\theta)}, \tag{3.14}$$

chosen so as to minimize the cost function [30, 34]

$$C(\theta) = \int W^2(\boldsymbol{y};\theta) p_{\boldsymbol{Y}^*}(\boldsymbol{y};\theta) d\boldsymbol{y}. \tag{3.15}$$

In the case of the variance scaling IS simulation method, the biased distribution is defined as

$$p_{\boldsymbol{Y}^*}(\boldsymbol{y};\theta) = \frac{p_{\boldsymbol{Y}}(\boldsymbol{y}/\theta)}{\theta}. \tag{3.16}$$

3.3.1 IS techniques for AWGN Channel

The adaptive IS method uses iterative Newton's method (or the gradient descent method) to find parameter θ for each value of the signal-to-noise ratio

$$\theta_{c+1} = \theta_c - \eta \frac{\frac{d}{d\theta}\widehat{C}(\theta_c)}{\frac{d^2}{d\theta^2}\widehat{C}(\theta_c)}, \tag{3.17}$$

where η represents the step size and

$$\frac{d}{d\theta}\widehat{C}(\theta) = \frac{1}{J}\sum_{j=1}^{J} \mathbb{1}_{\mathcal{D}}(\boldsymbol{y}_j) W(\boldsymbol{y}_j;\theta) \frac{d}{d\theta} W(\boldsymbol{y}_j;\theta), \tag{3.18}$$

$$\frac{d^2}{d\theta^2}\widehat{C}(\theta) = \frac{1}{J}\sum_{j=1}^{J} \mathbb{1}_{\mathcal{D}}(\boldsymbol{y}_j) W(\boldsymbol{y}_j;\theta) \frac{d^2}{d\theta^2} W(\boldsymbol{y}_j;\theta). \tag{3.19}$$

In the case of variance scaling, the biased distribution is defined as

$$p_{\boldsymbol{Y}^*}(\boldsymbol{y};\theta) = \frac{p_{\boldsymbol{Y}}(\frac{\boldsymbol{y}}{\theta})}{\theta} = \left(\frac{1}{\sqrt{2\pi}\sigma\theta}\right)^N e^{-\frac{\|\boldsymbol{y}\|^2}{2\sigma^2\theta^2}}. \tag{3.20}$$

3.3.2 Minimum Variance IS for BSC

In the case of minimum variance IS Bernoulli estimator [37] the noise vector $\boldsymbol{Y}^*$ is drawn as a multivariate Bernoulli distribution with parameter q, ($q \geq p$, where p is the crossover probability of BSC), chosen so as to minimize the variance of the IS estimator.

$$q = \arg\min_{q} \mathrm{Var}\left[\widehat{P}_{\mathrm{e}}^{\,\mathrm{IS}}\right]. \tag{3.21}$$

The likelihood ratio is defined as

$$W(\boldsymbol{y}; p, q) = \frac{p_{\boldsymbol{Y}}(\boldsymbol{y}; p)}{p_{\boldsymbol{Y}^*}(\boldsymbol{y}; q)} = \frac{p^{w_H(\boldsymbol{y})}(1-p)^{N-w_H(\boldsymbol{y})}}{q^{w_H(\boldsymbol{y})}(1-q)^{N-w_H(\boldsymbol{y})}}, \tag{3.22}$$

where $w_H(\cdot)$ represents the Hamming weight and is defined as

$$w_H(\boldsymbol{y}) = d_H(\boldsymbol{0}, \boldsymbol{y}). \tag{3.23}$$

Parameter $\hat{q}$ is estimated iteratively using the following rule

$$\hat{q}_{c+1} = \frac{1}{N} \frac{\sum_{j=1}^{J'} \mathbb{1}_{\mathcal{D}}(\boldsymbol{y}_j) w_H(\boldsymbol{y}_j) W^2(\boldsymbol{y}_j; p, \hat{q}_c)}{\sum_{j=1}^{J'} \mathbb{1}_{\mathcal{D}}(\boldsymbol{y}_j) W^2(\boldsymbol{y}_j; p, \hat{q}_c)}, \tag{3.24}$$

where J' represents the total number of iterations needed to estimate $\hat{q}$. A more detailed analysis of this method is given in [37].

Chapter 4
Quasi-Analytical Simulation Method

In this chapter we develop the quasi-analytical simulation method for estimating the error probability of a metric star domain decoder. We derive the upper bound on the estimation variance and use it to find the time complexity of the QA estimator. We show that our QA method is significantly (several orders of magnitude) faster than the MC method, especially at high SNR regime. We show that both AWGN and BSC are a special case of the geodesic channel model, and give details on implementing the QA method for them. These guidelines can then be applied to any continuous or discrete channel model, as long as it satisfies the geodesic property. We conclude this chapter with an analysis of the performance of our QA method.

4.1 General QA Simulation Method

Both MC and IS methods simulate the noise according to the real or biased distribution, and simultaneously check whether the corresponding channel output belongs to the decoding region of $\boldsymbol{x}$. Hereby, we introduce a QA procedure which is based on estimating the distance distribution of all vectors in $\mathcal{D}$ to the codeword $\boldsymbol{x}$. We then recalculate P_{e} using pdf of the noise from it. In the case of the BSC and other discrete channels with an MD decoder this procedure amounts to estimation of the distance distribution of coset leaders, and recalculation of P_{e} according to it [104].

If the channel output $\boldsymbol{Y} = \Omega(\boldsymbol{x})$ falls outside of the decoding region

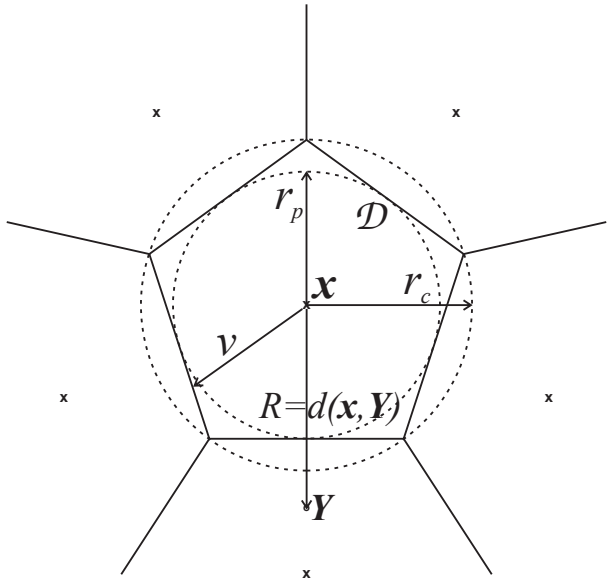

Figure 4.1: *Decoding region $\mathcal{D}$ of the codeword $\boldsymbol{x}$. The channel output $\boldsymbol{Y}$ falls outside of $\mathcal{D}$ resulting in a decoding error. r_p is the radius of the packing sphere and r_c is the radius of the covering sphere. v - distance from $\boldsymbol{x}$ to the boundary of $\mathcal{D}$.*

associated to $\boldsymbol{x}$, an error occurs (2.28). A simplified illustration of the decoding region is shown in Fig. 4.1. Random variable $R = d(\boldsymbol{x}, \boldsymbol{Y})$ in Fig. 4.1 represents the distance between the codeword and the channel output, and r_p and r_c represent the packing and covering radii. The following holds true for any $\boldsymbol{y} \in \mathcal{Y}$

$$\begin{aligned} d(\boldsymbol{x}, \boldsymbol{y}) \leq r_p &\Rightarrow \boldsymbol{y} \in \mathcal{D} \\ d(\boldsymbol{x}, \boldsymbol{y}) > r_c &\Rightarrow \boldsymbol{y} \notin \mathcal{D} \end{aligned} \tag{4.1}$$

Given a geodesic segment $\gamma_{[\boldsymbol{x},\boldsymbol{y}]}$ with $\gamma(0) = \boldsymbol{x}$ and $\gamma(1) = \boldsymbol{y} \notin \mathcal{D}$, there is a distance point $\boldsymbol{z} = \gamma(k^*) \in \mathcal{D}$ that is farthest from $\boldsymbol{x}$ (with

respect to d), that is

$$\boldsymbol{z} = \underset{d(\boldsymbol{x},\gamma(k))}{\arg\max}\{k \in [0,1] : \gamma(k) \in \mathcal{D}\}. \tag{4.2}$$

Let $\boldsymbol{Z}$ be a random distance point. Error probability with respect to $\boldsymbol{Z} = \boldsymbol{z}$ is by definition

$$P_{\mathrm{e}}(\boldsymbol{z}) = P[R > d(\boldsymbol{x}, \boldsymbol{Z})|\boldsymbol{Z} = \boldsymbol{z}]. \tag{4.3}$$

It follows that the error probability can be defined as

$$P_{\mathrm{e}} = E_{\boldsymbol{Z}}[P_{\mathrm{e}}(\boldsymbol{Z})] = P[R > V], \tag{4.4}$$

where $V = d(\boldsymbol{x}, \boldsymbol{Z})$ is an auxiliary random variable that represents the distance between the codeword and a random distance point. The domain of V is $[r_p, r_c]$, and since the tail distribution function is monotonically decreasing, the domain of $\overline{F}_R(V)$ is $\left[\overline{F}_R(r_c), \overline{F}_R(r_p)\right]$.

Theorem 4.1.1. *Error probability of a star domain decoder is defined as*

$$P_e = E_V[\overline{F}_R(V)] = E_R[F_V(R)]. \tag{4.5}$$

Proof. We assume R and V are continuous random variables. The proof for discrete case is the same, with the usual conversion of $\int f(x)dx \to \sum_x f(x)$.

Equation (4.50) can be written as

$$P_{\mathrm{e}} = P[R - V > 0]. \tag{4.6}$$

We introduce a new auxiliary random variable $A = R - V$.

$$P_{\mathrm{e}} = P[A > 0] = \int_0^\infty p_A(a)da, \tag{4.7}$$

where $p_A(\cdot)$ represents the pdf of random variable A. Since the probability density function of the difference of two independent random variables is equal to the correlation of their density functions,

$$p_A(a) = \int_{-\infty}^{\infty} p_R(v+a)p_V(v)dv, \tag{4.8}$$

the error probability can be redefined as

$$P_e = \int_0^{\infty} \left[\int_{-\infty}^{\infty} p_R(v+a)p_V(v)dv \right] da. \tag{4.9}$$

Since

$$\int_0^{\infty} p_R(v+a)da = \overline{F}_R(v). \tag{4.10}$$

After changing the order of integration the error probability in (4.9) can be written as

$$P_e = \int_{-\infty}^{\infty} \overline{F}_R(v)p_V(v)dv = E_V[\overline{F}_R(V)]. \tag{4.11}$$

It can similarly be shown that

$$P_e = P[0 > V - R] = E_R[F_V(R)]. \tag{4.12}$$

In fig. 4.2 we show the PDF of the Reed-Muller (1, 5) code and the tail of the Bernoulli distribution with parameter p = 0.1, 0.3 and 0.5. We see that this integral falls to zero as p is reduced.

■

This corresponds to the general simulation framework, presented in Chapter 3, with $T = \overline{F}_R(V)$ or $T = F_V(R)$. Following (3.1), the probability of error is correspondingly estimated as

$$\widehat{P}_e^{\,\mathrm{QA}} = \frac{1}{J}\sum_{j=1}^{J} \overline{F}_R(v_j), \tag{4.13}$$

where J represents a predefined number of measured distances. Unlike the MC and the IS method, where we estimate the error probability for one SNR value, our QA method is SNR invariant, since SNR is used to deterministically calculate $\overline{F}_R(v)$, $\forall v$, and the only random parameter v_j is independent of SNR. The main steps of the QA method are given in Algorithm 2.

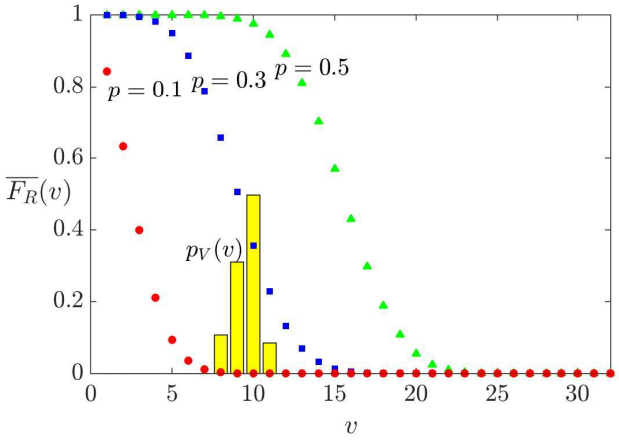

Figure 4.2: *Calculation of error probability of the RM(1, 5) code.*

Algorithm 2 *Generic QA Simulation method*

$\boldsymbol{x} \leftarrow \boldsymbol{X}$ {Initialize codeword}
$j \leftarrow 0$ {Total number of simulations}
$\widehat{P}_{\mathrm{e}}^{\mathrm{QA}} \leftarrow 0$ {Estimated error probability}
while $CONDITION$ **do**
  $j \leftarrow j + 1$
  Find v_j
  Update $\widehat{P}_{\mathrm{e}}^{\mathrm{QA}}$ {Using equation (4.13)}
end while

Theorem 4.1.2. *The variance of the QA estimator is upper bounded by*

$$Var[\widehat{P}_e{}^{QA}] \leq \frac{1}{J} P_e \overline{F}_R(r_p) \tag{4.14}$$

Proof. The variance of the QA estimator (3.3) is given by

$$\mathrm{Var}\left[\widehat{P}_{\mathrm{e}}^{\mathrm{QA}}\right] = \frac{1}{J}\left(E\left[\overline{F}_R^{\,2}(V)\right] - P_{\mathrm{e}}^2\right) \tag{4.15}$$

Given a random variable T with domain $[T_a, T_b]$ and a function $f(\cdot)$, that is convex over the domain of T, the upper bound on the expectation of $f(T)$ is given by the Edmundson-Madansky inequality [105]

$$E[f(T)] \leq \frac{T_b - E[T]}{T_b - T_a} f(T_a) + \frac{E[T] - T_a}{T_b - T_a} f(T_b). \tag{4.16}$$

By applying the Edmundson-Madansky inequality to $E\left[\overline{F}_R^{\,2}(V)\right]$ we get

$$\begin{aligned} E\left[\overline{F}_R^{\,2}(V)\right] \leq & \frac{\overline{F}_R(r_p) - P_{\mathrm{e}}}{\overline{F}_R(r_p) - \overline{F}_R(r_c)} \overline{F}_R^{\,2}(r_c) + \\ & \frac{P_{\mathrm{e}} - \overline{F}_R(r_c)}{\overline{F}_R(r_p) - \overline{F}_R(r_c)} \overline{F}_R^{\,2}(r_p) \end{aligned}, \tag{4.17}$$

which can be simplified to

$$E\left[\overline{F}_R^{\,2}(V)\right] \leq P_{\mathrm{e}}\left(\overline{F}_R(r_p) + \overline{F}_R(r_c)\right). \tag{4.18}$$

It follows that the variance of the QA estimator is upper bounded by

$$\mathrm{Var}\left[\widehat{P}_{\mathrm{e}}^{\mathrm{QA}}\right] \leq \frac{P_{\mathrm{e}}}{J}\left(\overline{F}_R(r_p) + \overline{F}_R(r_c) - P_{\mathrm{e}}\right). \tag{4.19}$$

Since $\overline{F}_R(r_p) >> P_{\mathrm{e}}\overline{F}_R(r_c)$ and $\overline{F}_R(r_p) \geq P_{\mathrm{e}} \geq \overline{F}_R(r_c)$, it follows that

$$\mathrm{Var}[\widehat{P}_{\mathrm{e}}^{\,\mathrm{QA}}] \leq \frac{1}{J} P_{\mathrm{e}} \overline{F}_R(r_p). \tag{4.20}$$

■

It follows that the number of measured distances needed to achieve a relative precision δ is upper bounded by

$$J \leq \frac{\overline{F}_R(r_p)}{\delta^2 P_{\mathrm{e}}}. \tag{4.21}$$

The distance v_j is estimated using a bisection method (which will be given later on for the examples of the BSC and the AWGN channel) with a complexity of $\mathcal{O}(\log_2 N)$, where N is the code length. The time complexity of the proposed QA method is then given by

$$\mathscr{T}_{\mathrm{QA}}(\delta, P_{\mathrm{e}}) = \mathcal{O}(J \log_2 N) = \mathcal{O}\left(\frac{\overline{F}_R(r_p)}{\delta^2 P_{\mathrm{e}}} \log_2 N\right). \tag{4.22}$$

We define the simulation gain of our QA method over the MC simulation method as

$$\tau = \frac{\mathscr{T}_{\mathrm{MC}}(\delta, P_{\mathrm{e}})}{\mathscr{T}_{\mathrm{QA}}(\delta, P_{\mathrm{e}})} = \mathcal{O}\left(\frac{1}{\overline{F}_R(r_p) \log_2 N}\right). \tag{4.23}$$

Fig. 4.3 shows the speedup of the QA simulation method over the MC method in the case of the BSC. Results are presented for $N = 512$ and different values of r_p and SNR.

In the case of a discrete channel and decoder equation (4.5) can be rewritten as

$$P_{\mathrm{e}} = \sum_{v=r_p}^{r_c} p_V(v) \overline{F}_R(v), \tag{4.24}$$

where $p_V(\cdot)$ represents the probability mass function of V. The QA estimator in (4.13) is then equivalent to

$$\widehat{P}_{\mathrm{e}}^{\mathrm{QA}} = \sum_{v} \overline{F}_R(v) \widehat{p}_V(v), \tag{4.25}$$

where $\widehat{p}_V(\cdot)$ represents the probability mass function of V that needs to be estimated.

Theorem 4.1.3. *Given a discrete channel and hard-decision decoder, the variance of the QA estimator is equal to*

$$Var[\widehat{P}_e^{QA}] = \sum_{v} \overline{F}_R^2(v) \frac{p_V(v)(1 - p_V(v))}{J} \tag{4.26}$$

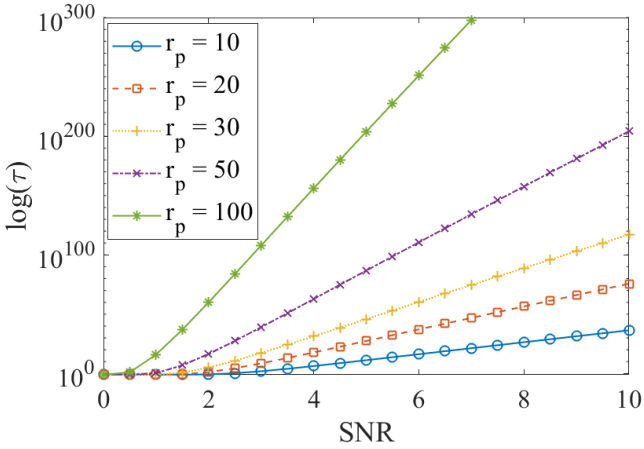

(a) Speedup as a function of SNR

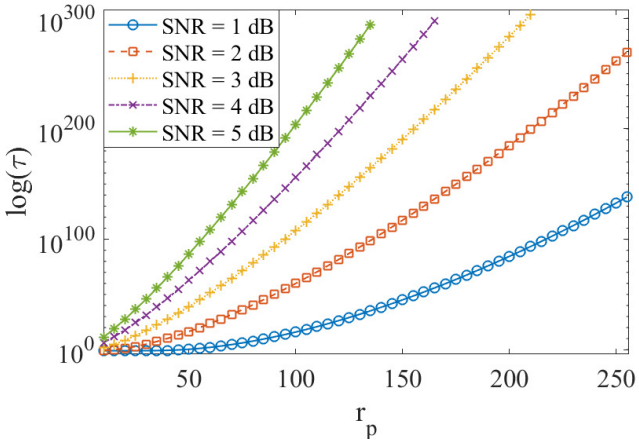

(b) Speedup as a function of r_p

Figure 4.3: *Speedup of the QA method over the MC in the case of the BSC, with* $N = 512$.

Proof. The variance of the QA estimator is given by

$$\mathrm{Var}[\widehat{P}_{\mathrm{e}}^{\mathrm{QA}}] = \mathrm{Var}\left[\sum_{v} \overline{F}_R(v)\widehat{p}_V(v)\right]. \tag{4.27}$$

Under the assumption that each generated sample of V is independent from each other and that $\overline{F}_R(v)$ is constant for specific value of v, variance of the QA estimator can be extended as

$$\mathrm{Var}[\widehat{P}_{\mathrm{e}}^{\mathrm{QA}}] = \sum_{v} \mathrm{Var}[\overline{F}_R(v)\widehat{p}_V(v)] = \sum_{v} \left(\overline{F}_R(v)\right)^2 \mathrm{Var}[\widehat{p}_V(v)]. \tag{4.28}$$

Since

$$p_V(v) = P[V = v] = E_V[\mathbb{1}_{\{v\}}(V)], \tag{4.29}$$

the probability function of V can be estimated using

$$\widehat{p}_V(v) = \frac{1}{J}\sum_{j=1}^{J} \mathbb{1}_{\{v\}}(v_j), \tag{4.30}$$

Estimator in (4.30) has a Binomial distribution with a known variance [106]

$$Var[\widehat{p}_V(v)] = \frac{p_V(v)(1-p_V(v))}{J}. \tag{4.31}$$

By substituting (4.31) in (4.28) the variance of the QA estimator becomes

$$Var[\widehat{P}_{\mathrm{e}}^{QA}] = \sum_{v} \overline{F_R}^2(v)\,\frac{p_V(v)(1-p_V(v))}{J}. \tag{4.32}$$

■

Theorem 4.1.4. *Given a discrete channel and a hard-decision decoder, the number of simulation runs J needed to achieve a given accuracy δ is upper bounded by*

$$J \leq \frac{1}{\delta^2}\sum_{v}\frac{1-p_V(v)}{p_V(v)} \tag{4.33}$$

Proof. Squaring both sides of (3.2) and replacing (4.26) and (4.24) in it gives

$$\delta^2 = \frac{Var[\widehat{P}_e^{QA}]}{P_e^2} = \frac{1}{J}\frac{\sum_v \overline{F_R}^2(v)p_V(v)\left(1-p_V(v)\right)}{\left(\sum_v p_V(v)\overline{F_R}(v)\right)^2}. \tag{4.34}$$

Using the Schwartz inequality

$$\left(\sum_i a_i\right)^2 \geq \sum_i (a_i)^2, \tag{4.35}$$

under the assumption that both sums converge and $a_i \geq 0$ for every i, the previous expression becomes

$$\delta^2 \leq \frac{1}{J}\frac{\sum_v \overline{F_R}^2(v)p_V(v)(1-p_V(v))}{\sum_v p_V^2(v)\overline{F_R}^2(v)}. \tag{4.36}$$

This expression can further be simplified by using the inequality

$$\frac{\sum_i a_i}{\sum_i b_i} \leq \sum_i \frac{a_i}{b_i}, \tag{4.37}$$

which holds under assumption that all sums in (4.36) converge and $a_i \geq 0$ and $b_i > 0$ for all i.

$$\delta^2 \leq \frac{1}{J}\sum_v \frac{\overline{F_R}^2(v)p_V(v)(1-p_V(v))}{p_V^2(v)\overline{F_R}^2(v)}, \tag{4.38}$$

which reduces to

$$\delta^2 \leq \frac{1}{J}\sum_v \frac{1-p_V(v)}{p_V(v)}. \tag{4.39}$$

It follows that the number of needed simulations to achieve accuracy δ is

$$J \leq \frac{1}{\delta^2}\sum_v \frac{1-p_V(v)}{p_V(v)}. \tag{4.40}$$

■

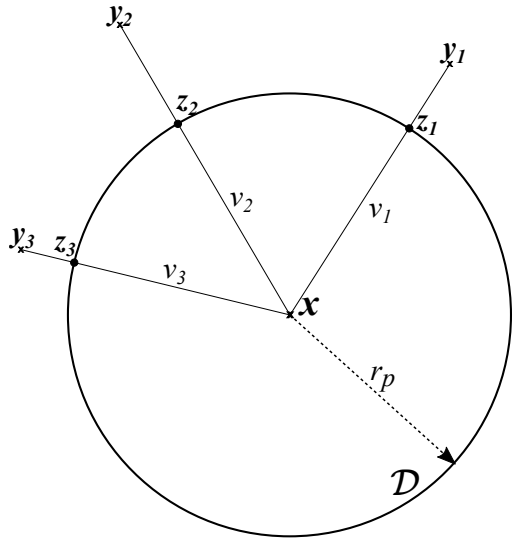

Figure 4.4: *Decoding region $\mathcal{D}$ of the codeword $\boldsymbol{x}$. r_p is the radius of the packing sphere and v_j is the distance from $\boldsymbol{x}$ to the distance point $\boldsymbol{z}_j$.*

We will give a simple example of using the proposed QA method to estimate the error probability of some arbitrary bounded distance decoder. This will be useful to point some additional facts about the practical implementation of our algorithm.

Example 4.1.5. Estimating the error probability of a general BD decoder (with respect to $\boldsymbol{x}$) shown in Fig. 4.4, defined as

$$D(\boldsymbol{y}) = \begin{cases} \boldsymbol{x}, & d(\boldsymbol{x}, \boldsymbol{y}) \leq r_p \\ \text{error}, & \text{otherwise} \end{cases}. \tag{4.41}$$

The function $\overline{F}_R(\cdot)$ is defined by the channel model and we assume it is known analytically or it can be numerically evaluated (which is usually the case). Numerical evaluation of $\overline{F}_R(\cdot)$ is computationally more expensive so it is recommended to use the maximum number of

measured distances (J) as a stopping rule (as opposed to formula (3.5)), and if a grater accuracy is needed to generate more distances (which is very fast). In this case we set $J = 3$ and the iterator $j = 0$.

We generate a random point $\boldsymbol{Y} = \boldsymbol{y}_1 \notin \mathcal{D}$ and increase the iterator to $j = 1$. When choosing a random point, it is important that the geodesic segment from $\boldsymbol{x}$ to $\boldsymbol{Y}$ is chosen uniformly at random. As there is at least one geodesic segment $\gamma_{[\boldsymbol{x},\boldsymbol{y}_1]}$ (which is guaranteed by the system model) we can use the bisection method to find the distance point $\boldsymbol{z}_1$ and calculate $v_1 = d(\boldsymbol{x}, \boldsymbol{z}_1)$. We repeat this procedure until $J = 3$ and then after calculating the relative precision we decide if we need to generate more points or if we can calculate the error probability using the formula (4.13).

Note that we only assume that the decoding region is a metric star domain. By using additional information about the decoder (e.g. bounded distance property) it is possible to additionally reduce the number of iterations needed (in this case to $J = 1$). If we know that the decoder used is a BD decoder with a known r_p our algorithm reduces to analytical evaluation of the error probability ($J = 0$).

If there is a point $\boldsymbol{y}$ such that $d(\boldsymbol{x}, \boldsymbol{y}) = \infty$ (as in the case of the octahedron code in Example 2.2.3) we say that the decoding region is "open". It is important to detect open regions or the simulation may halt. When an open region is found, the counter is incremented but the point is not taken into account when calculating the error probability (i.e. $\overline{F}_R(\infty) = 0$).

4.1.1 QA Simulation for the BSC

Given a BSC $\boldsymbol{Y} = \boldsymbol{x} + \boldsymbol{W}$, with $\mathcal{Y} = \mathbb{F}_2^N$, and a matched Hamming metric d_H, a geodesic segment $\gamma_{[\boldsymbol{x},\boldsymbol{Y}]}$ corresponds to a Hamming line (aka cube dominating path or Boolean line), defined as a sequence of points $\{\boldsymbol{a}_1, \boldsymbol{a}_2, \dots \boldsymbol{a}_K\}$, $K = d_H(\boldsymbol{x}, \boldsymbol{Y}) + 1$, with $\boldsymbol{a}_1 = \boldsymbol{x}$, $\boldsymbol{a}_K = \boldsymbol{Y}$ and $d_H(\boldsymbol{a}_k, \boldsymbol{a}_{k+1}) = 1, k = 1, \dots K - 1$ [107]. Each component of the noise vector $\boldsymbol{W} \in \mathbb{F}_2^N$ is generated according to a Bernoulli distribution $\mathcal{B}(p)$.

Sufficient condition for a decoder D to be star domain is given by

$$D(\boldsymbol{x}+\boldsymbol{w}) = \boldsymbol{x} \Rightarrow D(\boldsymbol{x}+\boldsymbol{w}\Lambda) = \boldsymbol{x}, \tag{4.42}$$

where $\Lambda \in \mathbb{F}_2^{N\times N}$ is a diagonal matrix.

Let $\mathcal{A}$ be a set of all lines $\{\boldsymbol{a}_1, \dots \boldsymbol{a}_{N+1}\}$, with $\boldsymbol{a}_1 = \mathbf{0}$ (all-zero vector) and $\boldsymbol{a}_{N+1} = \mathbf{1}$ (all-one vector). Given a line $\mathscr{A} \in \mathcal{A}$ there is a unique distance point $\boldsymbol{z}_{\mathscr{A}} = \boldsymbol{x} + \boldsymbol{a}^*$ where

$$\boldsymbol{a}^* = \underset{d_H(\boldsymbol{x},\boldsymbol{x}+\boldsymbol{a})}{\arg\max} \{\boldsymbol{a} \in \mathscr{A} : \boldsymbol{x}+\boldsymbol{a} \in \mathcal{D}\}. \tag{4.43}$$

Error probability can be defined as

$$P_{\mathrm{e}} = \frac{1}{|\mathcal{A}|} \sum_{\mathscr{A}\in\mathcal{A}} P[R > d_H(\boldsymbol{x}, \boldsymbol{z}_{\mathscr{A}})] = P[R > V], \tag{4.44}$$

where $|\mathcal{A}|$ is the cardinality of set $\mathcal{A}$, and V is an auxiliary random variable that represents the distance between the codeword and a random distance point. The tail distribution function of a Binomial random variable R is given by

$$\overline{F}_R(v) = (1-p)^N \sum_{n=v+1}^{N} \binom{N}{n} \left(\frac{p}{1-p}\right)^n. \tag{4.45}$$

In case of the BSC, distance v is found using a modified bisection algorithm for the discrete case, presented in Algorithm 3.

Algorithm 3 *Bisection method for the discrete case (e.g. BSC)*

$\mathscr{A} \leftarrow \{\boldsymbol{a}_1 \cdots \boldsymbol{a}_{N+1}\}$ {select a random line}
$\boldsymbol{a} \leftarrow \boldsymbol{a}_1 = \mathbf{0}$ {all zero vector}
$\boldsymbol{b} \leftarrow \boldsymbol{a}_{N+1} = \mathbf{1}$ {all one vector}
$k \leftarrow \lceil \frac{N+1}{2} \rceil$
repeat
  $\boldsymbol{c} \leftarrow \boldsymbol{a}_k$
  if $D(\boldsymbol{x} + \boldsymbol{c}) = \boldsymbol{x}$ **then**
    $\boldsymbol{a} \leftarrow \boldsymbol{c}$
    $k = k + \lfloor \frac{d_H(\boldsymbol{a},\boldsymbol{b})}{2} \rfloor$
  else
    $\boldsymbol{b} \leftarrow \boldsymbol{c}$
    $k = k - \lfloor \frac{d_H(\boldsymbol{a},\boldsymbol{b})}{2} \rfloor$
  end if
until $d_H(\boldsymbol{a}, \boldsymbol{b}) = 1$ {Distance point found}
$v_i = d_H(\boldsymbol{x}, \boldsymbol{a})$

4.1.2 QA Simulation for the AWGN Channel

Given an AWGN channel $\boldsymbol{Y} = \boldsymbol{x} + \boldsymbol{W}$, with $\mathcal{Y} = \mathbb{R}^N$ and a matched Euclidean metric, a geodesic segment $\gamma_{[\boldsymbol{x},\boldsymbol{Y}]}$ corresponds to a straight line segment (in $\mathbb{R}^N$) between the codeword $\boldsymbol{x}$ and the channel output $\boldsymbol{Y}$. Each component of the noise vector $\boldsymbol{W} \in \mathbb{R}^N$ is generated according to a zero mean Normal distribution $\mathcal{N}(0, \sigma^2)$ with variance σ^2.

Sufficient condition for a decoder D to be star domain is given by

$$D(\boldsymbol{x} + \boldsymbol{w}) = \boldsymbol{x} \Rightarrow D(\boldsymbol{x} + \alpha\boldsymbol{w}) = \boldsymbol{x}, \ \forall \alpha \in [0, 1], \tag{4.46}$$

Let $\mathcal{E}$ be a set of feasible directions at codeword $\boldsymbol{x}$ [108] with $\boldsymbol{e} \in \mathcal{E}$, and $d(\boldsymbol{x}, \boldsymbol{e}) = 1$. Random noise vector can be written as $\boldsymbol{W} = R\boldsymbol{E}$, where random variable R represents the magnitude of the noise vector in some random direction $\boldsymbol{E} \in \mathcal{E}$. Error probability can then be defined

as

$$P_{\mathrm{e}} = \frac{1}{area(\mathcal{E})} \int_{\boldsymbol{e}\in\mathcal{E}} \left[\int_0^{\infty} p_R(r) \overline{\mathbb{1}}_{\mathcal{D}}(\boldsymbol{x} + r\boldsymbol{e}) dr \right] d\boldsymbol{e}, \tag{4.47}$$

Under the assumption that $\mathcal{D}$ is a star domain, for each $\boldsymbol{e} \in \mathcal{E}$ there is a unique distance point $\boldsymbol{z}_{\boldsymbol{e}} = \boldsymbol{x} + v_{\boldsymbol{e}}\boldsymbol{e}$, where

$$v_{\boldsymbol{e}} = d(\boldsymbol{x}, \boldsymbol{z}_{\boldsymbol{e}}) = \arg\max_r \{r \geq 0 : \boldsymbol{x} + r\boldsymbol{e} \in \mathcal{D}\}. \tag{4.48}$$

Error probability can now be defined as

$$P_{\mathrm{e}} = \frac{1}{area(\mathcal{E})} \int_{\boldsymbol{e}\in\mathcal{E}} \left[\int_{v_{\boldsymbol{e}}}^{\infty} p_R(r) dr \right] d\boldsymbol{e}, \tag{4.49}$$

or more precisely

$$P_{\mathrm{e}} = \frac{1}{area(\mathcal{E})} \int_{\boldsymbol{e}\in\mathcal{E}} P[R > v_{\boldsymbol{e}}] d\boldsymbol{e} = P[R > V], \tag{4.50}$$

where V is an auxiliary random variable that represents the distance between the codeword and a distance point in some random direction $\boldsymbol{E}$. In the case of the AWGN, random variable R has a χ_N distribution with a tail distribution function

$$\overline{F}_R(v) = \overline{\Gamma}\left(\frac{N}{2}, \frac{v^2}{2\sigma^2}\right). \tag{4.51}$$

Function $\overline{\Gamma}(s, x)$ is the regularized upper incomplete gamma function

$$\overline{\Gamma}(s, x) = \frac{\Gamma(s, x)}{\Gamma(s)} \tag{4.52}$$

where

$$\Gamma(s, x) = \int_x^{\infty} t^{s-1} e^{-t} dt, \tag{4.53}$$

is the upper incomplete gamma function and

$$\Gamma(s) = \int_0^{\infty} t^{s-1} e^{-t} dt \tag{4.54}$$

is the gamma function.

The steps for finding the distance v are given in Algorithm 4. This procedure can be used for any continuous noise vector distribution.

Algorithm 4 *Bisection method for the continuous case (e.g. AWGN)*

$\boldsymbol{w} \leftarrow \boldsymbol{W}$ {Generate a random error sequence}
$\boldsymbol{e} = \frac{\boldsymbol{w}}{\|\boldsymbol{w}\|}$ {unit energy noise specifying its direction only}
$a \leftarrow 0$, $b \leftarrow 1$
while $D(b * \boldsymbol{e}) = \mathbf{0}$ {Until the error occurs for the first time} **do**
  $a \leftarrow b$, $b \leftarrow b * 2$
end while
repeat
  $c \leftarrow (a + b)/2$
  if $D(\boldsymbol{x} + c * \boldsymbol{e}) = \boldsymbol{x}$ **then**
    $a \leftarrow c$
  else
    $b \leftarrow c$
  end if
until $b - a < \varepsilon$ (predefined precision)
$v_j \leftarrow c$

4.2 Analysis of the QA Simulation Method

For the purpose of analyzing the performance of the QA estimator, we use small codes coupled with an MD decoder because they have analytically known error probability. In the case of the AWGN channel, we use the octahedron code [109], and in the case of the BSC we use the Reed–Muller RM(1, 5) code of length $N = 32$ and dimension $K = 6$. [110, 111].

$\widehat{P}_{\mathrm{e}}^{QA}$ such that J takes values from a set of logarithmically spaced points in the interval of $[10^2, 10^6]$, was calculated for E_b/N_0 ranging from $-1.6dB$ to $10dB$ with a step of $0.1dB$, and compared to the ana-

lytically known P_{e}. Average relative error (3.6) with $I = 100$ was used as a measure of accuracy.

Fig. 4.5 shows the accuracy of the QA estimator as a function of generated samples, for fixed values of E_b/N_0. The average relative error decreases linearly in log scale as the number of samples (J) grows.

Fig. 4.6 shows the accuracy of the QA estimator as a function of E_b/N_0, for fixed values of J. As it can be seen the accuracy of the estimator slowly decreases with E_b/N_0, and as J grows it becomes more stable.

Fig. 4.7 shows the comparison of the QA estimated error probability ($\widehat{P}_{\mathrm{e}}^{QA}$), with $J = 10000$ measured distances, and the analytically calculated error probability (P_{a}). By increasing J the difference would become even smaller.

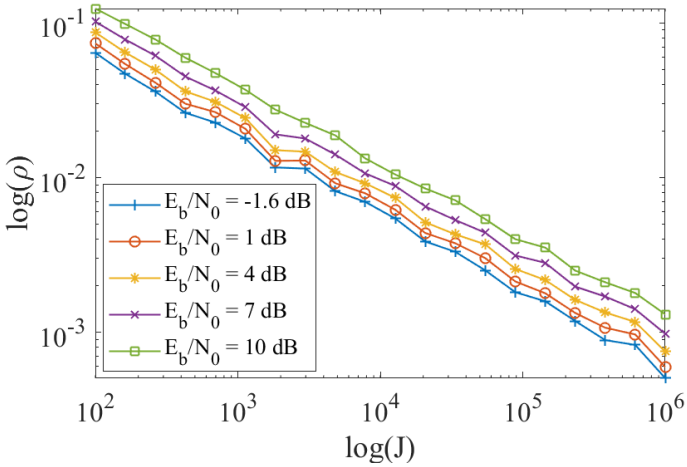

(a) Octahedron code

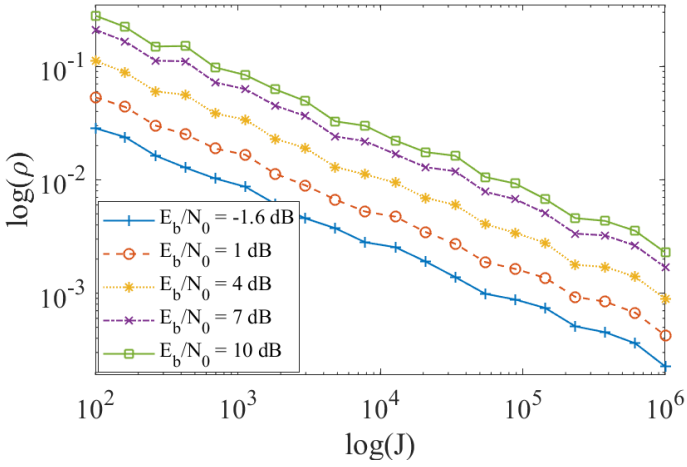

(b) RM(1, 5) code

Figure 4.5: *QA Estimator accuracy as a function of measured distances.*

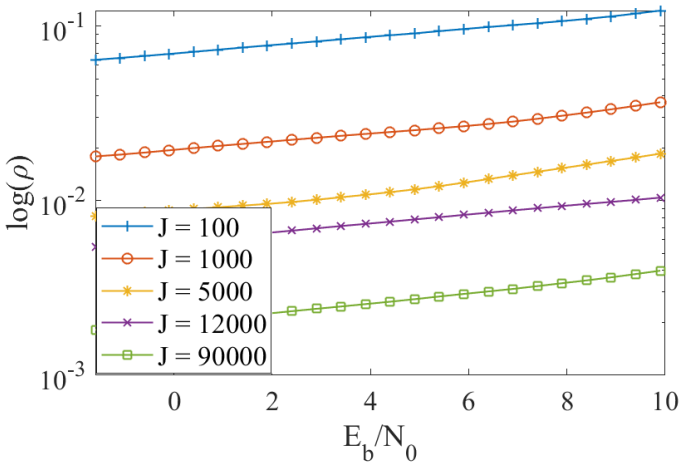

(a) Octahedron code

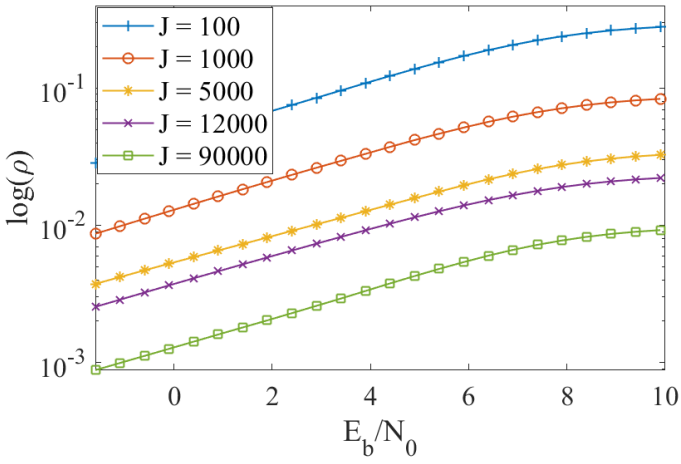

(b) RM(1, 5) code

Figure 4.6: *QA Estimator accuracy as a function of* E_b/N_0.

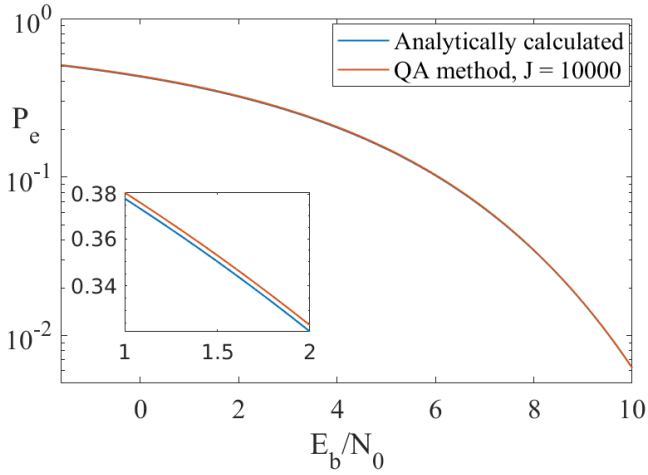

(a) Octahedron code, with J = 10000

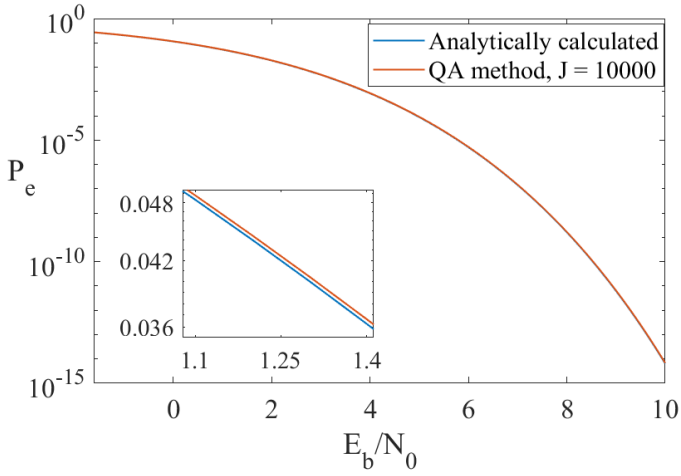

(b) RM(1, 5) code, with J = 10000

Figure 4.7: *Comparison of analytically calculated and QA estimated error probability for different values of* E_b/N_0.

Chapter 5

Numerical Results

This chapter concludes part I of the thesis. A comparison of our QA method and MC and IS methods is first given. We show that our QA method is at least 10^3 times faster then the MC method and at least 10 times faster then the current state of the art IS method, for the same accuracy. Some comments about future work are given at the end of this chapter.

5.1 Comparison of Different Simulation Methods

We will now demonstrate our QA method for the case of AWGN and BSC, and we will compare it to the MC and IS methods, described in Chapter 3, in terms of accuracy and speed.

In the case of the BSC, we used low rate BCH codes [85] of length 63, 127 and 255, couppled with an MD decoder. For the purpose of comparing different simulation methods in the case of the AWGN, we used binary polar codes [47] of length 128, 256, 512 and 1024 with rate 1/2. At the receiver we used a SCD, as described in [47]. We also give results for the Reed-Muller RM(1, 5) code coupled with the OSD. The generator matrix of an (N, K) polar code, where $N = 2^M$, can be generated by taking Arikan's kernel G_2, building its Kronecker product M times (building $G_2^{\otimes M}$) and selecting K rows corresponding to the highest mutual information. Bits of the remaining $N - K$ channels are frozen (usually set to 0) [17,47]. The generator matrix of an (N, K) RM

code is generated by taking K rows with the highest Hamming weight from $G_2^{\otimes M}$ [17, 112]. OSD and the successive cancellation decoding of binary polar codes are described in Chapter 2.2.1 and Chapter 2.2.2, respectively. For the transmission over the AWGN channel we use a simple binary phase shift keying (BPSK) modulation scheme.

For these codes error probability was first estimated using the MC and IS simulation methods for different values of E_b/N_0. The performance of polar codes was estimated for E_b/N_0 ranging from $-1.6dB$ to $3.3dB$, with a step of $0.1dB$ (a total of 50 SNR values), while the performance of BCH codes and RM(1, 5) code was estimated for E_b/N_0 ranging from $-1.6dB$ to $5.8dB$, with a step of $0.1dB$ (a total of 75 SNR values). Each SNR value was run with a sequential stopping rule of $\widehat{\delta} = 0.05$. An additional sequential stopping rule of 2^{31} simulation runs per SNR point was used. The QA method was used to estimate the error probability at the same SNR values as both MC and IS methods. As our QA method is SNR-invariant simulation was run until an average relative error of $\widehat{\delta} = 0.05$ was reached (global stopping rule).

All three simulation methods are compared in terms of the total number of simulation runs needed, and the results for the polar codes with sequential decoding are given in Table 5.1, the results for the RM(1, 5) code with OSD are given in Table 5.2 and the results for the BCH codes with MD decoding are given in Table 5.3. Fig. 5.1 shows the error probability curves of different polar codes obtained by the QA simulation method. The difference between the MC, IS and QA simulation methods for the example of (256, 128) polar code is shown in Fig. 5.3(a) and a detailed view is shown in Fig. 5.3(b). Fig. 5.2 presents the error probability of the RM(1, 5) code under OSD decoding with 1, 3 and 6 (maximum likelihood) refactoring steps. The difference between the MC, IS and QA simulation methods for the example of BCH (127, 8, 31) is shown in Fig. 5.4(a) and a detailed view is shown in Fig. 5.4(b).

Table 5.1: *Run time comparison of different simulation methods for (N,K) Polar Codes with PSCD*

Polar codes	MC method	IS method	QA method
K = 64, N = 128	$2 \cdot 10^7$	$1.3 \cdot 10^5$	$3.5 \cdot 10^4$
K = 128, N = 256	$3.7 \cdot 10^7$	$3.7 \cdot 10^5$	$4.7 \cdot 10^4$
K = 256, N = 512	$2.5 \cdot 10^7$	$2.9 \cdot 10^5$	$6 \cdot 10^4$
K = 512, N = 1024	$1.8 \cdot 10^6$	$7.3 \cdot 10^5$	$9.5 \cdot 10^4$

Table 5.2: *Run time comparison of different simulation methods for the RM(1, 5) code with OSD*

OSD order	MC method	IS method	QA method
Refactoring steps: 1	$8.1 \cdot 10^6$	$4.1 \cdot 10^6$	$7.1 \cdot 10^4$
Refactoring steps: 3	$3.7 \cdot 10^7$	$7.8 \cdot 10^6$	$7.1 \cdot 10^4$
Refactoring steps: 6	$3.7 \cdot 10^7$	$8.7 \cdot 10^6$	$7.3 \cdot 10^4$

Table 5.3: *Run time comparison of different simulation methods for (N,K,T) BCH codes with MD decoder*

BCH codes	MC method	IS method	QA method
K = 7, N = 63, T = 15	$1.8 \cdot 10^9$	$1.2 \cdot 10^6$	$2.8 \cdot 10^4$
K = 8, N = 127, T = 31	$9.2 \cdot 10^9$	$5.6 \cdot 10^6$	$2.6 \cdot 10^5$
K = 9, N = 255, T = 63	$1.8 \cdot 10^{10}$	$2.26 \cdot 10^7$	$3.7 \cdot 10^5$

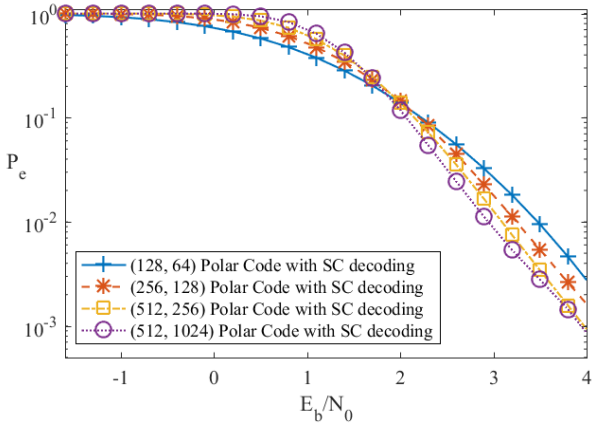

Figure 5.1: *Quasi-analytical error probability of Polar Codes, using QA simulation method.*

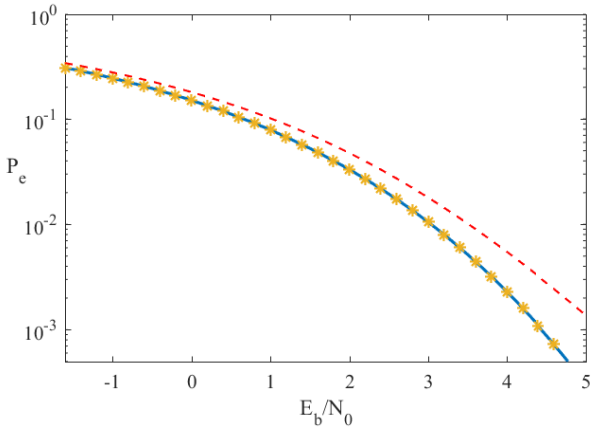

Figure 5.2: *Quasi-analytical error probability of RM(1, 5) code with ordered statistics decoding and 1 refactoring step (– –), 3 refactoring steps (∗) and 6 refactoring steps (—).*

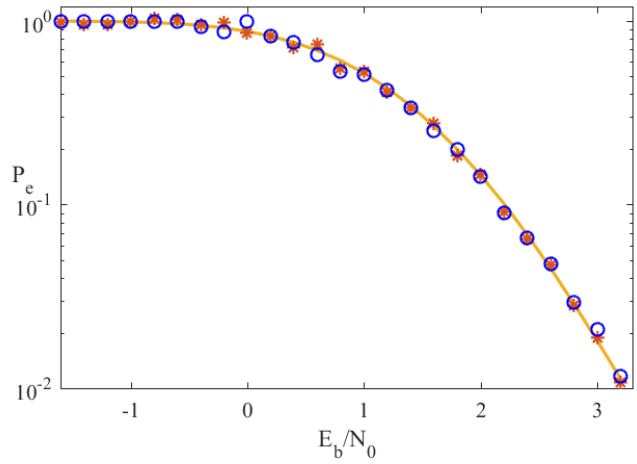

(a) Error probability of (256,128) polar code

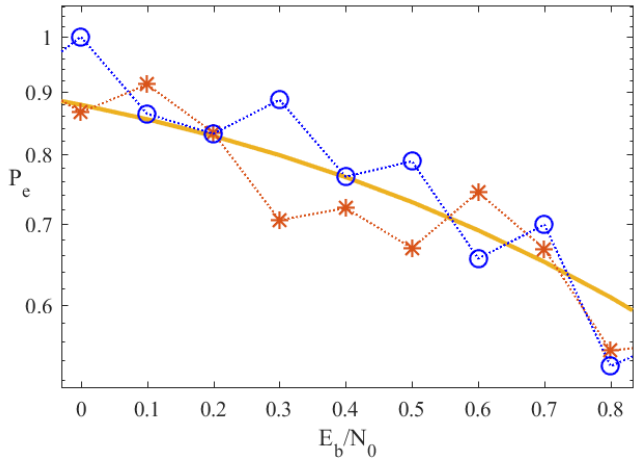

(b) Detailed view

Figure 5.3: *Error Probability of (256,128) polar code using QA (—), MC (∘) and IS (∗) simulation methods.*

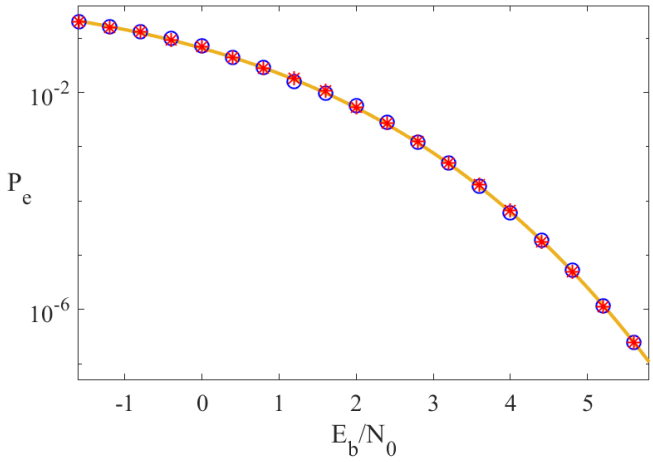

(a) Error probability of BCH (127, 8, 31) code

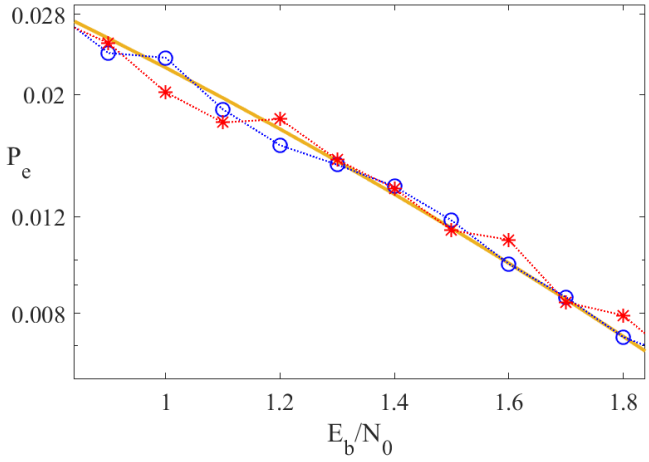

(b) Detailed view

Figure 5.4: *Error Probability of BCH (127, 8, 31) code using QA (—), MC (∘) and IS (∗) simulation methods.*

5.2 Conclusion

This part introduced a novel Quasi-Analytical (QA) method for estimating the error probability of a communication system. The QA method was compared to the classical Monte Carlo and Importance Sampling methods and it was shown that it outperforms them in both accuracy and speed, especially at high SNR regime.

Although this method can be used to accurately predict the waterfall region of the message passing decoders, a modification of the algorithm is needed to estimate the error floor. This goes beyond this thesis and will be addressed in a sequel.

Future work will also address applications of our QA method to estimate the error probability of more complex communication systems.

Part II

Trellis Coded Modulation Design by Optimized Set Partitioning

Chapter 6
Multidimensional Coded Modulation

This chapter sets the mathematical foundation for the development of our algorithm (for designing spherical codes that are optimized for set partitioning) in the next chapter. We first give an overview of multidimensional modulation schemes with an emphasis on spherical codes. We introduce the problem of spherical code design and discuss how they can be used to design a multidimensional coded modulation. Trellis coded modulation technique is presented with an emphasis on encoder and decoder implementation.

6.1 Multidimensional Modulation

Claude E. Shannon was the first to show that a real signal (of finite bandwidth) can mathematically be represented as a point in Euclidean space [76, 113]. This was very important for the development of digital communications and especially digital modulations. In the case of quadrature modulations, bits are mapped to real signals of the following form

$$s(t) = I(t)\cos(2\pi f_c t) + Q(t)\sin(2\pi f_c t), \tag{6.1}$$

where t represents time, f_c represents the carrier frequency and $I(t)$ and $Q(t)$ represent the *in-phase* and *quadrature* components of the signal. It follows that every digital signal of this form can be represented as a point $[I(t), Q(t)] \in \mathbb{R}^2$, which is called a modulation symbol (or constellation point).

Recent advances in MIMO, and optical and visible-light communication systems allow the use of additional "dimensions" [63–65, 69, 70], which can result in a modest coding gain and better energy savings [114]. It is also possible to combine T N-dimensional symbols (without coding) into an NT-dimensional symbol, but implementation of such a system also involves added complexity and latency, which may outweigh the performance gains [114]. Significant performance gain can be achieved by coding sequences of symbols in such a way that not all sequences are possible [114]. This approach is called coded modulation [85].

Constellation is an algebraic representation of the modulation signal space. The constellation of an N-dimensional modulation is a finite set $\mathcal{C} \subset \mathbb{R}^N$ of N-dimensional real vectors (constellation points), and the size, $M = |\mathcal{C}|$, of a constellation is the number of its points [115, 116]. The distance between points $\boldsymbol{x}_i$, $\boldsymbol{x}_j \in \mathcal{C}$ $(i \neq j)$ is defined as

$$d_{i,j} = \|\boldsymbol{x}_i - \boldsymbol{x}_j\|. \tag{6.2}$$

Performance of $\mathcal{C}$ is characterized by the minimum distance, defined as

$$d_{\min} = \min_{i \neq j} d_{i,j}, \tag{6.3}$$

and the average constellation energy, defined as [117]

$$P(\mathcal{C}) = \frac{1}{MN} \sum_{\boldsymbol{x} \in \mathcal{C}} \|\boldsymbol{x}\|^2. \tag{6.4}$$

By increasing the energy, $d_{\min}$ is also increased and error rate is improved, but this will also increase the cost of the system, and in many cases is impractical. When designing a constellation we usually assume $P(\mathcal{C}) = 1$, and try to maximize the minimum distance. It is well known that the problem of designing a good multidimensional constellation for the bandwidth-limited AWGN channel is equivalent to packing points within a unit sphere in $\mathbb{R}^N$ [113]. This is known as the sphere packing problem [76, 117, 118]. Two practical approaches for solving the sphere packing problem include lattice constellations [76, 117, 118] and spherical codes [76, 119–121].

6.1.1 Lattice Constellations

Given a *plane lattice* Λ [76, 117, 118, 122], a lattice constellation (aka lattice code) is defined as a set of lattice points (translated by a vector $\boldsymbol{c}$, i.e. a coset) that lie inside a compact bounding region $\mathcal{R} \subset \mathbb{R}^N$ [76, 117, 118]

$$\mathcal{C}(\Lambda, \mathcal{R}) = (\Lambda + \boldsymbol{c}) \cap \mathcal{R}. \tag{6.5}$$

Lattice codes have good minimum distance and algebraic properties (i.e. geometrically uniform), which is useful for designing low complexity encoding and decoding algorithms [117, 118, 123–126].

6.1.2 Spherical Codes

A constellation, $\mathcal{C}(M, N)$, where every N-dimensional vector is a point on the surface of a unit sphere (every signal in the signal space has the same unit energy), is called a spherical code [75–78]. The equi-energy property of spherical codes makes them very useful for fading channels. In higher dimensions all lattice constellations approach spherical codes. This is a consequence of the sphere hardening phenomenon [113, 127].

Sphere hardening claims that by the law of large numbers, all points will (almost surely) lie in a small shell around the surface of the sphere, or more formally: for any $\epsilon > 0$ and any Gaussian iid vector $\boldsymbol{X} \in \mathbb{R}^N$, with components generated according to the $\mathcal{N}(0, \sigma^2)$ distribution, the following holds true

$$N \to \infty \Rightarrow P[N(\sigma - \epsilon) \leq \|\boldsymbol{X}\|^2 \leq N(\sigma + \epsilon)] \to 1. \tag{6.6}$$

The configuration of points with the largest $d_{\min}$ for a given N and M is called the densest packing and the corresponding spherical code is often called the best (N, M) spherical code. For $N = 3$ and $M = 12$ the best spherical code is given by a regular icosahedron [76] (Fig. 6.1a).

A list of densest packings and best lattices is available at [76, 128].

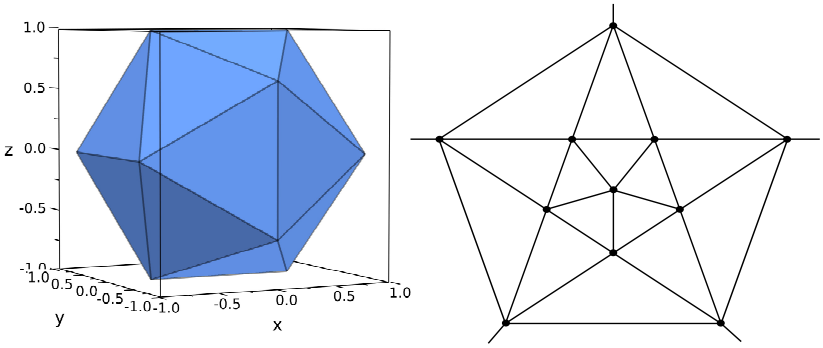

Figure 6.1: *Icosahedron code and its stereographic projection.*

6.2 Visualization of 3D Spherical Codes

Stereographic projection [129] is a mapping that projects a sphere onto a plane, and, as such, it is a useful tool for visualizing 3D spherical codes. The result of the stereographic projection of a 3D spherical code is a planar graph, often called the Schlegel diagram [130, 131]. The procedure for generating the Schlegel diagram of a spherical code, used in this thesis, is given in Algorithm 5. For simplicity we assume that the center of projection is the point $[0, 0, 1]$. If a different point $\boldsymbol{p}$ is chosen as the center of projection, the constellation is first rotated so that $\boldsymbol{p} = [0, 0, 1]$.

If a point corresponding to one of the codewords is chosen as the center of projection, that point will be mapped to infinity. This is visualized as a straight line going from points that are at a minimum distance from the center of projection (Fig 6.1b).

Besides Schlegel diagrams, spherical codes are often represented as polar plots. This is useful if constellation points are represented using spherical coordinates [132].

Algorithm 5 *Stereographic projection*

Input:
constellation $\mathcal{C} \subset \mathbb{R}^3$,
distance $d_{\min}$,
for $i \in \{1, 2, ..., M\}$ **do**
$\boldsymbol{x}_i^* \leftarrow [\frac{x_{i,1}}{1-x_{i,3}}, \frac{x_{i,2}}{1-x_{i,3}}]$ {$[0, 0, 1]$ is the center of projection}
end for
for $i \in \{1, 2, ..., M\}$ **do**
for $j \in \{1, 2, ...M\}$ **do**
if $i \neq j$ **then**
$d_{i,j} \leftarrow \|\boldsymbol{x}_i - \boldsymbol{x}_j\|$ {Find the distance between distinct points.}
if $d_{i,j} = d_{\min}$ **then**
Connect points $\boldsymbol{x}_i^*$ and $\boldsymbol{x}_j^*$
end if
end if
end for
end for

6.3 Design of Spherical Codes

Problem of designing an (M, N) spherical code is usually stated as an optimization problem of distributing M points on an N-dimensional unit sphere so that the minimum distance between any pair of points is maximized (packing problem),

Optimization problem 6 *Packing problem*

$$\begin{aligned} &\text{minimize} && -\min_{i \neq j} \|\boldsymbol{x}_j - \boldsymbol{x}_i\| \\ &\text{subject to} && \|\boldsymbol{x}_i\| = 1;\ i = 1, \ldots, M. \end{aligned} \tag{6.7}$$

As the cost function in (6.7) locally depends only on the distance between two points, it is common to model the constellation points as repealing particles (repealing by the conservative central force). The packing problem can then be restated as the minimization of the total potential energy (V) of the constellation (generalized Thomson problem). The new optimization problem is

Optimization problem 7 *Total potential energy minimization*

$$\begin{aligned} &\text{minimize} && V = \sum_{i<j} V_{ij}^{\beta-2} \\ &\text{subject to} && \|\boldsymbol{x}_i\| = 1;\ i = 1, \ldots, M, \end{aligned} \tag{6.8}$$

where

$$V_{ij} = \frac{\gamma}{\|\boldsymbol{x}_j - \boldsymbol{x}_i\|} \tag{6.9}$$

represents the interaction energy occurring between the two particles, β is the exponent of the inverse power law and

$$\gamma = \min_{i \in \{1,\ldots,M\} \setminus \{j\}} \|\boldsymbol{x}_j - \boldsymbol{x}_i\| \tag{6.10}$$

is a constant used to prevent overflow (or underflow).

As $\beta \to \infty$, the cost function in (6.8) is dominated by the smallest distance and the force equilibrium (the stationary point of V) is attained. As V is a differentiable function, this optimization problem is usually solved using a gradient descent or Newton's method. In order to satisfy the constraint, vectors are either normalized after every iteration [78] or represented using spherical coordinates (distance maximization is equivalent to angle maximization) [77]. Both approaches have been shown to converge to a local optimum. There is however no guarantee that the local optimum is also a global optima, so in order to obtain results as good as possible, optimization procedure is repeated multiple times with a different initial configuration.

6.4 Trellis Coded Modulation

TCM is a combined coding and modulation technique for digital transmission over a bandwidth-limited channel, which allows the achievement of significant coding gains over conventional uncoded modulation schemes, without compromising bandwidth efficiency.

TCM was first proposed by Gottfried Ungerboeck in his 1976 paper [71], followed by a more detailed description in [72] and [73, 74]. TCM with multidimensional constellations (aka multidimensional TCM) was introduced in [133]. TCM became very popular in the early nineties and was adopted in satellite, modem and mobile communication standards [134–136]. Today it is mostly used in space and optical communication systems [63, 64].

The main idea of TCM, proposed by Ungerboeck, was to maximize the Euclidean distance between sequences of modulation symbols. This was accomplished by coding on subsets of constellations using techniques and principles from channel coding theory (e.g. convolutional codes, trellis diagrams, Viterbi algorithm). TCM codes coupled with a sequential decoder are known to achieve up to a 5.8 dB coding gain (reaching the cut-off rate of a bandwidth-limited AWGN channel) [137, 138]. Theoretically, an NT-dimensional lattice constellation can achieve the same coding gain as an N-dimensional TCM of length T, but at a higher decoding complexity. In order to approach the Shannon capacity more closely, a powerful extension of the TCM, known as multilevel coding [85, 139, 140] is often used. Multilevel codes are often coupled with some powerful multistage decoding technique that has a much better performance/complexity trade-off then classical ML and near-ML decoders [141–143].

6.4.1 Set Partitioning

The main idea of TCM is to separate codewords in such a way as to maximize the squared Euclidean distance between codewords in the

same subset. This is called *set partitioning*. Set partitioning of classical 1D and 2D modulation schemes is straightforward and is demonstrated in Example 6.4.1 for the case of an 8-PSK modulation.

Example 6.4.1. Set partitioning of an 8-PSK constellation is shown in Fig. 6.4.1. We first label all points with labels "A" and "B" in such a way that no two adjacent points have the same label. After that, we partition the constellation $\mathcal{C}$ into subset $\mathcal{C}_A$, which contains only points with label "A", and subset $\mathcal{C}_B$, which contains only points with label "B". We repeat this to get subsets $\mathcal{C}_{AA}$, $\mathcal{C}_{AB}$, $\mathcal{C}_{BA}$ and $\mathcal{C}_{BB}$.

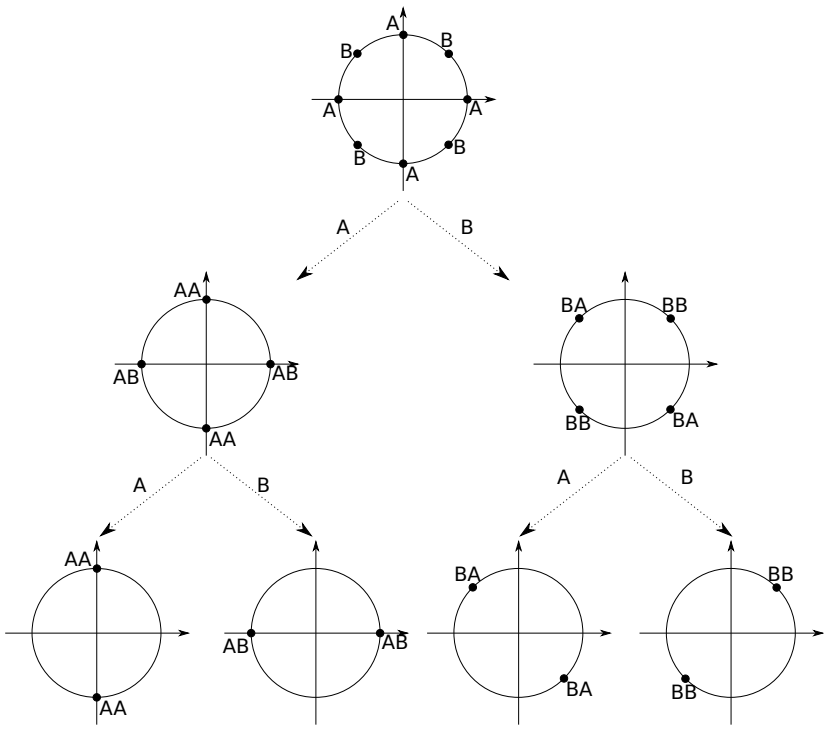

Figure 6.2: *Set Partitioning of an 8-PSK modulation.*

Lattice constellations can be effectively partitioned into subsets by exploiting group-theoretic properties of lattices [138]. Set partitioning of spherical codes is more complicated, as there is generally no nice geometric structure that can be exploited. Example 6.4.2 shows set partitioning of the icosahedron code.

Example 6.4.2. Set partitioning of the icosahedron code is shown in Fig. 6.4.2. All five ■ symbols represent the same point at infinity (the center of projection).

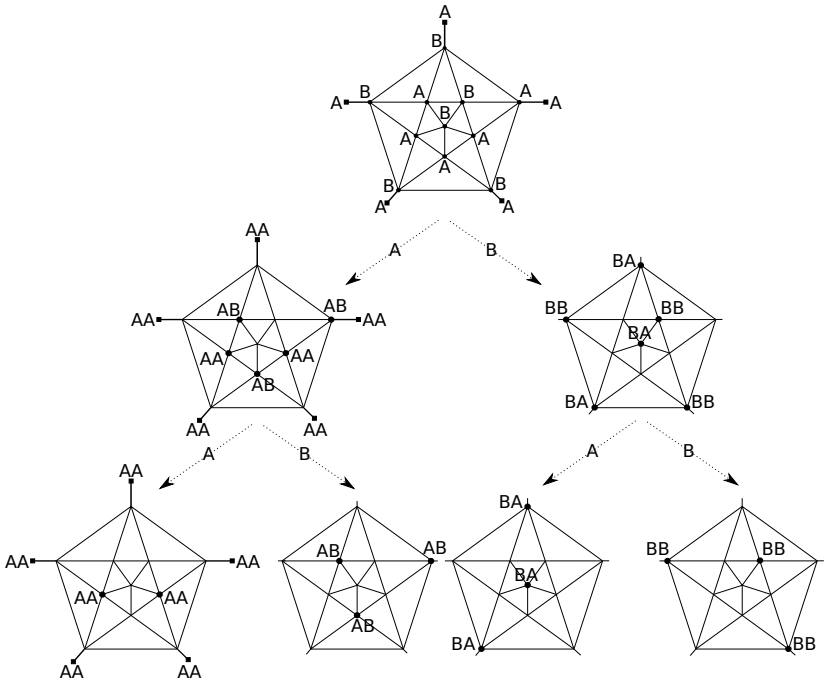

Figure 6.3: *Set Partitioning of the icosahedron code.*

We start by selecting two points that are at $d_{\min}$ from each other, and give them labels "A" and "B". In a greedy manner, we select one

point that is furthest from all points with label "A" and give it the same label. We do the same for "B". We repeat this until all points are labeled. This will divide the constellation $\mathcal{C}$ into subsets $\mathcal{C}_A$ and $\mathcal{C}_B$. We repeat the labeling step in order to get partitions $\mathcal{C}_{AA}$, $\mathcal{C}_{AB}$, $\mathcal{C}_{BA}$ and $\mathcal{C}_{BB}$. Set partitioning improves $d_{\min}$ from 1.0514 to $1,7013$.

A simple procedure for set partitioning of spherical codes is presented in Algorithm 8. This procedure is computationally expensive, but as it is done only once per code, during the design phase, it does not affect the TCM encoding or decoding complexity.

Algorithm 8 *Set partitioning of spherical codes*

Input:
constellation $\mathcal{C}$, distance $d_{\min}$, CONDITION
{CONDITION represents a stopping criterion (e.g num. of subsets)}
SetPartitionProcedure$(\mathcal{C}, d_{min})$:
if CONDITION **then**
Return $\mathcal{C}$
end if
$\mathcal{C}_A \leftarrow \{\}$, $\mathcal{C}_B \leftarrow \{\}$
Find $\boldsymbol{x}_i, \boldsymbol{x}_j \in \mathcal{C}$ such that $d_{i,j} = d_{\min}$
$\mathcal{C}_A \leftarrow \boldsymbol{x}_i$, $\mathcal{C}_B \leftarrow \boldsymbol{x}_j$,$\mathcal{C} \rightarrow \boldsymbol{x}_i, \boldsymbol{x}_j$ {Remove $\boldsymbol{x}_i, \boldsymbol{x}_j$ from $\mathcal{C}$}
repeat
Find $\boldsymbol{x} \in \mathcal{C}$, farthest from $\mathcal{C}_A$
$\mathcal{C}_A \leftarrow \boldsymbol{x}$, $\mathcal{C} \rightarrow \boldsymbol{x}$
Find $\boldsymbol{x} \in \mathcal{C}$, farthest from $\mathcal{C}_B$
$\mathcal{C}_B \leftarrow \boldsymbol{x}$, $\mathcal{C} \rightarrow \boldsymbol{x}$
until $\mathcal{C} = \{\}$
Find $d^A_{\min}$ and $d^B_{\min}$.
Call *SetPartitionProcedure*$(\mathcal{C}_A, d^A_{\min})$
Call *SetPartitionProcedure*$(\mathcal{C}_B, d^B_{\min})$

6.4.2 TCM Encoding

Figure 6.4 shows a TCM encoder. Some of the input bits are encoded using a convolutional encoder (usually of rate $\frac{K}{K+1}$). Encoded bits are used to select a subset (or more precisely a sequence of subsets), while uncoded bits are used to select a point from a subset.

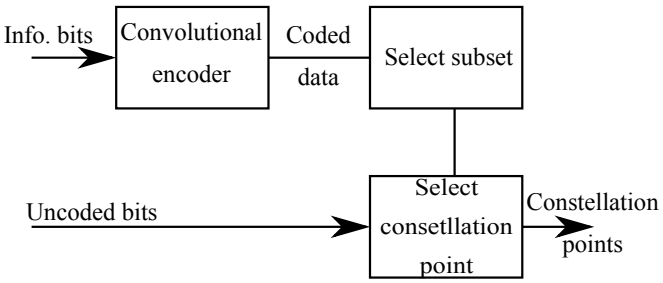

Figure 6.4: *TCM encoder.*

TCM code is usually represented using a trellis diagram [85]. Each point $\boldsymbol{x} \in \mathcal{C}$ is assigned to a transition in the trellis. Points belonging to the same subset are assigned to parallel transitions (Fig. 6.5a).

Encoded bits are used to select a path (Fig. 6.5b) in the trellis, while uncoded bits are used to select one of the parallel transitions (point from a subset) for each trellis segment.

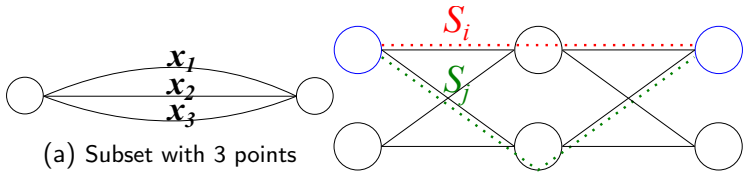

(a) Subset with 3 points

(b) Trellis segment with 2 paths (sequences of subsets): S_i and S_j

Figure 6.5: *Trellis representation of a TCM code.*

Any two paths S_i and S_j $(i \neq j)$ from a trellis that diverge in one state and merge in another, after more than one transition, have path distance $d_{\mathrm{p}}(S_i, S_j)$ (Fig. 6.5b). Let the minimum path distance in a trellis be d_{p}. The free Euclidean distance of a TCM code is defined as

$$d^2_{\mathrm{free}} = \min(d_{\mathrm{p}}, d_{\mathrm{ip}}), \tag{6.11}$$

where d_{ip} represents the intra-partition distance. Given an AWGN channel with noise variance σ^2, error probability of a TCM code, at high SNR, can be approximated as

$$P_{\mathrm{e}} \approx \exp\left\{\frac{-d^2_{\mathrm{free}}}{2\sigma^2}\right\}. \tag{6.12}$$

6.4.3 Viterbi Decoding

The Viterbi decoding algorithm is a dynamic programming algorithm for finding the "shortest" (the most likely) path in a trellis with respect to a given metric. The choice of metric depends on the problem, for example the squared Euclidean distance is used in case of the TCM.

An N-dimensional TCM codeword of length T, $\boldsymbol{x} = [\boldsymbol{x}_1, ..., \boldsymbol{x}_T] \in \mathbb{R}^{NT}$, is sent over the bandwidth-limited AWGN channel. At the receiver a channel output $\boldsymbol{Y} = \boldsymbol{x} + \boldsymbol{W}$ is detected and decoded using the Viterbi decoding algorithm [85].

Viterbi algorithm keeps track of several possible paths with the best accumulated metric. At every stage $t \in \{1, 2, ...T\}$, the Viterbi algorithm merges all the surviving paths that arrive in each state, and keeps only the ones with the smallest metric. The paths are then updated by finding the closest point $\boldsymbol{x}_t$ to the channel output $\boldsymbol{y}_t$ and adding the distance $\|\boldsymbol{x}_t - \boldsymbol{y}_t\|$ to the accumulated metric path for every state in the trellis. Once the end of the trellis has been reached, the best surviving path is chosen as the correct codeword.

Chapter 7

Optimized Set Partitioning

In this chapter we introduce the problem of TCM design by optimized set partitioning. We present an optimization problem and develop an algorithm, based on the repulsive force method, for solving it. The algorithm is then used to design several 3D TCM codes, which are compared to the best known spherical codes with the same number of points. We show that it is possible to achieve a coding gain over conventional spherical codes - especially at high SNR. Some comments about future work are given at the end of this chapter.

7.1 Problem Formulation and Algorithm

Instead of designing a "good" spherical code (a code with a good minimum distance) which is to be partitioned into subsets, we propose to a-priori divide randomly generated constellation points into subsets and then:

1. maximize the minimum distance between the points belonging to the same subset (intra-partition distance),

2. maximize the minimum distance between subsets, given the memory of the underlying trellis code.

The number of subsets and points in each subset is defined by the TCM. We will refer to this approach as optimized set partitioning (OSP).

The initial configuration of points is generated by choosing M vectors with components drawn according to the Normal $\mathcal{N}(0,1)$ distri-

bution. This guarantees that all vectors have a uniformly random orientation in space. The vectors are then normalized to the surface of the unit sphere. The initial set of points is divided into D (D divides M) subsets, with M/D points in each subset. The choice of subsets is arbitrary.

The optimized set partitioning is a multi-objective optimization problem. In order to maximize the free distance over the minimum distance we first modify the formula for the interaction energy between the two particles (equation (6.9)) to

$$V_{ml}(\alpha) = \frac{\gamma}{\alpha\|\boldsymbol{x}_l - \boldsymbol{x}_m\|},\ \alpha = \begin{cases}\alpha_1, & \mathbb{1}_{\mathcal{X}_m}(\boldsymbol{x}_l) = 1\\ \alpha_2, & \text{otherwise}\end{cases}, \tag{7.1}$$

with $\alpha_1 + \alpha_2 = 1$ and $\alpha_2 > \alpha_1$. This ensures that the particles belonging to the same subset will exert greater force than the other particles.

Linear scalarization is the simplest method to convert a multi-objective optimization problem into a single objective optimization problem.

Optimization problem 9 *Optimized set partitioning*

$$\begin{aligned}\text{minimize}\quad & V = (1-\lambda)\sum_{m<l}\left(V_{ml}(\alpha_1)\mathbb{1}_{\mathcal{X}_m}(\boldsymbol{x}_l)\right)^{\beta}\\ & \quad +\lambda\sum_{m<l}\left(V_{ml}(\alpha_2)\overline{\mathbb{1}}_{\mathcal{X}_m}(\boldsymbol{x}_l)\right)^{\beta}\\ \text{subject to}\quad & \|\boldsymbol{x}_m\| = 1;\ m = 1,\ldots,M,\end{aligned} \tag{7.2}$$

We solve this optimization problem using the conjugate gradient method, because of its simplicity. As in [78] the constraint is satisfied by normalizing the vectors after every iteration. The conservative central force from point $\boldsymbol{x}_m$ to point $\boldsymbol{x}_l$ is defined as

$$\boldsymbol{F}_{m\to l} = \begin{cases}-\nabla_{\boldsymbol{x}_l} V_{ml}^{\beta-2}(\alpha_1), & \mathbb{1}_{\mathcal{X}_m}(\boldsymbol{x}_l)\\ -\nabla_{\boldsymbol{x}_l} V_{ml}^{\beta-2}(\alpha_2), & \text{otherwise}\end{cases}. \tag{7.3}$$

$$\boldsymbol{F}_{m\to l} \propto \begin{cases} \left(\frac{\gamma}{\alpha_1\|\boldsymbol{x}_l-\boldsymbol{x}_m\|}\right)^{\beta} \alpha_1(\boldsymbol{x}_l-\boldsymbol{x}_m), & \mathbb{1}_{\mathcal{X}_m}(\boldsymbol{x}_l) \\ \left(\frac{\gamma}{\alpha_2\|\boldsymbol{x}_l-\boldsymbol{x}_m\|}\right)^{\beta} \alpha_2(\boldsymbol{x}_l-\boldsymbol{x}_m), & \text{otherwise} \end{cases}. \tag{7.4}$$

The total resulting force other particles exert on particle $\boldsymbol{x}_l$ is given by

$$\boldsymbol{F}_{\to l} = -\nabla_{\boldsymbol{x}_l} V = \sum_{m\in\{1,\dots,M\}\setminus\{l\}} \boldsymbol{F}_{m\to l}. \tag{7.5}$$

In order to avoid numerical problems, we first calculate the direction of the force and then move the point in that direction. The direction of the force is calculated as

$$\boldsymbol{F}^*_{\to l} = \frac{\boldsymbol{F}_{\to l}}{\|\boldsymbol{F}_{\to l}\|}. \tag{7.6}$$

New value of $\boldsymbol{x}_l$ can be calculated using a simple update rule

$$\boldsymbol{x}_l^{k+1} = \boldsymbol{x}_l^k + \frac{\gamma}{2\beta}\boldsymbol{F}^*_{\to l}. \tag{7.7}$$

Let $\mathcal{C}' = \{\boldsymbol{x}'_1, \dots \boldsymbol{x}'_M\}$ be a constellation generated by applying the proposed algorithm to the original constellation $\mathcal{C} = \{\boldsymbol{x}_1, \dots \boldsymbol{x}_M\}$. Then, the total move norm L_{MOV} is defined as

$$L_{\mathrm{MOV}}(\mathcal{C}, \mathcal{C}') = \sum_{m=1}^{M} \|\boldsymbol{x}_m - \boldsymbol{x}'_m\|. \tag{7.8}$$

Whenever β is increased too rapidly, the vectors are forced into a state of a numerical deadlock. To avoid this we use the same strategy (Algorithm 10) as presented in [78].

Algorithm 10 *β update rule*

Input:
constellation $\mathcal{C}$
Initialization:
$a = 1$, $b = 2$
Update procedure:
Set $\beta = 2^b$
Calculate $\mathcal{C}'$, and $L_{\mathrm{MOV}}(\mathcal{C}, \mathcal{C}')$
Set $\beta = 2^{b(1+1/a)}$
Calculate $\mathcal{C}''$, and $L_{\mathrm{MOV}}(\mathcal{C}, \mathcal{C}'')$
if $L_{\mathrm{MOV}}(\mathcal{C}, \mathcal{C}') > L_{\mathrm{MOV}}(\mathcal{C}, \mathcal{C}'')$ **then**
$\mathcal{C} = \mathcal{C}'$
else
$\mathcal{C} = \mathcal{C}''$
$b = b(1 + \frac{1}{a})$
end if

7.2 Simulation Results

We used optimized set partitioning to generate three 3D spherical codes with $M = 12$, 16 and 24. This codes are used to design a TCM code with memory 3, length 36 (trellis was terminated after 36 segments) and generator polynomials, given in the standard left-alligned octal notation, $(74, 64)$. This codes are compared to TCM codes designed using classical 3D spherical codes that correspond to the densest packings with the same number of points. Set partitioning of classical codes was done using Algorithm 8. Viterbi decoding algorithm was used at the receiver side.

All codes are compared in terms of the first error probability [27, 85] (which is equivalent to the block error probability in the case of

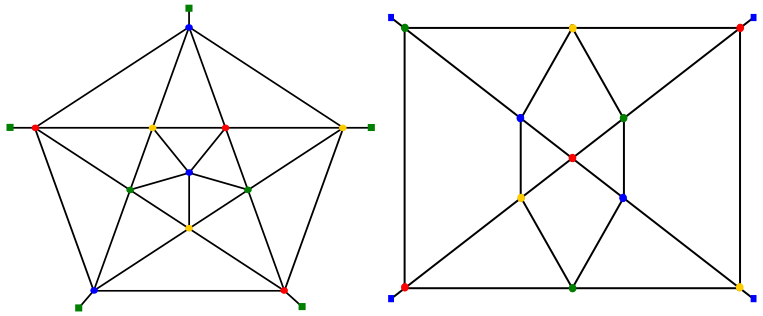

(a) Icoashedron (b) Cuboctahedron

Figure 7.1: *Set partitions of icosahedron and cuboctahedron cdoes*

convolutional codes), for the case of the AWGN channel with E_b/N_0 ranging from $-1.6db$ to $14dB$. Error probability was estimated using the QA simulation method described in part I of this thesis, with 10^7 measured distances. We show, that even compared to the best known codes, it is still possible to get a coding gain using weaker codes that are optimized for the specific TCM.

Table 7.1 shows a comparison of the minimum and *intra-partition* distances and the distance gain achieved using our method.

Table 7.1: *Comparison of the minimum and intra-partition distance for different* (M, N) *spherical codews*

Code		Classical	OSP	Distance gain
$M = 12,\ N = 3$	$d_{\min}$	1.051462	1.0	−0.051462
	d_{ip}	1.7013	1.73205	+0.03075
$M = 16,\ N = 3$	$d_{\min}$	0.88057	0.7966	−0.08397
	d_{ip}	1.5390	1.5926	+0.0536
$M = 24,\ N = 3$	$d_{\min}$	0.744206	0.71483	−0.029376
	d_{ip}	1.254	1.3208	+0.0668

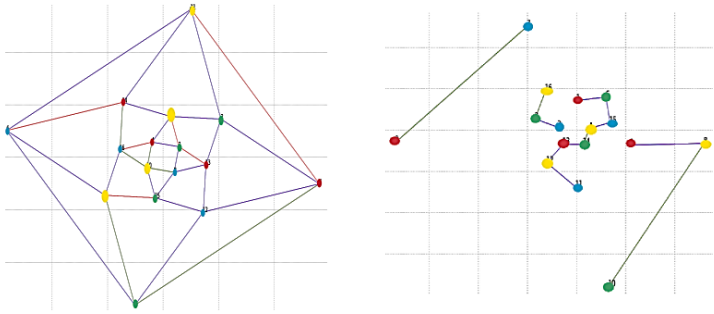

(a) Classical (16,3) (b) OSP (16,3)

Figure 7.2: *Set partitions of two (16,3) spherical codes.*

Figure 7.1a shows the stereographic projection and set partitions of the icosahedron code. Using optimized set partitioning we got a spherical code corresponding to the cuboctahedron, with set partitions shown in Fig. 7.1b. Figures 7.2a and 7.2b show stereographic projections corresponding to the two (16,3) codes and their set partitions. Figures 7.3a and 7.3b show the stereographic projections corresponding to the two (24,3) codes and their set partitions.

Figure 7.4 shows error rate probability comparison of the icosahedron and the cuboctahedron (which was obtained using the OSP method) code. Cuboctahedron has a small coding gain at high SNR. This is expected as the d_{ip} of the two codes is very similar. Figure 7.5 shows error rates for the classical and OSP generated (16,3) code. Comparison of the classical and OSP generated (24,3) code is given in Fig. 7.6. We see that a crucial coding gain is achieved over the classical spherical code. As was expected, achieved coding gain is directly proportional to the achieved *intra-partition* distance gain.

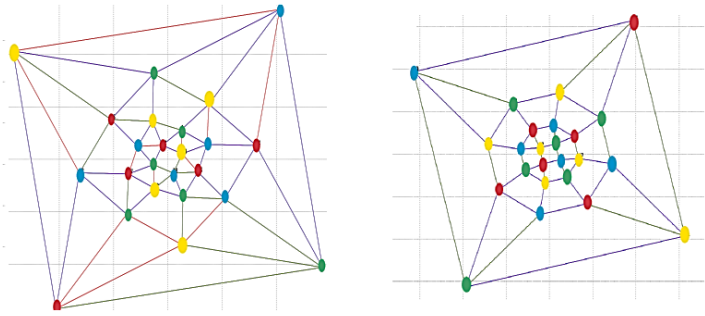

(a) Classical (24,3) (b) OSP (24,3)

Figure 7.3: *Set partitions of two (24,3) spherical codes.*

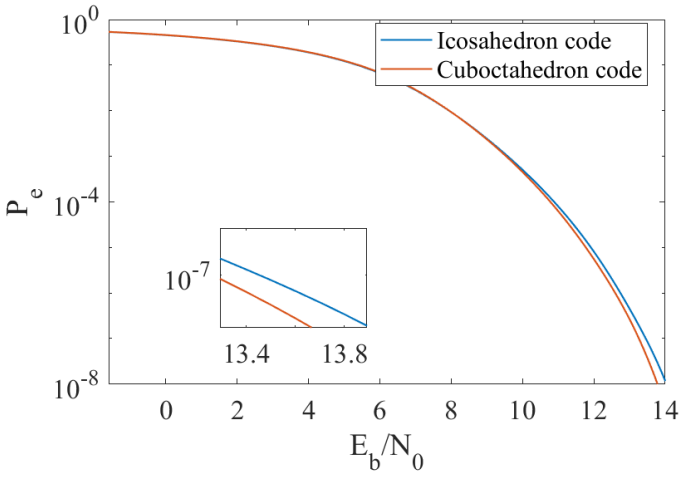

Figure 7.4: *QA estimated BLER comparison of two (12, 3) spherical codes.*

7.3 Conclusion

In this chapter we presented a novel approach to constructing TCM from spherical codes, optimized for set partitioning. It was shown that

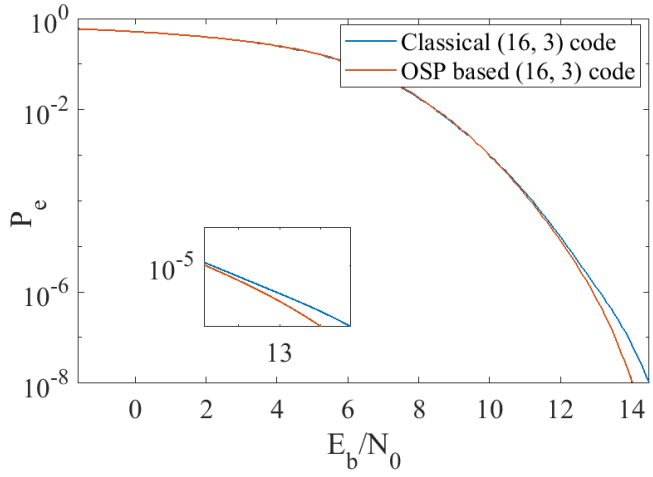

Figure 7.5: *QA estimated BLER comparison of two (16, 3) spherical codes.*

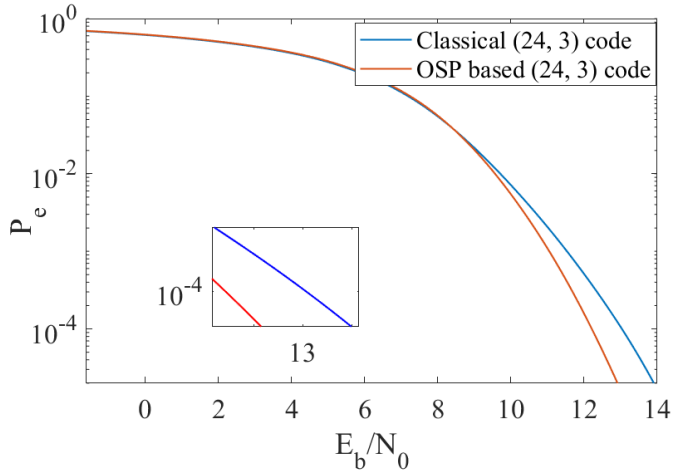

Figure 7.6: *QA estimated BLER comparison of two (24, 3) spherical codes.*

this approach allows for construction of new multidimensional modulation schemes that achieve better performance to classical schemes when combined with TCM.

Different coded modulation schemes might benefit from different partitioning strategies. By introducing additional restrictions it is possible to reduce the encoding complexity but probably at the result of coding gain. This needs to be investigated further.

Bibliography

[1] M. Shirvanimoghaddam, M. Sadegh Mohamadi, R. Abbas, A. Minja, B. Matuz, G. Han, Z. Lin, Y. Li, S. Johnson, and B. Vucetic, "Short Block-length Codes for Ultra-Reliable Low-Latency Communications," *IEEE Communications Magazine*, 2018.

[2] Petar Popovski, Kasper F. Trillingsgaard, Osvaldo Simeone, and Giuseppe Durisi, "5G wireless network slicing for eMBB, URLLC, and mMTC: A communication-theoretic view," *CoRR*, vol. abs/1804.05057, 2018.

[3] H. Ji, S. Park, J. Yeo, Y. Kim, J. Lee, and B. Shim, "Ultra-reliable and low-latency communications in 5g downlink: Physical layer aspects," *IEEE Wireless Communications*, vol. 25, no. 3, pp. 124–130, JUNE 2018.

[4] Carsten Bockelmann, Nuno Pratas, Hosein Nikopour, Kelvin Au, Tommy Svensson, Cedomir Stefanovic, Petar Popovski, and Armin Dekorsy, "Massive machine-type communications in 5G: physical and MAC-layer solutions," *IEEE Communications Magazine*, vol. 54, no. 9, pp. 59–65, 2016.

[5] Nuno K. Pratas, Sarath Pattathil, Cedomir Stefanovic, and Petar Popovski, "Massive machine-type communication (mMTC) access with integrated authentication," in *IEEE International Conference on Communications, ICC 2017, Paris, France, May 21-25, 2017*, 2017, pp. 1–6.

[6] P. Popovski, J. J. Nielsen, C. Stefanovic, E. d. Carvalho, E. Strom, K. F. Trillingsgaard, A. S. Bana, D. M. Kim, R. Kotaba, J. Park, and R. B. Sorensen, "Wireless access for ultra-reliable low-latency communication: Principles and building blocks," *IEEE Network*, vol. 32, no. 2, pp. 16–23, March 2018.

[7] Mehdi Bennis, Mérouane Debbah, and H. Vincent Poor, "Ultra-reliable and low-latency wireless communication: Tail, risk and scale," *Proceedings of the IEEE (in press)*, 2018.

[8] F. Boccardi, R. W. Heath, A. Lozano, T. L. Marzetta, and P. Popovski, "Five disruptive technology directions for 5G," *IEEE Communications Magazine*, vol. 52, no. 2, pp. 74–80, February 2014.

[9] A. M. Cipriano, P. Gagneur, G. Vivier, and S. Sezginer, "Overview of ARQ and HARQ in beyond 3G systems," in *2010 IEEE 21st International Symposium on Personal, Indoor and Mobile Radio Communications Workshops*, Sept 2010, pp. 424–429.

[10] Arjun Anand and Gustavo de Veciana, "Resource allocation and HARQ optimization for URLLC traffic in 5g wireless networks," *CoRR*, vol. abs/1804.09201, 2018.

[11] Kasper Fløe Trillingsgaard and Petar Popovski, "Generalized HARQ protocols with delayed channel state information and average latency constraints," *IEEE Trans. Information Theory*, vol. 64, no. 2, pp. 1262–1280, 2018.

[12] Y. Polyanskiy, H. V. Poor, and S. Verdu, "Feedback in the non-asymptotic regime," *IEEE Transactions on Information Theory*, vol. 57, no. 8, pp. 4903–4925, Aug 2011.

[13] Haobo Wang, Nathan Wong, Alexander M. Baldauf, Christopher K. Bachelor, Sudarsan V. S. Ranganathan, Dariush Divsalar, and Richard D. Wesel, "An information density approach to analyzing and optimizing incremental redundancy with feedback," in *2017 IEEE International Symposium on Information Theory, ISIT*, June 2017, pp. 261–265.

[14] A. R. Williamson, T. Chen, and R. D. Wesel, "Variable-length convolutional coding for short blocklengths with decision feedback," *IEEE*

Transactions on Communications, vol. 63, no. 7, pp. 2389–2403, July 2015.

[15] 3rd Generation Partnership project, "R1-1804849 - Remaining Issues on URLLC Data Channel Coding," Apr. 2018, 3GPP TSG RAN WGI Meeting#92bis - Discussion and Decision.

[16] G. Liva, L. Gaudio, and T. Ninacs, "Code design for short blocks: A survey," in *Proc. EuCNC*, Athens, Greece, June 2016.

[17] J. Van Wonterghem, A. Alloumf, J. J. Boutros, and M. Moeneclaey, "Performance comparison of short-length error-correcting codes," in *2016 Symposium on Communications and Vehicular Technologies (SCVT)*, Nov 2016, pp. 1–6.

[18] M. Sybis, K. Wesolowski, K. Jayasinghe, V. Venkatasubramanian, and V. Vukadinovic, "Channel coding for ultra-reliable low-latency communication in 5G systems," in *2016 IEEE 84th Vehicular Technology Conference (VTC-Fall)*, Sept 2016, pp. 1–5.

[19] M. P. C. Fossorier and Shu Lin, "Soft-decision decoding of linear block codes based on ordered statistics," *IEEE Transactions on Information Theory*, vol. 41, no. 5, pp. 1379–1396, Sep 1995.

[20] J. Van Wonterghem, Amira Alloum, J J Boutros, and Marc Moeneclaey, "On performance and complexity of OSD for short error correcting codes in 5g-nr," in *BalkanCom2017*, 06 2017.

[21] C. Shannon, "The zero error capacity of a noisy channel," *IRE Transactions on Information Theory*, vol. 2, no. 3, pp. 8–19, September 1956.

[22] Marat V. Burnashev, "Data transmission over a discrete channel with feedback," *Problems Inf. Transmission*, vol. 12, no. 4, pp. 250–265, 1976.

[23] Dejan E. Lazic and Vojin Senk, "A direct geometrical method for bounding the error exponent for any specific family of channel codes - I: cutoff rate lower bound for block codes," *IEEE Trans. Information Theory*, vol. 38, no. 5, pp. 1548–1559, 1992.

[24] Kasra Vakilinia, Sudarsan V. S. Ranganathan, Dariush Divsalar, and Richard D. Wesel, "Optimizing transmission lengths for limited feedback with nonbinary LDPC examples," *IEEE Trans. Communications*, vol. 64, no. 6, pp. 2245–2257, 2016.

[25] Haobo Wang, Sudarsan V. S. Ranganathan, and Richard D. Wesel, "Approaching capacity using incremental redundancy without feedback," in *2017 IEEE International Symposium on Information Theory, ISIT 2017, Aachen, Germany, June 25-30, 2017*, 2017, pp. 161–165.

[26] Carsten Bockelmann, Nuno K. Pratas, Gerhard Wunder, Stephan Saur, Monica Navarro, David Gregoratti, Guillaume Vivier, Elisabeth de Carvalho, Yalei Ji, Cedomir Stefanovic, Petar Popovski, Qi Wang, Malte Schellmann, Evangelos A. Kosmatos, Panagiotis Demestichas, Miruna Raceala-Motoc, Peter Jung, Slawomir Stanczak, and Armin Dekorsy, "Towards massive connectivity support for scalable mMTC communications in 5G networks," *IEEE Access*, vol. 6, pp. 28969–28992, 2018.

[27] Vojin Šenk, Dejan Lazić, et al., *Zastitno Kodovanje sa Statistickim Prepoznavanjem Oblika*, Vojnoizadavacki i novinski centar, 1989.

[28] "Minimum requirements related to technical performance for IMT-2020 radio interface(s) - draft," 2017.

[29] 3rd Generation Partnership project, "R1-1608770 - Flexibility Evaluation of Channel Coding Schemes for NR," Oct. 2016, 3GPP TSG RAN WGI Meeting#86 - Discussion and Decision.

[30] Michel C. Jeruchim, Philip Balaban, and K. Sam Shanmugan, Eds., *Simulation of Communication Systems: Modeling, Methodology and Techniques*, Kluwer Academic Publishers, Norwell, MA, USA, 2nd edition, 2000.

[31] William Tranter, K. Shanmugan, Theodore Rappaport, and Kurt Kosbar, *Principles of Communication Systems Simulation with Wireless Applications*, Prentice Hall Press, Upper Saddle River, NJ, USA, first edition, 2003.

[32] Rajan Srinivasan, *Importance sampling : applications in communications and detection*, Springer, Berlin, New York, 2002.

[33] James Antonio Bucklew, *Introduction to rare event simulation*, Springer series in statistics. Springer, New York, 2004.

[34] P. J. Smith, M. Shafi, and Hongsheng Gao, "Quick simulation: a review of importance sampling techniques in communications systems," *IEEE*

Journal on Selected Areas in Communications, vol. 15, no. 4, pp. 597–613, May 1997.

[35] M. Ferrari and S. Bellini, "Importance sampling simulation of concatenated block codes," *Communications, IEE Proceedings-*, vol. 147, no. 5, pp. 245–251, Oct 2000.

[36] G. Romano, A. Drago, and D. Ciuonzo, "Sub-optimal importance sampling for fast simulation of linear block codes over bsc channels," in *Wireless Communication Systems (ISWCS), 2011 8th International Symposium on*, Nov 2011, pp. 141–145.

[37] G. Romano and D. Ciuonzo, "Minimum-variance importance-sampling Bernoulli estimator for fast simulation of linear block codes over binary symmetric channels," *Wireless Communications, IEEE Transactions on*, vol. 13, no. 1, pp. 486–496, January 2014.

[38] Vojin Šenk and Predrag Radivojac, "An efficient simulation procedure for estimating the error probability of channel codes," *Proceedings of ITP, Symposium on Information Technology and Application*, pp. 21–24, 1995.

[39] Predrag Radivojac and Vojin Šenk, "An improved simulation procedure for estimating the error probability of channel codes," *Proceedings of YU-INFO, Symposium on Computer Science*, pp. 21–24, 1996.

[40] A. Mahadevan and J.M. Morris, "SNR-invariant importance sampling for hard-decision decoding performance of linear block codes," *Communications, IEEE Transactions on*, vol. 55, no. 1, pp. 100–111, Jan 2007.

[41] Vojin Šenk and Dejan Lazić, "A new quazi-analytical method of Monte Carlo simulation, and an appication," *Proceedings of IASTED International Symposium - Simulation and Modeling*, pp. 29–32, 1989.

[42] M.T. Core, R. Campbell, P. Quan, and J. Wada, "Semianalytic BER for PSK," *Wireless Communications, IEEE Transactions on*, vol. 8, no. 4, pp. 1644–1648, April 2009.

[43] DingDing Lu, S. Gupta, and M. Marcu, "Estimation of very low BER using quasi-analytical method," in *Electromagnetic Compatibility, 2008. EMC 2008. IEEE International Symposium on*, Aug 2008, pp. 1–4.

[44] Abhiji Bhattacharyya and Neetu Sood, "Semianalytical BER estimation of SC-QPSK under Nakagami-m frequency selective fading channel with diversity reception," in *Inter. Journal of Information and Electronics Engineering*, Jan 2014, vol. 4, pp. 67–69.

[45] A. Mahmood and R. Jäntti, "Packet error rate analysis of uncoded schemes in block-fading channels using extreme value theory," *IEEE Communications Letters*, vol. 21, no. 1, pp. 208–211, Jan 2017.

[46] E.R. Berlekamp, *Key papers in the development of coding theory*, IEEE Press selected reprint series. Institute of Electrical and Electronics Engineers, 1974.

[47] E. Arikan, "Channel polarization: A method for constructing capacity-achieving codes for symmetric binary-input memoryless channels," *IEEE Transactions on Information Theory*, vol. 55, no. 7, pp. 3051–3073, July 2009.

[48] Eren Şaşoğlu, "Polarization and polar codes," *Foundations and Trends® in Communications and Information Theory*, vol. 8, no. 4, pp. 259–381, 2012.

[49] E. Arikan and E. Telatar, "On the rate of channel polarization," in *2009 IEEE International Symposium on Information Theory*, June 2009, pp. 1493–1495.

[50] T. Tanaka and R. Mori, "Refined rate of channel polarization," in *2010 IEEE International Symposium on Information Theory*, June 2010, pp. 889–893.

[51] A. Eslami and H. Pishro-Nik, "On finite-length performance of polar codes: Stopping sets, error floor, and concatenated design," *IEEE Transactions on Communications*, vol. 61, no. 3, pp. 919–929, March 2013.

[52] Valerio Bioglio, Carlo Condo, and Ingmar Land, "Design of polar codes in 5g new radio," *CoRR*, vol. abs/1804.04389, 2018.

[53] A. Sharma and M. Salim, "Polar code: The channel code contender for 5g scenarios," in *2017 International Conference on Computer, Communications and Electronics (Comptelix)*, July 2017, pp. 676–682.

[54] K. Chen, K. Niu, and J. R. Lin, "List successive cancellation decoding of polar codes," *Electronics Letters*, vol. 48, no. 9, pp. 500–501, April 2012.

[55] I. Tal and A. Vardy, "List decoding of polar codes," *IEEE Transactions on Information Theory*, vol. 61, no. 5, pp. 2213–2226, May 2015.

[56] S. A. Hashemi, C. Condo, and W. J. Gross, "Fast and flexible successive-cancellation list decoders for polar codes," *IEEE Transactions on Signal Processing*, vol. 65, no. 21, pp. 5756–5769, Nov 2017.

[57] C. Xia, Y. Fan, J. Chen, C. Tsui, C. Zeng, J. Jin, and B. Li, "An implementation of list successive cancellation decoder with large list size for polar codes," in *2017 27th International Conference on Field Programmable Logic and Applications (FPL)*, Sept 2017, pp. 1–4.

[58] K. Niu and K. Chen, "Stack decoding of polar codes," *Electronics Letters*, vol. 48, no. 12, pp. 695 –697, June 2012.

[59] K. Chen, K. Niu, and J. Lin, "Improved successive cancellation decoding of polar codes," *IEEE Transactions on Communications*, vol. 61, no. 8, pp. 3100–3107, August 2013.

[60] Petar Popovski, Jimmy Jessen Nielsen, Cedomir Stefanovic, Elisabeth de Carvalho, Erik G. Ström, Kasper F. Trillingsgaard, Alexandru-Sabin Bana, Dong-Min Kim, Radoslaw Kotaba, Jihong Park, and René B. Sørensen, "Ultra-reliable low-latency communication (URLLC): principles and building blocks," *CoRR*, vol. abs/1708.07862, 2017.

[61] Taner Cevik and Serdar Yilmaz, "An overview of visible light communication systems," *International Journal of Computer Networks and Communications*, vol. 7, no. 6, 2015.

[62] M. Karlsson and E. Agrell, Eds., *Enabling Technologies for High Spectral-efficiency Coherent Optical Communication Networks, Ch. 2 - Multidimensional Optimized Optical Modulation Formats*, Chalmers Publication Library, 2016.

[63] David S. Millar, Toshiaki Koike-Akino, Sercan Ö. Arik, Keisuke Kojima, Kieran Parsons, Tsuyoshi Yoshida, and Takashi Sugihara, "High-dimensional modulation for coherent optical communications systems," *Opt. Express*, vol. 22, no. 7, pp. 8798–8812, Apr 2014.

[64] A. Alvarado and E. Agrell, "Four-dimensional coded modulation with bit-wise decoders for future optical communications," *Journal of Lightwave Technology*, vol. 33, no. 10, pp. 1993–2003, May 2015.

[65] J. He, Z. Wang, and H. Liu, "An efficient 4-D 8PSK TCM decoder architecture," *IEEE Transactions on Very Large Scale Integration (VLSI) Systems*, vol. 18, no. 5, pp. 808–817, May 2010.

[66] X. Zhang, Y. He, Y. Cai, M. Su, X. Zhou, Y. Chen, S. Chen, Y. Xiang, L. Chen, C. Su, Y. Li, and D. Fan, "Coherent separation detection for orbital angular momentum multiplexing in free-space optical communications," *IEEE Photonics Journal*, vol. 9, no. 3, pp. 1–11, June 2017.

[67] A. Demeter and C. Z. Kertesz, "Simulation of free-space communication using the orbital angular momentum of radio waves," in *2014 International Conference on Optimization of Electrical and Electronic Equipment (OPTIM)*, May 2014, pp. 846–851.

[68] Jian Wang, Jeng-Yuan Yang, Irfan M. Fazal, Nisar Ahmed, Yan Yan, Hao Huang, Yongxiong Ren, Yang Yue, Samuel Dolinar, Moshe Tur, and Alan E. Willner, "Terabit free-space data transmission employing orbital angular momentum multiplexing," *Nature Photonics*, vol. 6, pp. 488 EP –, Jun 2012, Article.

[69] B. Allen, A. Tennant, Q. Bai, and E. Chatziantoniou, "Wireless data encoding and decoding using OAM modes," *Electronics Letters*, vol. 50, no. 3, pp. 232–233, January 2014.

[70] C. Zhang and L. Ma, "Trellis-coded OAM-QAM union modulation with single-point receiver," *IEEE Communications Letters*, vol. 21, no. 4, pp. 690–693, April 2017.

[71] G. Ungerboeck and I. Csajka, "On improving data-link performance by increasing channel alphabet and introducing sequence coding," *Proc. IEEE Int. Symp. Information Theory (ISIT)*, June 1976.

[72] Gottfried Ungerboeck, "Channel coding with multilevel/phase signals," *IEEE Trans. Information Theory*, vol. 28, no. 1, pp. 55–66, 1982.

[73] G. Ungerboeck, "Trellis-coded modulation with redundant signal sets Part I: Introduction," *IEEE Communications Magazine*, vol. 25, no. 2, pp. 5–11, February 1987.

[74] G. Ungerboeck, "Trellis-coded modulation with redundant signal sets Part II: State of the art," *IEEE Communications Magazine*, vol. 25, no. 2, pp. 12–21, February 1987.

[75] A. Minja, I. Stanojević, and V. Šenk, "Tcm design optimizing set partitioning of 3-dimensional spherical codes," in *2013 21st Telecommunications Forum Telfor (TELFOR)*, Nov 2013, pp. 373–376.

[76] J.H. Conway and N.J.A. Sloane, *Sphere packings, lattices, and groups*, Grundlehren der mathematischen Wissenschaften. Springer-Verlag, 1993.

[77] Kari J. Nurmela and Kari J. Nurmela, "Constructing spherical codes by global optimization methods," 1995.

[78] Ivan Stanojević, Vojin Šenk, and Veljko Milutinović, "Application of maxeler dataflow supercomputing to spherical code design," *Transactions on Internet Research*, vol. 9, no. 2, pp. 1–4, 07 2013.

[79] M. Firer and J. L. Walker, "Matched metrics and channels," *IEEE Transactions on Information Theory*, vol. 62, no. 3, pp. 1150–1156, March 2016.

[80] Elena Deza and Michel-Marie Deza, *Dictionary of Distances*, Elsevier, Amsterdam, 2006.

[81] M.R. Bridson and A. Häfliger, *Metric Spaces of Non-Positive Curvature*, Grundlehren der mathematischen Wissenschaften. Springer Berlin Heidelberg, 2011.

[82] C. R. Smith, "A characterization of star-shaped sets," *The American Mathematical Monthly*, vol. 75, no. 4, pp. 386, April 1968.

[83] E. Viterbo and J. Boutros, "A universal lattice code decoder for fading channels," *IEEE Transactions on Information Theory*, vol. 45, no. 5, pp. 1639–1642, July 1999.

[84] B. Hassibi and H. Vikalo, "On the sphere-decoding algorithm i. expected complexity," *IEEE Transactions on Signal Processing*, vol. 53, no. 8, pp. 2806–2818, Aug 2005.

[85] S. Lin and D.J. Costello, *Error Control Coding*, Pearson-Prentice Hall, second edition, 2004.

[86] Marc P. C. Fossorier, "Reliability-based soft-decision decoding with iterative information set reduction," *IEEE Trans. Information Theory*, vol. 48, no. 12, pp. 3101–3106, 2002.

[87] A. Valembois and M. Fossorier, "Box and match techniques applied to soft-decision decoding," *IEEE Transactions on Information Theory*, vol. 50, no. 5, pp. 796–810, May 2004.

[88] W. Jin and M. Fossorier, "Probabilistic sufficient conditions on optimality for reliability based decoding of linear block codes," in *2006 IEEE International Symposium on Information Theory*, July 2006, pp. 2235–2239.

[89] Y. Wu and C. N. Hadjicostis, "Soft-decision decoding of linear block codes using preprocessing and diversification," *IEEE Trans. Inf. Theor.*, vol. 53, no. 1, pp. 378–393, Jan. 2007.

[90] Wenyi Jin and Marc P. C. Fossorier, "Enhanced box and match algorithm for reliability-based soft-decision decoding of linear block codes," in *GLOBECOM*. 2006, IEEE.

[91] Y. Wu and C. N. Hadjicostis, "Soft-decision decoding using ordered recodings on the most reliable basis," *IEEE Transactions on Information Theory*, vol. 53, no. 2, pp. 829–836, Feb 2007.

[92] Wenyi Jin and Marc P. C. Fossorier, "Reliability-based soft-decision decoding with multiple biases," *IEEE Trans. Information Theory*, vol. 53, no. 1, pp. 105–120, 2007.

[93] Yingquan Wu and Marc P. C. Fossorier, "Soft-decision decoding using time and memory diversification," in *ISIT*. 2008, pp. 76–80, IEEE.

[94] Y. Polyanskiy, H. V. Poor, and S. Verdu, "Channel coding rate in the finite blocklength regime," *IEEE Transactions on Information Theory*, vol. 56, no. 5, pp. 2307–2359, May 2010.

[95] R. Mori and T. Tanaka, "Performance and construction of polar codes on symmetric binary-input memoryless channels," in *2009 IEEE International Symposium on Information Theory*, June 2009, pp. 1496–1500.

[96] R. Mori and T. Tanaka, "Performance of polar codes with the construction using density evolution," *IEEE Communications Letters*, vol. 13, no. 7, pp. 519–521, July 2009.

[97] Tom Richardson and Ruediger Urbanke, *Modern Coding Theory*, Cambridge University Press, New York, NY, USA, 2008.

[98] Pascal Giard, Gabi Sarkis, Alexios Balatsoukas-Stimming, YouZhe Fan, Chi-Ying Tsui, Andreas Burg, Claude Thibeault, and Warren J. Gross, "Hardware decoders for polar codes: An overview," *CoRR*, vol. abs/1606.00737, 2016.

[99] Thomas H. Cormen, Charles E. Leiserson, Ronald L. Rivest, and Clifford Stein, *Introduction to Algorithms, Third Edition*, The MIT Press, 3rd edition, 2009.

[100] C. Leroux, A. J. Raymond, G. Sarkis, and W. J. Gross, "A semi-parallel successive-cancellation decoder for polar codes," *IEEE Transactions on Signal Processing*, vol. 61, no. 2, pp. 289–299, Jan 2013.

[101] G.D. Forney, "Geometrically uniform codes," *Information Theory, IEEE Transactions on*, vol. 37, no. 5, pp. 1241–1260, Sep 1991.

[102] Zbigniew A. Kotulski and Wojciech Szczepinski, *Error Analysis with Applications in Engineering*, Springer, 2009.

[103] X. R. Li and Z. Zhao, "Relative error measures for evaluation of estimation algorithms," in *2005 7th International Conference on Information Fusion*, July 2005, vol. 1, pp. 8 pp.–.

[104] Florence Jessie "MacWilliams and Neil James Alexander" Sloane, *The theory of error correcting codes*, "North-Holland mathematical library". "North-Holland Pub. Co. New York", 1977.

[105] John R. Birge and Franois Louveaux, *Introduction to Stochastic Programming*, Springer Publishing Company, Incorporated, 2nd edition, 2011.

[106] Sheldon M. Ross, *A First Course in Probability*, Prentice Hall, Upper Saddle River, N.J., fifth edition, 1998.

[107] U. Blass, I. Honkala, M. Karpovsky, and S. Litsyn, "Short dominating paths and cycles in the binary hypercube," *Annals of Combinatorics*, vol. 5, 2001.

[108] Stephen Boyd and Lieven Vandenberghe, *Convex Optimization*, Cambridge University Press, New York, NY, USA, 2004.

[109] A. Minja, I. Stanojević, and V. Šenk, "Novel quasi-analytical simulation method for estimating the error probability in AWGN channel," in *Telecommunications and Signal Processing (TSP), 2014 37th International Conference on*, July 2014, pp. 1–5.

[110] E. Berlekamp and L. Welch, "Weight distributions of the cosets of the (32,6) reed-muller code," *IEEE Transactions on Information Theory*, vol. 18, no. 1, pp. 203–207, Jan 1972.

[111] A. Minja, I. Stanojević, and V. Šenk, "Novel quasi-analytical simulation method for estimating the error probability over the BSC," in *Telecommunications and Signal Processing (TSP), 2015 38th International Conference on*, July 2015, pp. 309–313.

[112] M. Mondelli, S. H. Hassani, and R. L. Urbanke, "From polar to reed-muller codes: A technique to improve the finite-length performance," *IEEE Transactions on Communications*, vol. 62, no. 9, pp. 3084–3091, Sept 2014.

[113] Claude Elwood Shannon, "A mathematical theory of communication," *The Bell System Technical Journal*, vol. 27, no. 3, pp. 379–423, 7 1948.

[114] G. Forney, R. Gallager, G. Lang, F. Longstaff, and S. Qureshi, "Efficient modulation for band-limited channels," *IEEE Journal on Selected Areas in Communications*, vol. 2, no. 5, pp. 632–647, September 1984.

[115] G. D. Forney and L. F. Wei, "Multidimensional constellations. I. introduction, figures of merit, and generalized cross constellations," *IEEE Journal on Selected Areas in Communications*, vol. 7, no. 6, pp. 877–892, Aug 1989.

[116] G. D. Forney, "Multidimensional constellations. ii. voronoi constellations," *IEEE Journal on Selected Areas in Communications*, vol. 7, no. 6, pp. 941–958, Aug 1989.

[117] Ram Zamir, *Lattice Coding for Signals and Networks: A Structured Coding Approach to Quantization, Modulation, and Multiuser Information Theory*, Cambridge University Press, New York, NY, USA, 2014.

[118] S.I.R. Costa, F. Oggier, A. Campello, J.C. Belfiore, and E. Viterbo, *Lattices Applied to Coding for Reliable and Secure Communications*,

SpringerBriefs in Mathematics. Springer International Publishing, 2018.

[119] D. E. Lazić, "Class of block codes for the gaussian channel," *IET Electronics Letters*, vol. 16, no. 5, pp. 185–186, Feb 1980.

[120] D. E. Lazić, D. P. Drajić, and V. Šenk, "A table of some small-size three-dimensional best spherical codes," in *Procedings of the IEEE International Symposium on Information Theory*, 1982.

[121] D. E. Lazić and V. Šenk, "A new packing of 19 equal circles on a sphere," *Bulletins for Applied Mathematics (Technical University of Budapest)*, vol. 57, no. 709/91, pp. 93–97, 1991.

[122] M. Artin, *Algebra*, Pearson Prentice Hall, 2011.

[123] A. Mejri and G. Rekaya-Ben Othman, "Efficient decoding algorithms for the compute-and-forward strategy," *IEEE Transactions on Communications*, vol. 63, no. 7, pp. 2475–2485, July 2015.

[124] O. Ordentlich, J. Zhan, U. Erez, M. Gastpar, and B. Nazer, "Practical code design for compute-and-forward," in *2011 IEEE International Symposium on Information Theory Proceedings*, July 2011, pp. 1876–1880.

[125] W. Nam, S. Chung, and Y. H. Lee, "Nested lattice codes for gaussian relay networks with interference," *IEEE Transactions on Information Theory*, vol. 57, no. 12, pp. 7733–7745, Dec 2011.

[126] N. Sommer, M. Feder, and O. Shalvi, "Low-density lattice codes," *IEEE Transactions on Information Theory*, vol. 54, no. 4, pp. 1561–1585, April 2008.

[127] John M Wozencraft and Irwin Mark Jacobs, *Principles of communication engineering*, Wiley, New York, NY, 1965.

[128] Gabriele Nebe and Neil Sloane, "A catalogue of lattices," `http://www.math.rwth-aachen.de/~Gabriele.Nebe/LATTICES/`, Accessed: 2018-09-17.

[129] B.A. Rozenfel'd and N.D. Sergeeva, *Stereographic projection*, Little mathematics library. Mir Publishers, 1977.

[130] V. Schlegel, *Theorie der homogen zusammengesetzten Raumgebilde, von Dr. Victor Schlegel ....*, Druck von E. Blochmann und Sohn, 1883.

[131] H.S.M. Coxeter, *Regular Polytopes*, Dover books on advanced mathematics. Dover Publications, 1973.

[132] D. A. Kottwitz, "The densest packing of equal circles on a sphere," *Acta Crystallographica Section A*, vol. 47, no. 3, pp. 158–165, May 1991.

[133] Lee-Fang Wei, "Trellis-coded modulation with multidimensional constellations," *IEEE Transactions on Information Theory*, vol. 33, no. 4, pp. 483–501, July 1987.

[134] G. Caire, G. Taricco, and E. Biglieri, "Bit-interleaved coded modulation," *IEEE Transactions on Information Theory*, vol. 44, no. 3, pp. 927–946, May 1998.

[135] Xiaodong Li and J. A. Ritcey, "Bit-interleaved coded modulation with iterative decoding," *IEEE Communications Letters*, vol. 1, no. 6, pp. 169–171, Nov 1997.

[136] P. Fines and A. H. Aghvami, "A trellis coded 16-qam modem for land mobile communications," in *IEE Colloquium on Land Mobile Satellite Systems*, June 1992, pp. 6/1–6/4.

[137] Fu-Quan Wang and D. J. Costello, "Sequential decoding of trellis codes at high spectral efficiencies," *IEEE Transactions on Information Theory*, vol. 43, no. 6, pp. 2013–2019, Nov 1997.

[138] G. D. Forney and G. Ungerboeck, "Modulation and coding for linear gaussian channels," *IEEE Transactions on Information Theory*, vol. 44, no. 6, pp. 2384–2415, Oct 1998.

[139] U. Wachsmann, R. F. H. Fischer, and J. B. Huber, "Multilevel codes: theoretical concepts and practical design rules," *IEEE Transactions on Information Theory*, vol. 45, no. 5, pp. 1361–1391, July 1999.

[140] H. Herzberg, "Multilevel turbo coding with a short latency," in *Proceedings of IEEE International Symposium on Information Theory*, June 1997, pp. 112–.

[141] A. R. Calderbank, "Multilevel codes and multistage decoding," *IEEE Transactions on Communications*, vol. 37, no. 3, pp. 222–229, March 1989.

[142] P. A. Martin and D. P. Taylor, "On multilevel codes and iterative multistage decoding," *IEEE Transactions on Communications*, vol. 49, no. 11, pp. 1916–1925, Nov 2001.

[143] J. B. Soriaga, H. D. Pfister, and P. H. Siegel, "Determining and approaching achievable rates of binary intersymbol interference channels using multistage decoding," *IEEE Transactions on Information Theory*, vol. 53, no. 4, pp. 1416–1429, April 2007.